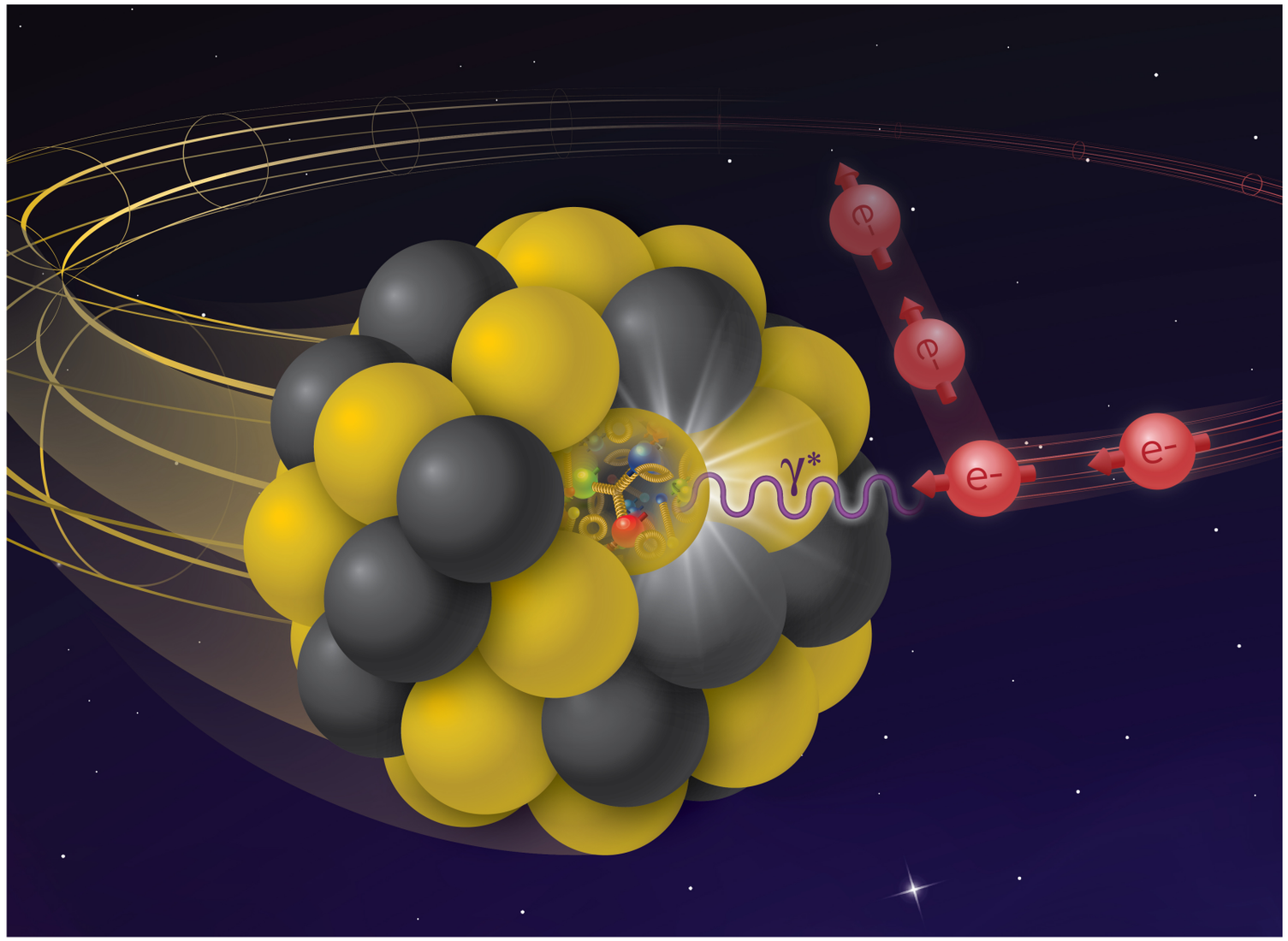

eA physics at Electron Ion Collider
with focus on small x and diffraction

Anna Stąśto

Penn State University

INT Program INT-23-1A, 'Intersection of nuclear structure and high-energy nuclear collisions', February 20-24, 2023

What can be explored at EIC in eA collisions ?

Capabilities of EIC

Beams with different A: from *light nuclei* to the ***heavy nuclei***

Polarized electron and nucleon beams. Possibility of polarized light ions.

Variable center of mass energies 20 -140 GeV

High luminosity $10^{33} - 10^{34} cm^{-2} s^{-1}$

Physics with nuclear beams

How are parton distributions changed in nuclei ? Nuclear PDFs, proton & neutron structure

How and when partons saturate in nuclei ? Parton saturation

How nucleons/nuclei stay intact in high energy collision?
What is the nature of color singlet exchange ? Diffraction and shadowing

How partons interact with nuclear medium ? Hadronization in medium

Nature of the strong force, correlations in nuclei ? EMC effect, short range correlations

EIC Yellow Report 2021

From the Yellow Report Chapter 1:

The purpose of the Yellow Report Initiative is to advance the state and detail of the documented physics studies (White Paper, Institute for Nuclear Theory program proceedings) and detector concepts (Detector and R&D Handbook) in preparation for the realization of the EIC. The effort aims to provide the basis for further development of concepts for experimental equipment best suited for science needs, including complementarity of two detectors towards future Technical Design Reports.

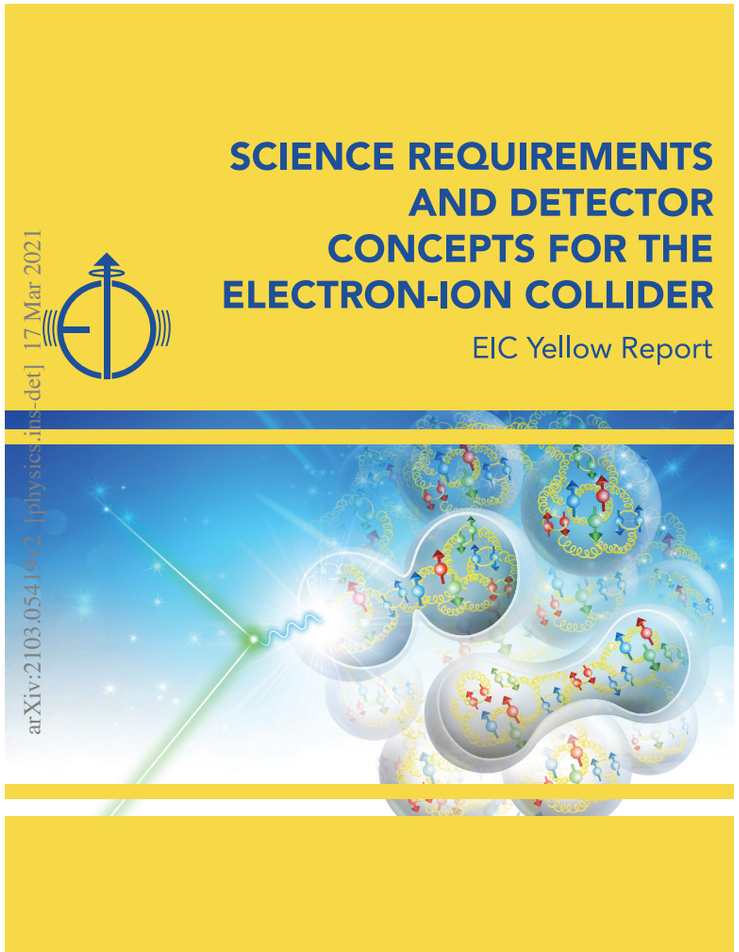

One year effort

4 workshops, 902 pages, 415 authors, 151 institutions

Organisation

Physics Working Group

- Inclusive Reactions
- Semi-Inclusive Reactions
- Jets & Heavy Quarks
- Exclusive Reactions
- Diffraction & Tagging

Detector Working Group

- Tracking
- Particle ID
- Calorimetry (EM + Hadronic)
- Far-forward detectors
- DAQ/Electronics
- Central Detector/Integration & Magnet
- Forward Detector/IR integration
- Polarimetry/Ancillary Detectors
- Detector Complementarity

Yellow Report arXiv:2103.05419

EIC Yellow Report 2021

Contents

Title Page i

Author List iii

Abstract

Table of Contents

Volume I: Executive Summary

1 The Electron-Ion Collider

2 Physics Measurements and Requirements

2.1 Introduction
2.2 Origin of Nucleon Spin
2.3 Origin of Nucleon Mass
2.4 Multi-Dimensional Imaging of the Nucleon
2.5 Imaging the Transverse Spatial Distributions of Partons
2.6 Physics with High-Energy Nuclear Beams at the EIC
2.7 Nuclear Modifications of Parton Distribution Functions
2.8 Passage of Color Charge Through Cold QCD Matter
2.9 Connections to Other Fields
2.10 Summary of Machine Design Parameters

xi

12 The Case for Two Detectors

12.1 Boundary Conditions and Important Relations
12.2 Dedicated Detector Designs versus General Purpose Detecto
12.3 Motivation for Two Detectors: Technology Considerations
12.4 Motivation for Two Detectors: Complementarity of Physics
12.5 Opportunities from Fixed Target Mode Operation
12.6 Summary

13 Integrated EIC Detector Concepts

13.1 Hall infrastructure
13.2 Safety and Environmental Protection
13.3 Installation
13.4 Detector Alignment
13.5 Access and Maintenance

14 Detector R&D Goals and Accomplishments 66

14.1 Silicon-Vertex Tracking . . . 665
14.2 Tracking . . . 669
14.3 Particle Identification . . . 677
14.4 Electromagnetic and Hadronic Calorimetry . . . 688
14.5 Auxiliary Detectors . . . 692
14.6 Data Acquisition . . . 697
14.7 Electronics . . . 699

Acknowledgements 703

Appendices 707

Appendix A Deep Inelastic Scattering Kinematics 707

A.1 Structure functions . . . 707

xiv

2.11 Summary of Detector Requirements . . . 19

3 Detector Concepts 23

3.1 Tracking and Vertexing Detector Systems . . . 24
3.2 Particle Identification Detector Systems . . . 25
3.3 Calorimeter Detector Systems . . . 26
3.4 Auxiliary Detector Systems . . . 27

7 EIC Measurements and Studies 52

7.1 Global Properties and Parton Structure of Hadrons . . . 52
7.2 Multi-dimensional Imaging of Nucleons, Nuclei, and Mesons . . . 105
7.3 The Nucleus: A Laboratory for QCD . . . 146
7.4 Understanding Hadronization . . . 186
7.5 Connections with Other Fields . . . 214
7.6 Connected Theory Efforts . . . 248

8 Detector Requirements 258

8.1 Inclusive Measurements . . . 260
8.2 Semi-Inclusive Measurements . . . 283
8.3 Jets and Heavy Quarks . . . 294
8.4 Exclusive Measurements . . . 323
8.5 Diffractive Measurements and Tagging . . . 365

A.4 Breit frame . . . 711
A.5 Helicity studies . . . 712

Appendix B Organizational Structure 713

Appendix C Yellow Report Workshops 717

References 743

8.6 Summary of Requirements . . . 393

Volume III: Detector 397

9 Introduction to Volume III 399

9.1 General EIC Detector Considerations . . . 400
9.2 Reference EIC Detector . . . 402

quirements 406

y, Luminosities . . . 406
ion . . . 410
. . . 413
. . . 415
. . . 427
. . . 432

434

. . . 434
. . . 436
. . . 483
. . . 511
. . . 519
. . . 546
. . . 572
hallenges . . . 583
. . . 591
n . . . 606
vation . . . 630
r . . . 634

Kinematics of DIS

Inelastic scattering off proton

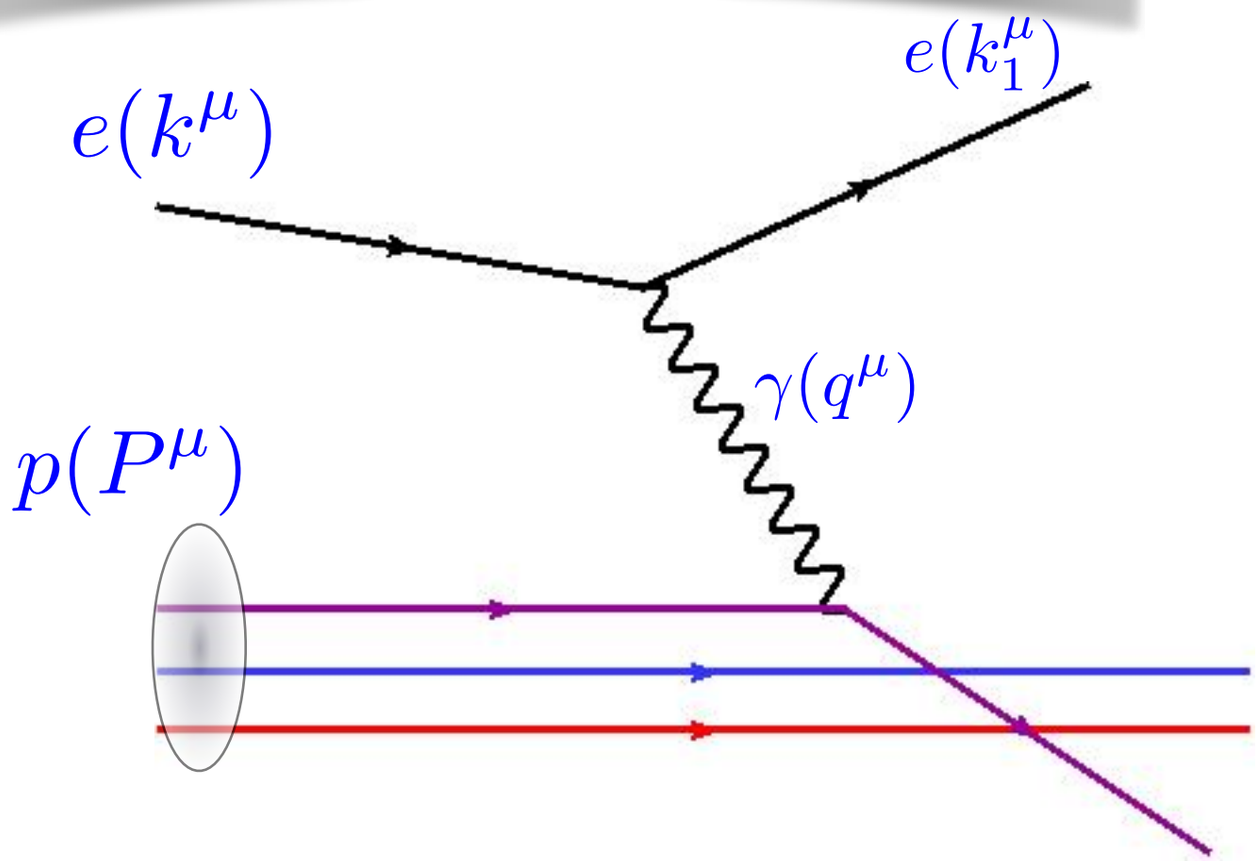

Elastic scattering off parton (quark)

$$Q^2 = -q^2$$ Photon virtuality : resolving power

$$x = \frac{Q^2}{2P \cdot q} \simeq \frac{Q^2}{Q^2 + W^2}$$ Bjorken x

$$W^2 = (p+q)^2$$ total energy of photon-proton system

$$s = (p+k)^2$$ total cms energy

x has the interpretation of the longitudinal momentum fraction of the proton carried by the struck quark

$Q^2 = -q^2$ Resolving power ⟺ high energy W ⟺ small x

Global structure of nuclei

DIS cross section

$$Y_+ = 1 + (1-y)^2$$

$$\frac{d^2\sigma}{dxdQ^2} = \frac{2\pi\alpha_{\rm em}^2}{xQ^4} Y_+ \sigma_{\rm r}(x,Q^2)$$

Reduced cross section and structure functions

$$\sigma_{\rm r}(x,Q^2) = F_2(x,Q^2) - \frac{y^2}{Y_+} F_L(x,Q^2)$$

Precise measurement of **nuclear structure functions** for wide range of nuclei and **wide kinematic range**

Extraction of **nuclear PDFs** which are essential for understanding **nuclear structure**

Initial conditions for Quark-Gluon Plasma

Sys. uncertainties at most few %, stat. negligible

Proton, deuteron and wide range nuclei structure function within **one facility:** reduction of uncertainties

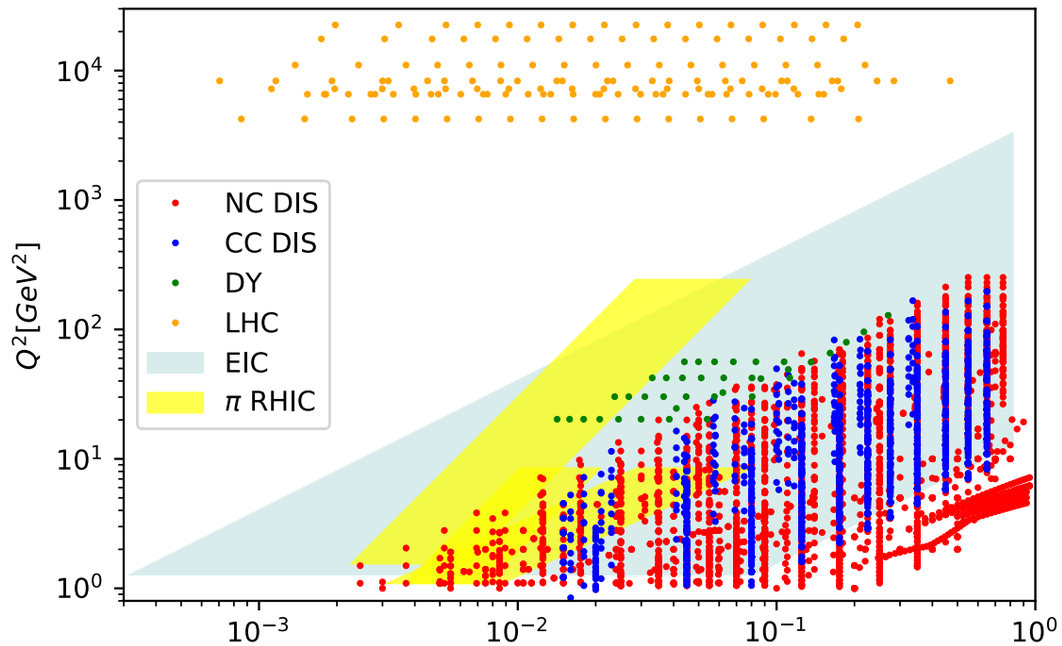

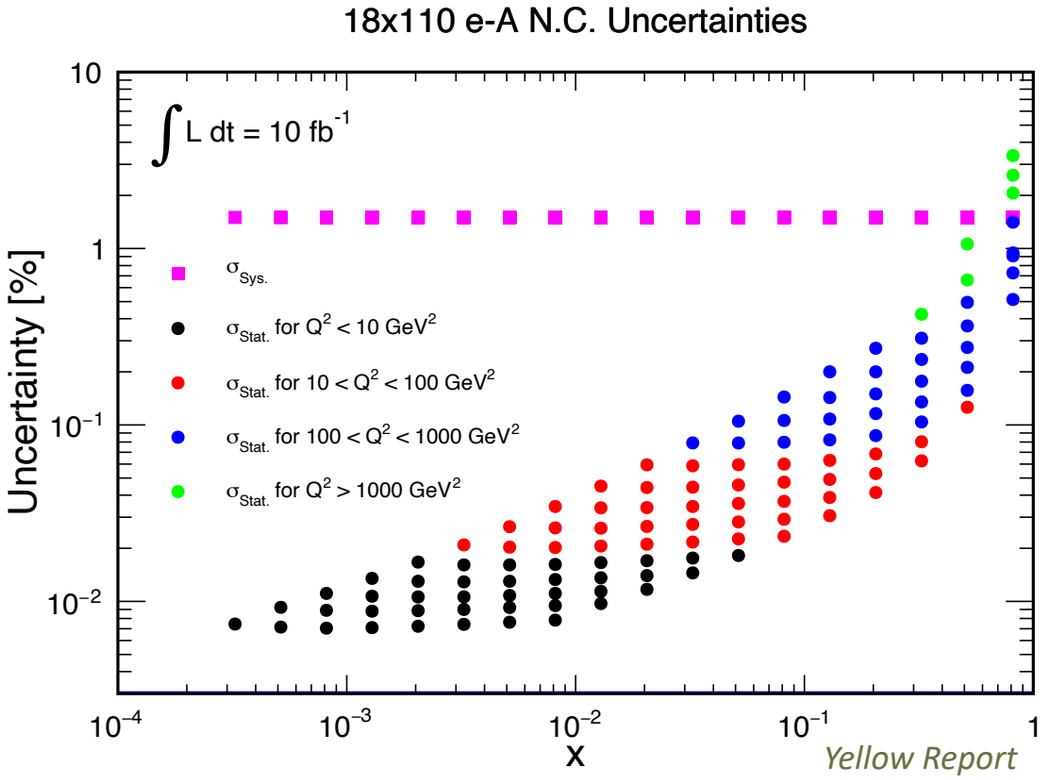

Nuclear structure

Deep Inelastic Scattering : $$\frac{d^2\sigma^{ep\to eX}}{dxdQ^2} = \frac{4\pi\alpha^2_{e.m.}}{xQ^4}\left[\left(1-y+\frac{y^2}{2}\right)F_2(x,Q^2) - \frac{y^2}{2}F_L(x,Q^2)\right]$$

Nuclear ratio for structure function

$$R^A_{F_2}(x,Q^2) = \frac{F_2^A(x,Q^2)}{A\,F_2^{\text{nucleon}}(x,Q^2)}$$

Nuclear effects $R^A \neq 1$

Schematic picture

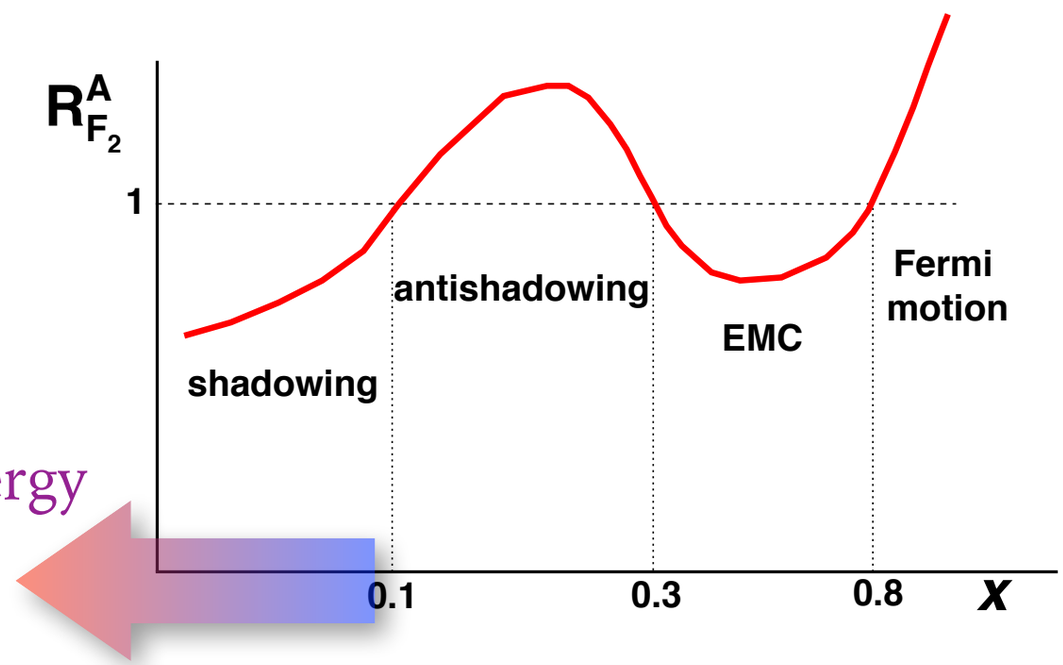

High energy

- Fermi motion $x \geq 0.8$
- EMC region $0.25 - 0.3 \leq x \leq 0.8$
- Antishadowing region $0.1 \leq x \leq 0.25 - 0.3$
- Shadowing region $x \leq 0.1$

Global nuclear structure: structure functions

Aschenauer, Fazio, Lamont, Paukkunen, Zurita

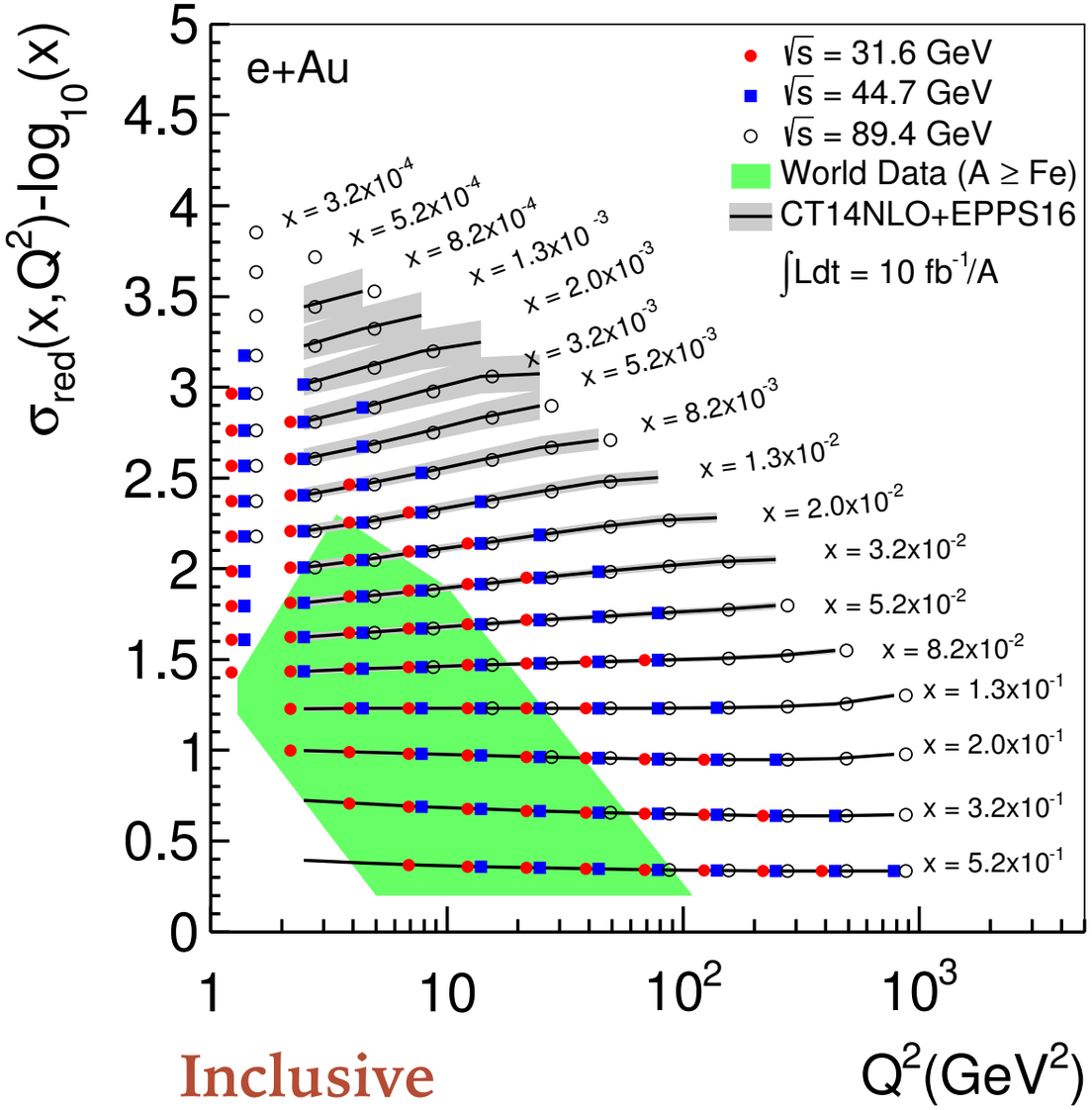

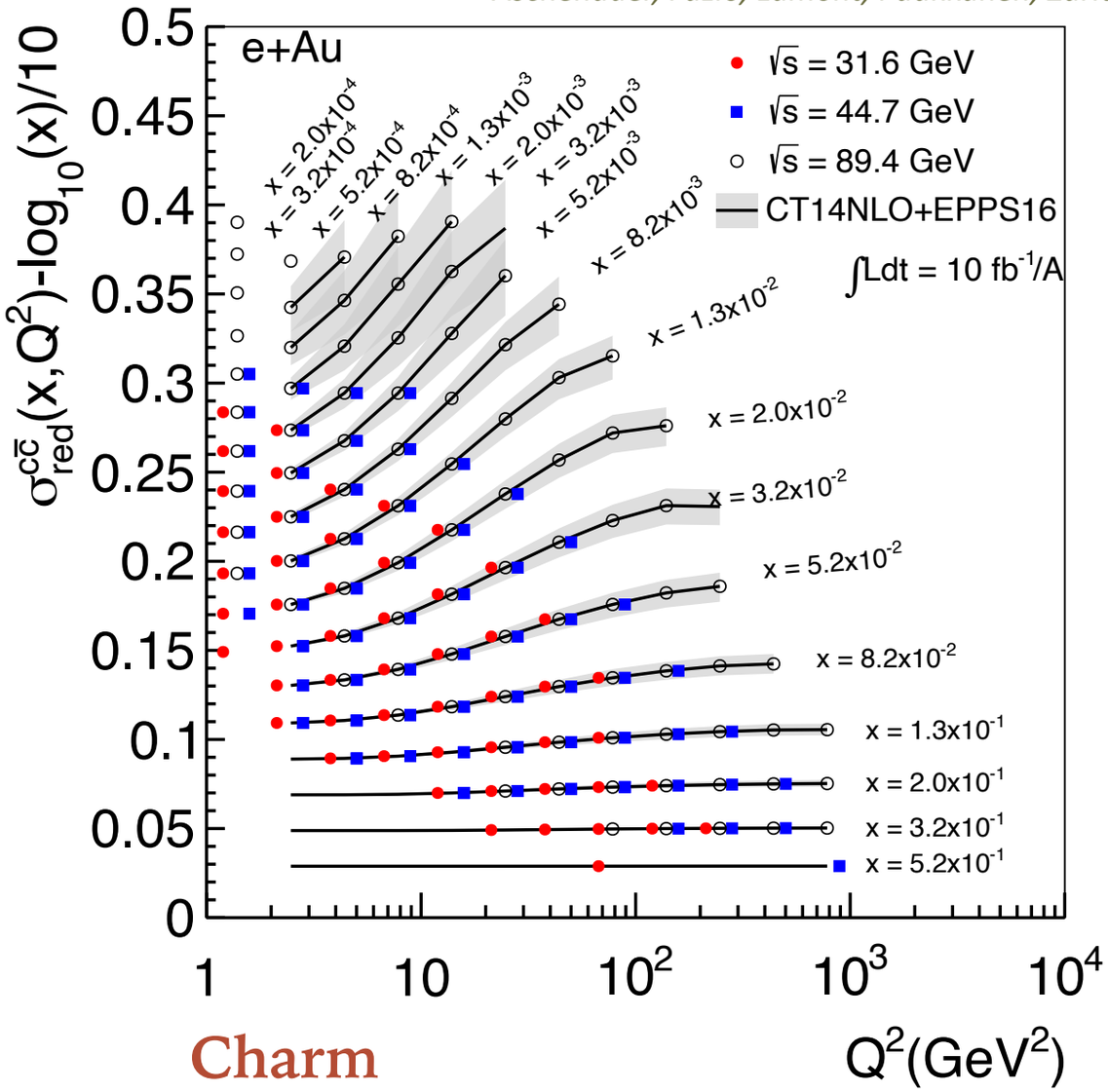

Precision measurements of the reduced cross section: inclusive and charm component in nuclei

Errors much smaller than the uncertainties of QCD predictions

Impact of EIC on nuclear PDFs

Collinear factorization

$$F_{2,L}(x,Q^2) = \sum_j \int_x^1 dz\, C_{2,L}(Q/\mu, x/z; \alpha_s)\, f_j(z,\mu) + \ldots$$

DGLAP evolution : linear evolution with scale

$$\frac{d}{d\ln\mu^2} f_j(z,\mu) = \sum_k \int \frac{d\xi}{\xi} P_{jk}(\xi,\alpha_s) f_k(z/\xi,\mu)$$

Yellow Report

Nuclear modification in this framework:

initial condition at low scales, **linear evolution with scale**

Significant impact of EIC measurements on nuclear PDFs

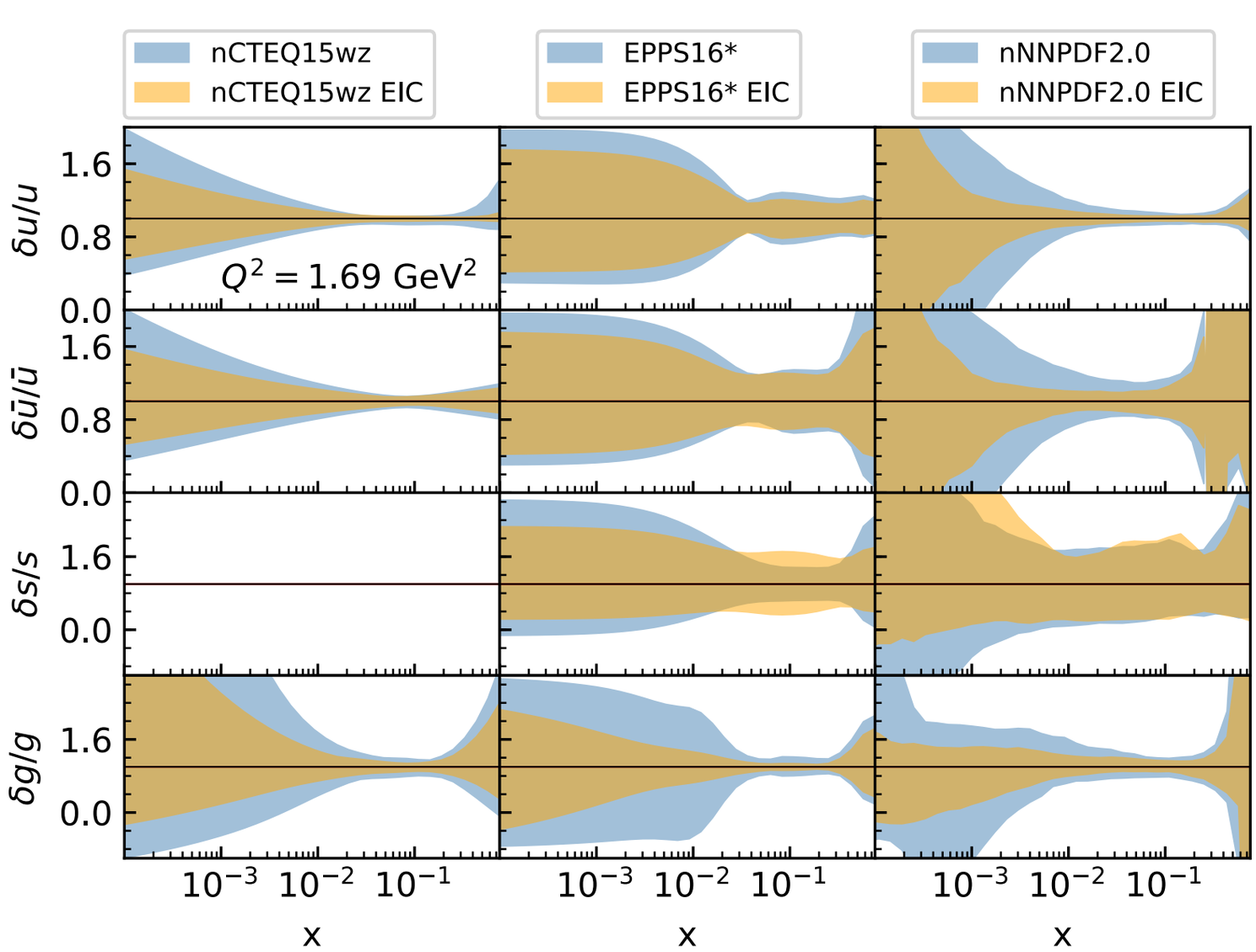

Heavy flavor impact on gluon PDF

Impact of **charm cross section** on the gluon PDF at high x

Charm is produced mainly in the photon-gluon fusion process

Dedicated efforts to study of feasibility of measurement of charm from D decays to K and pion

Significant impact on gluon at x>0.1. Sensitivity to EMC effect.

Further constraints: F_L

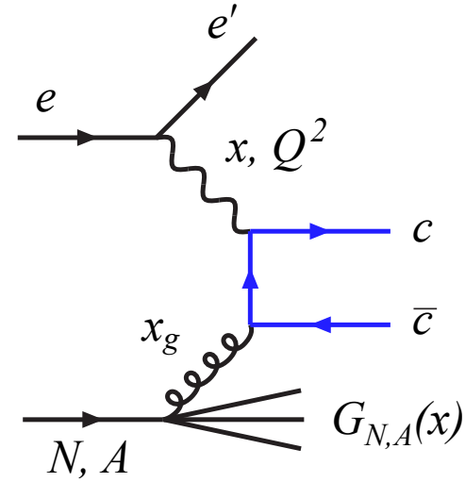

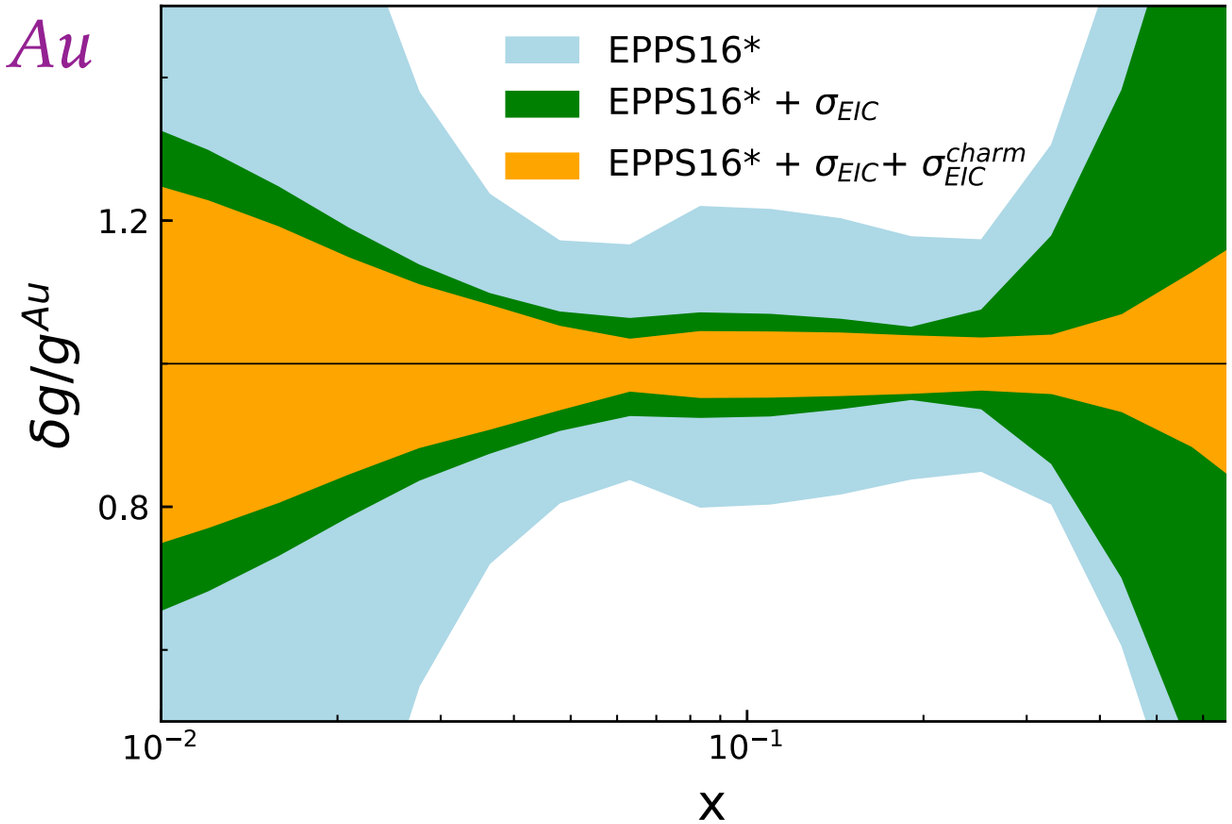

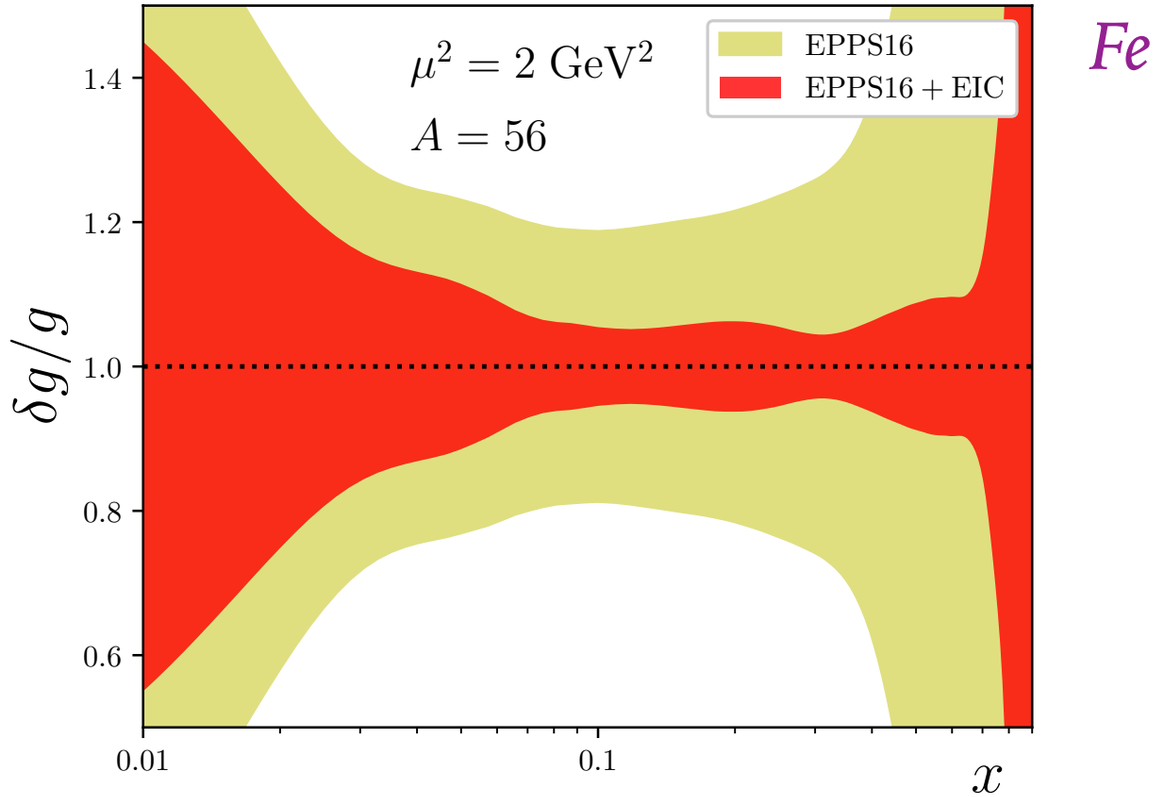

Small x problem

$$F_{2,L}(x,Q^2) = \sum_j \int_x^1 dz\, C_{2,L}(Q/\mu, x/z; \alpha_s)\, f_j(z,\mu) + \ldots$$

gluons

valence quarks

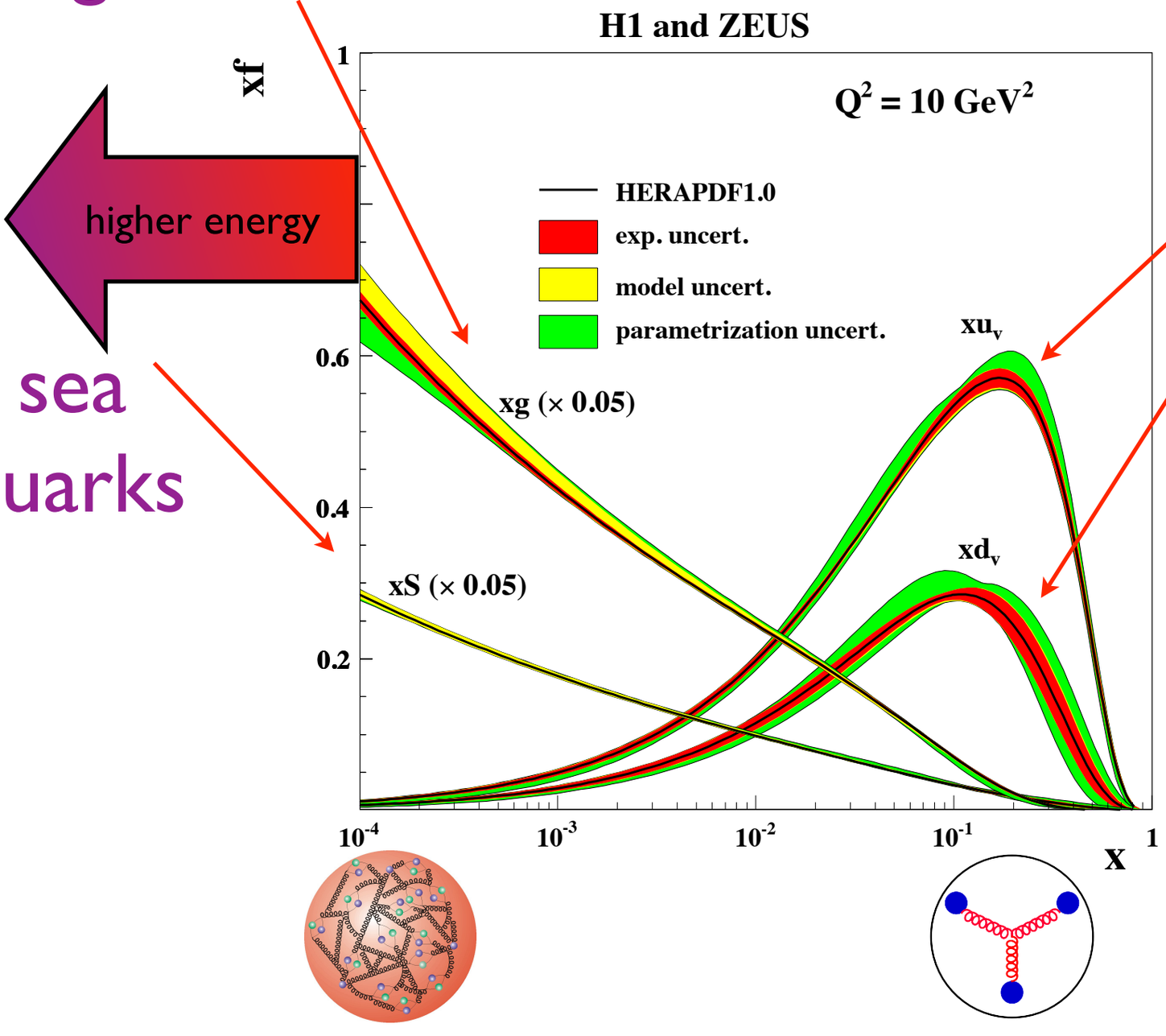

higher energy

sea quarks

Gluon density increases rapidly with decreasing x

What happens at very low x ?

Can the gluon density grow indefinitely ?

Collinear approach to parton evolution

$\gamma^* N$ as a template

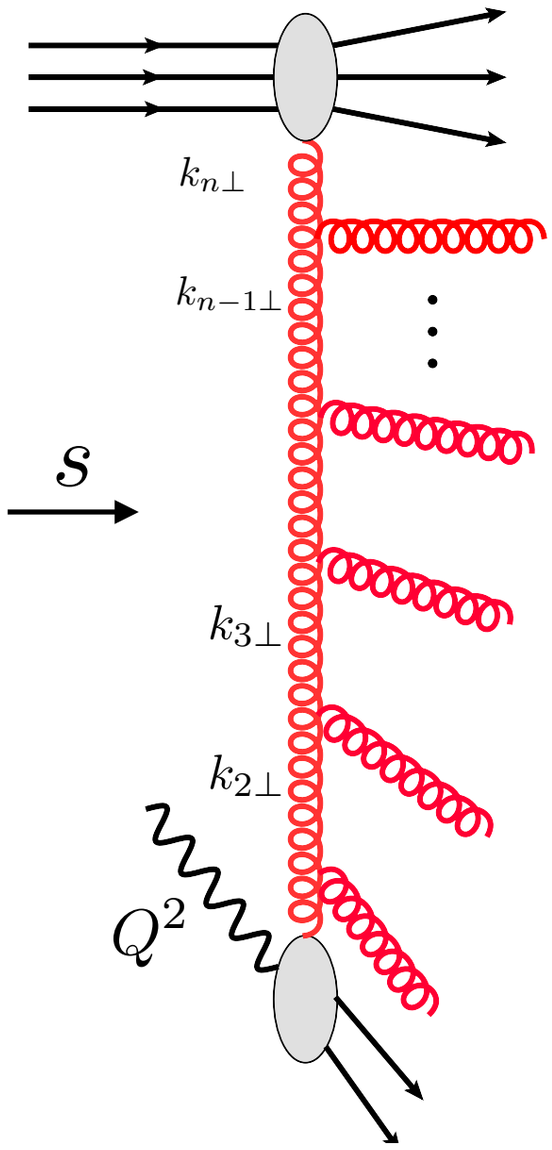

Large parameter

$$Q^2 \to \infty$$

s total energy is fixed

Probing small distances

Strong ordering in transverse momenta

$$Q^2 \gg k_{1\perp}^2 \gg k_{2\perp}^2 \gg k_{3\perp}^2 \cdots \gg k_{n\perp}^2$$

Resummation of large logarithms

$$\int_{\mu_0^2}^{Q^2} \frac{dk_{1\perp}^2}{k_{1\perp}^2} g^2 \int_{\mu_0^2}^{k_{1\perp}^2} \frac{dk_{2\perp}^2}{k_{2\perp}^2} g^2 \int_{\mu_0^2}^{k_{2\perp}^2} \frac{dk_{3\perp}^2}{k_{3\perp}^2} g^2 \cdots \int_{\mu_0^2}^{k_{n-1\perp}^2} \frac{dk_{n\perp}^2}{k_{n\perp}^2} g^2 \simeq \left(g^2 \log \frac{Q^2}{\mu_0^2} \right)^n$$

Collinear approach: DGLAP evolution

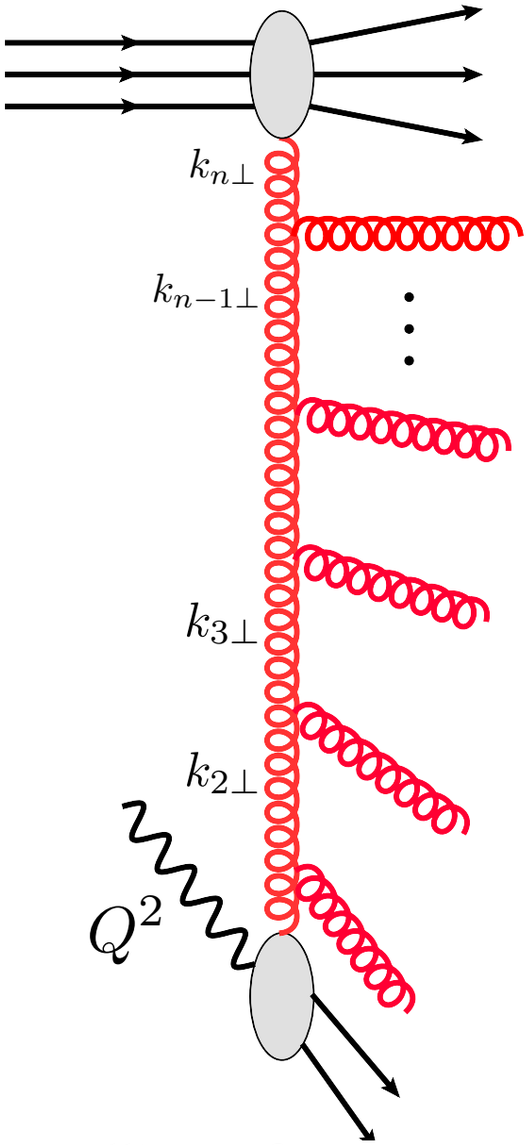

DGLAP evolution equation for parton densities

$$\frac{\partial f_i(x,Q^2)}{\partial \log(Q^2)} = \sum_j \int_x^1 \frac{dz}{z} P_{j\to i}(z) f_j(\frac{x}{z}, Q^2)$$

Splitting functions calculated perturbatively

$$P_{j\to i}(z) = \alpha_s P^{(LO)}_{j\to i}(z) + \alpha_s^2 P^{(NLO)}_{j\to i}(z) + \alpha_s^3 P^{(NNLO)}_{j\to i}(z) + \dots$$

Parton densities: distributions in longitudinal momenta at a given scale

$$f_i(x,Q^2)$$

Collinear factorization of the cross section

$$d\sigma(x,Q^2) = \sum_i f_i \otimes d\hat{\sigma}^i + \mathcal{O}(\Lambda^2/Q^2)$$

$d\hat{\sigma}^i$ partonic cross section, calculable perturbatively

High energy or small x limit

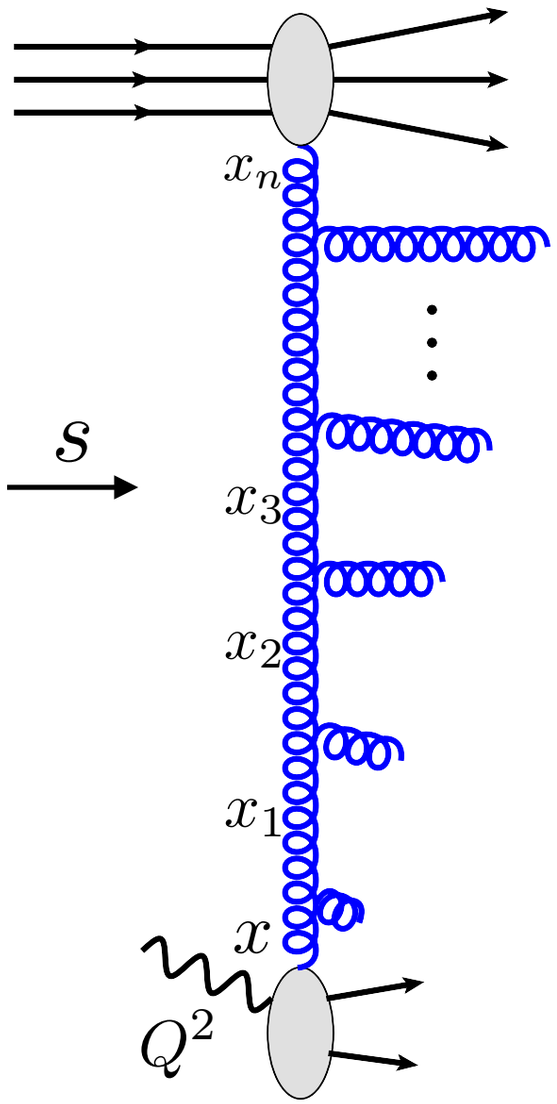

Large parameter

$$s \to \infty$$

Q^2 fixed, perturbative

High energy or Regge limit

$$s \gg Q^2 \gg \Lambda^2$$

Light cone proton momentum

$$p^+ = p^0 + p^z$$

$$k_i^+ = x_i p^+$$

Strong ordering in longitudinal momenta

$$x \ll x_1 \ll x_2 \ll \cdots \ll x_n$$

Perturbative coupling but large logarithm

$$\bar{\alpha}_s \ll 1$$

$$\ln \frac{1}{x} \simeq \ln \frac{s}{Q^2} \gg 1$$

Large logarithms

$$\frac{\alpha_s N_c}{\pi} \int_x^1 \frac{dz}{z} = \frac{\alpha_s N_c}{\pi} \ln \frac{1}{x} = \bar{\alpha}_s \ln \frac{1}{x}$$

Leading logarithmic resummation

$$\left(\bar{\alpha}_s \ln \frac{1}{x} \right)^n$$

High energy limit: BFKL evolution

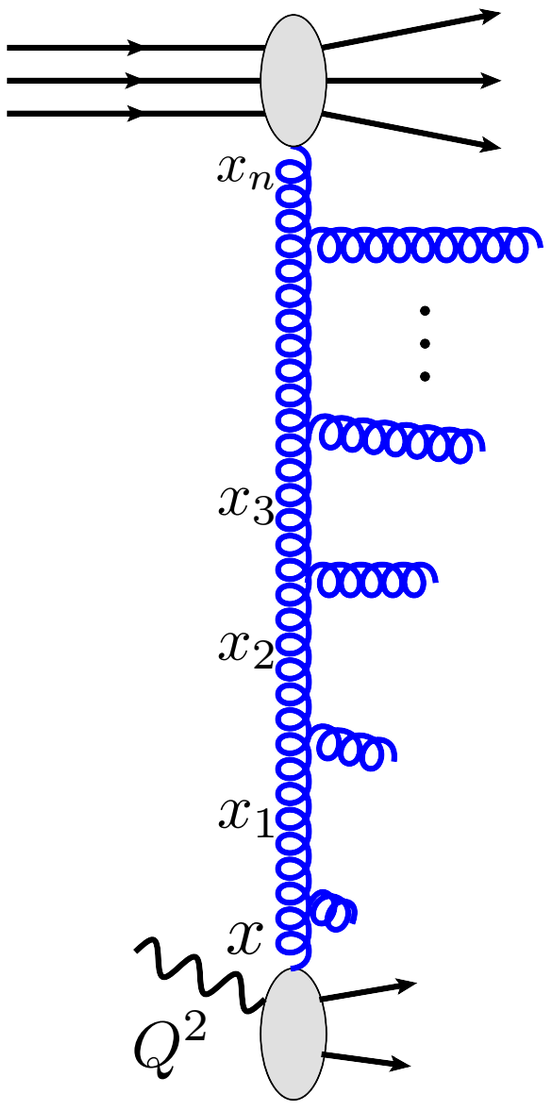

compare with DGLAP-collinear approach

Resummation performed by BFKL evolution equation

$$\frac{\partial \mathcal{F}_g(x,k_T)}{\partial \ln 1/x} = \int d^2k'_T\, \mathcal{K}(k_T,k'_T)\, \mathcal{F}_g(x,k'_T)$$

Branching kernel (perturbative expansion)

$$\mathcal{K} = \bar{\alpha}_s \mathcal{K}^{LLx} + \bar{\alpha}_s^2 \mathcal{K}^{NLLx} + \bar{\alpha}_s^3 \mathcal{K}^{NNLLx} + \dots$$

QCD N=4 SYM

Unintegrated, (transverse momentum dependent) gluon density

$$\mathcal{F}_g(x,k_T) \sim x^{-\lambda}$$

$$\frac{\partial f_i(x,Q^2)}{\partial \log(Q^2)} = \sum_j \int_x^1 \frac{dz}{z} P_{j\to i}(z) f_j(\frac{x}{z},Q^2)$$

Combining DGLAP and BFKL: low x resummation

BFKL expansion has large higher orders: need resummation

Ciafaloni, Colferai, Salam, AS

Altarelli, Ball, Forte; Thorne; Thorne, White

Combine the information from both expansions

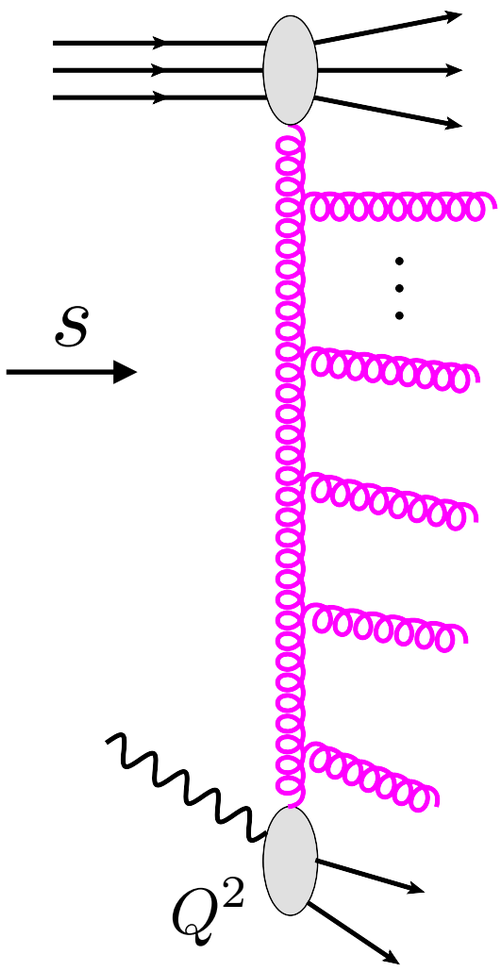

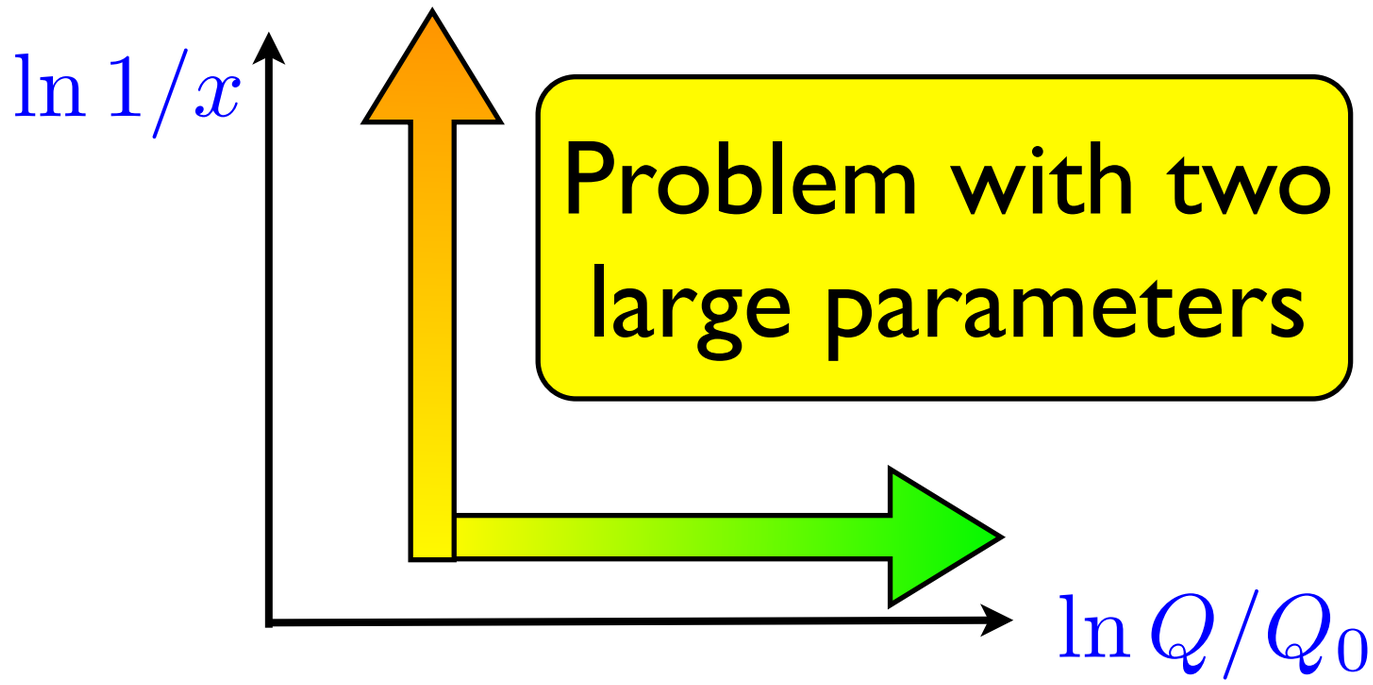

$\left(\frac{\alpha_s N_c}{\pi} \ln \frac{1}{x}\right)^n$ logarithms of energy

$\left(\frac{\alpha_s N_c}{\pi} \ln \frac{Q}{Q_0}\right)^n$ logarithms of scale (related to transverse momentum)

For accurate predictions at EIC resummed calculations which can interpolate between large, moderate and low x are necessary

Another problem at low x: parton saturation

QCD at high energy (low x) and/or high density (large A) predicts **saturation** of gluons

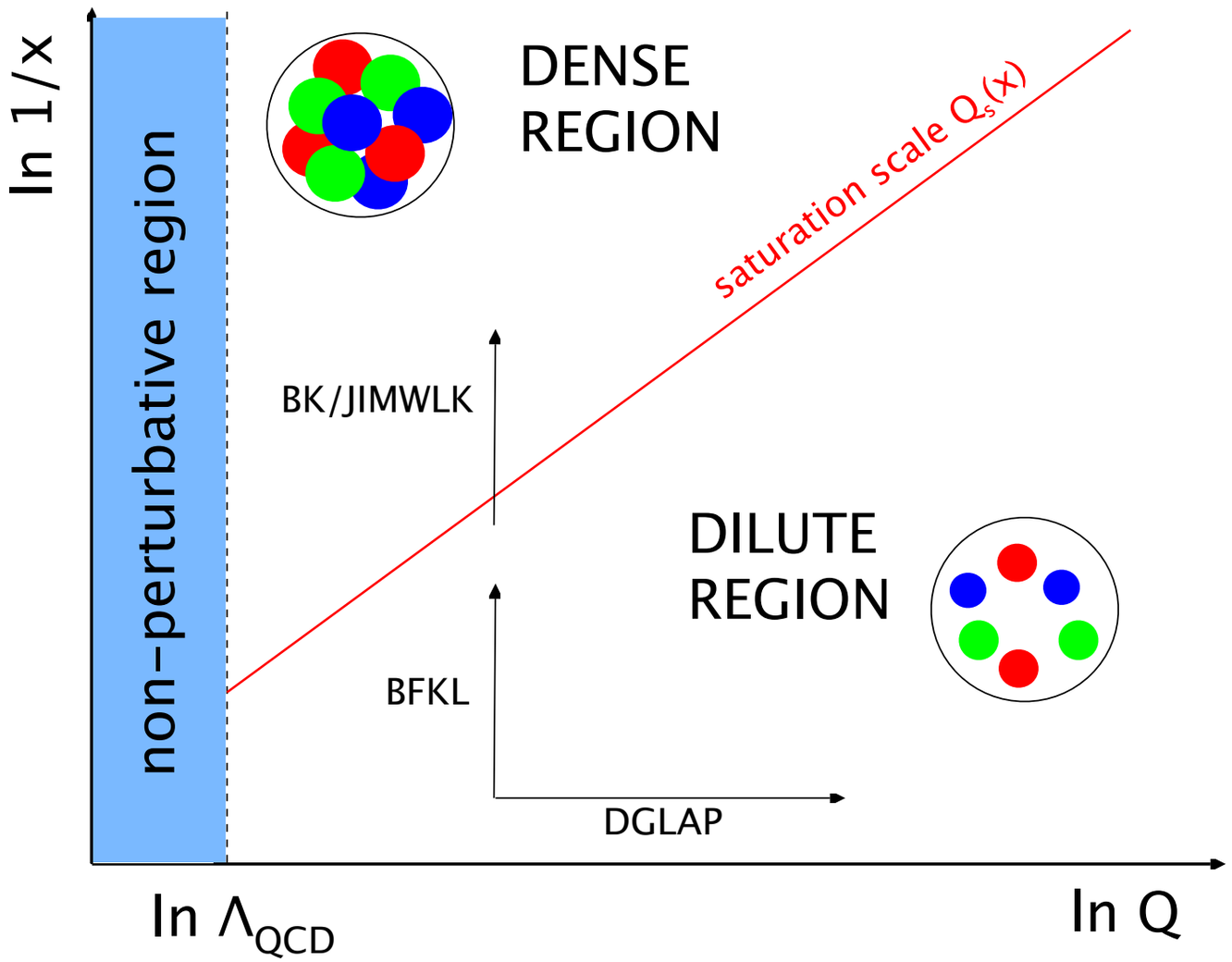

Splitting of gluons must be accompanied by **recombination**, important at high density

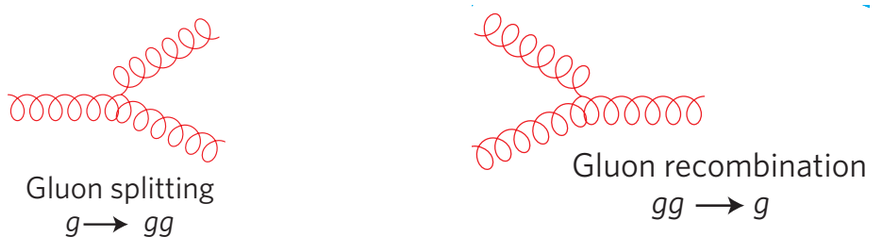

Evolution equations become non-linear ! (Balitsky-Kovchegov : BK equation, JIMWLK hierarchy)

$$\frac{\partial}{\partial \ln 1/x} f(x,k) = K \otimes [f - f^2]$$

Nonlinear evolution generates **saturation** scale

$$Q_s^2(x,A) \sim \frac{A^{1/3}}{x^\lambda}$$

Normalization of the saturation scale needs to be fixed in experiment

Color Glass Condensate: effective theory at high energy/density

Nuclei provide enhancement of the density

$$Q_s^2(x,A) \sim \frac{A^{1/3}}{x^{\lambda}}$$

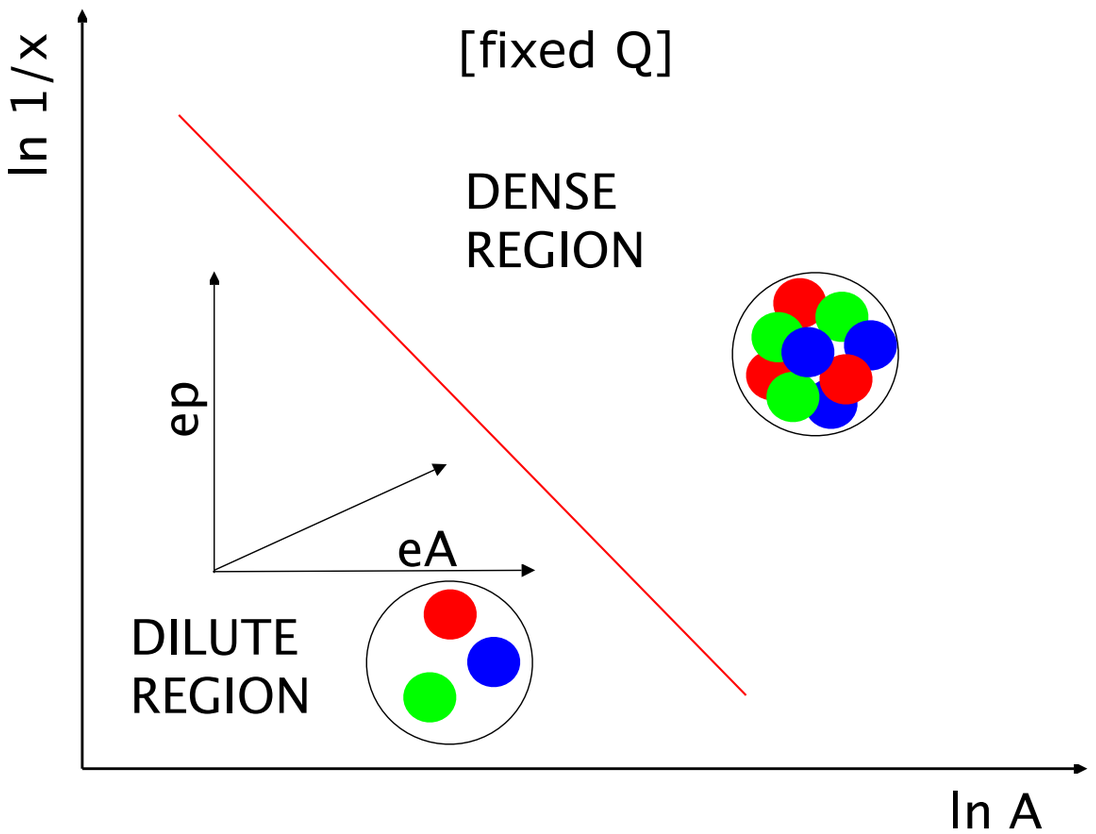

Impressive progress in higher order calculations at NLO in CGC in the context of DIS:

Nonlinear evolution equations to NLO in QCD and to NNLO in N=4 SYM

Resummation of higher orders in nonlinear evolution

Impact factors for inclusive structure functions

Impact factors for heavy quarks

Exclusive vector meson production and diffractive dijets

Inclusive dijet and hard photon final states

CGC calculations entering era of high precision

Necessary for EIC, which will probe moderate to low x

Opportunities at the EIC to test saturation using nuclei

Testing saturation through inclusive structure functions at EIC

Study differences in evolution between **linear DGLAP** evolution and **nonlinear** evolution with **saturation**

Matching of both approaches in the region where saturation effects expected to be small

Quantify differences away from the matching region: **differences in evolution dynamics**

$$\frac{F_{2,L}^{\mathrm{BK}} - F_{2,L}^{\mathrm{Rew}}}{F_{2,L}^{\mathrm{BK}}}$$

Armesto, Lappi,Mantysaari,PaukkunenmTevio

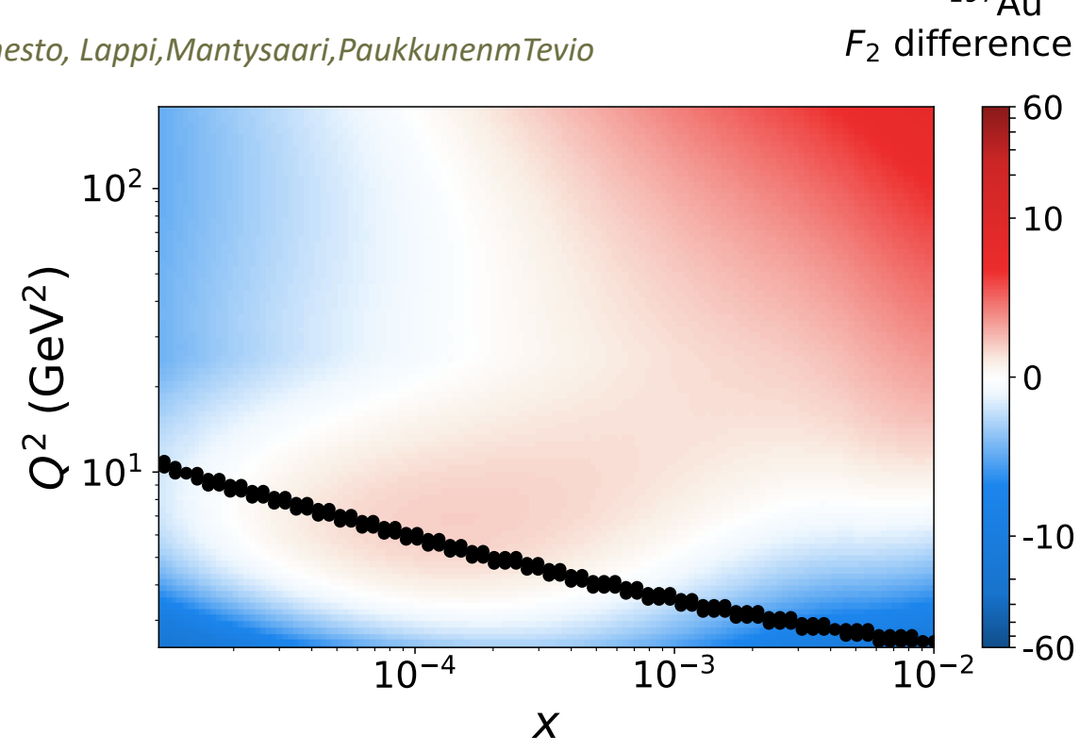

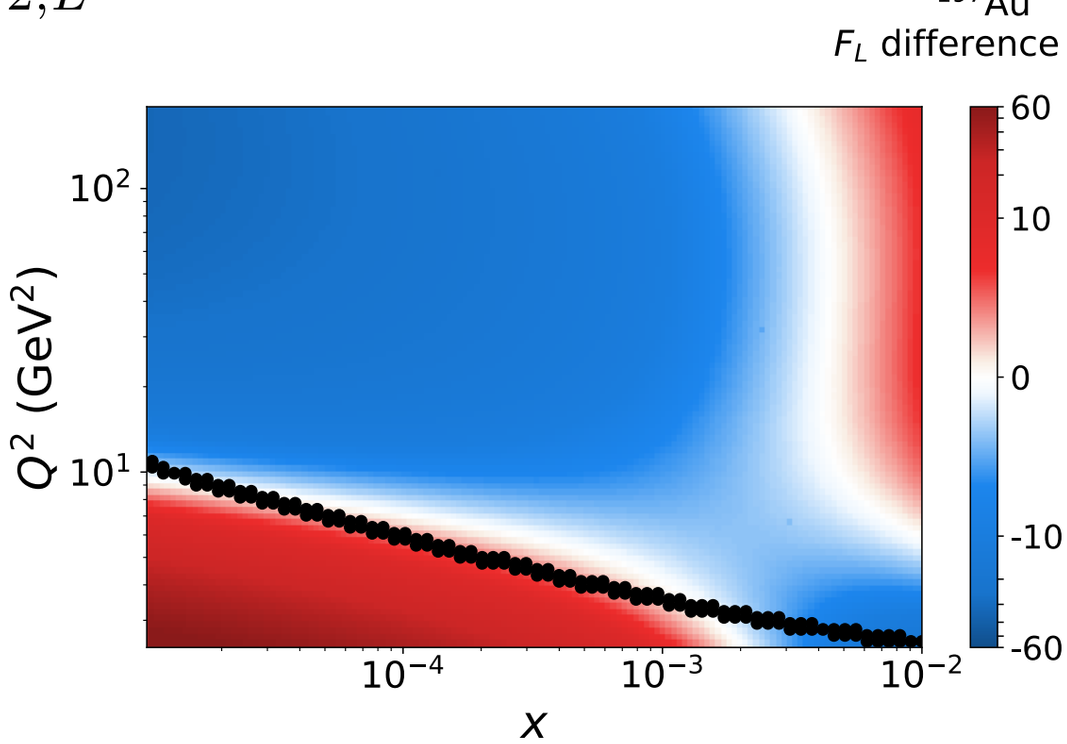

Heavy nucleus: difference between DGLAP and nonlinear are few % for F_2^A and up to 20% for F_L^A.

Longitudinal structure function can provide good sensitivity at EIC

Testing saturation through (de)correlations of hadrons

Azimuthal **(de)correlations of two hadrons** (dijets) in DIS in eA: direct test of the **Weizsacker -Williams unintegrated gluon distribution**

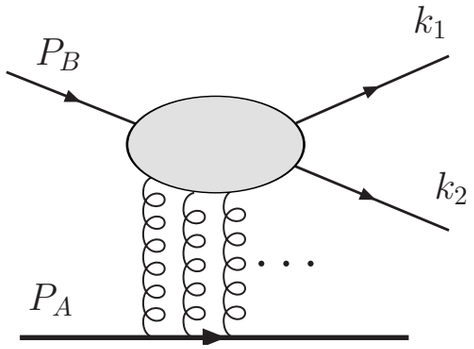

$$C(\Delta\phi) = \frac{1}{\frac{d\sigma^{\gamma^*+A\to h_1+X}_{\rm SIDIS}}{dz_{h1}}} \frac{d\sigma^{\gamma^*+A\to h_1+h_2+X}_{\rm tot}}{dz_{h1}dz_{h2}d\Delta\phi}$$

$$\frac{d\sigma^{\gamma^*+A\to h_1+h_2+X}}{dz_{h1}dz_{h2}d^2p_{h1T}d^2p_{h2T}} \sim \mathcal{F}(x_g, q_T) \otimes \mathcal{H}(z_q, k_{1T}, k_{2T}) \otimes D_q(z_{h1}/z_q, p_{1T}) \otimes D_q(z_{h2}/z_q, p_{2T})$$

Clear differences between the ep and eA: **suppression** of the correlation peak in **eA** due to **saturation** effects (including the **Sudakov resummation)**

Further observables: azimuthal correlations of dihadrons/ dijets in diffraction, photon+jet/dijet. These processes will allow to test various **CGC correlators**

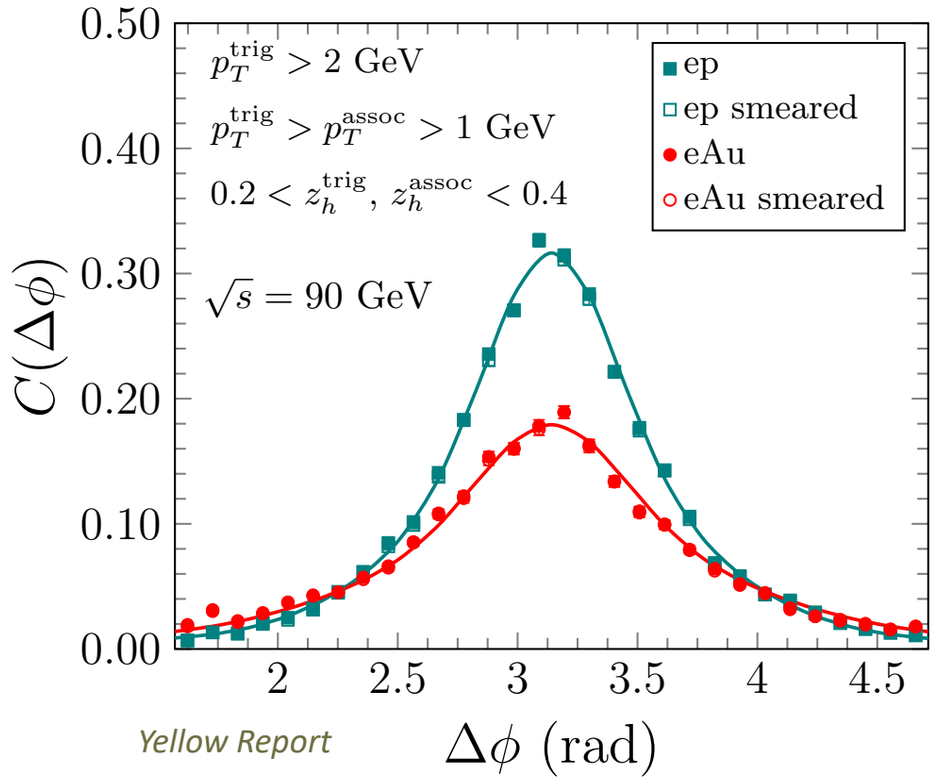

Yellow Report

Diffraction in DIS

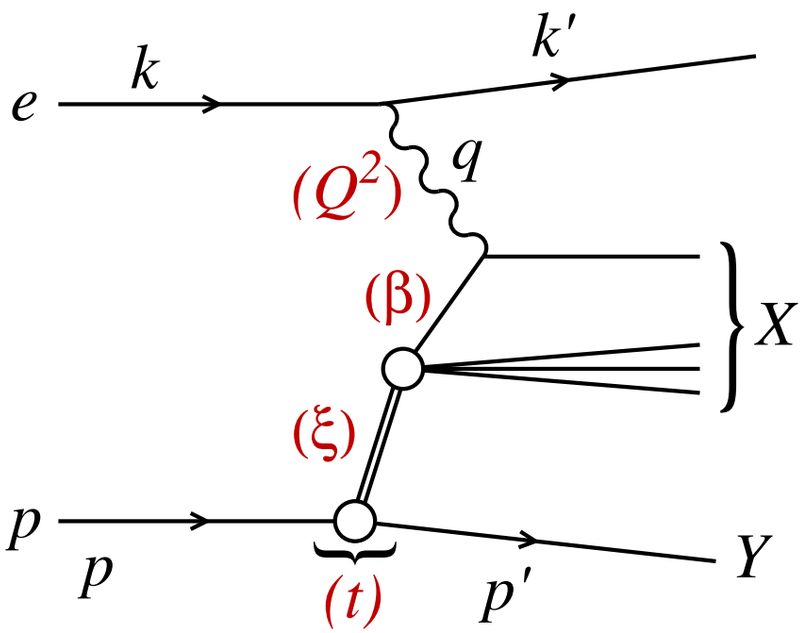

Diffraction: a reaction characterized by a large rapidity gap in the final state

Diffractive DIS variables:

$$\xi \equiv x_{IP} = \frac{Q^2 + M_X^2 - t}{Q^2 + W^2}$$

$$x = \xi\beta$$

momentum fraction of the Pomeron w.r.t hadron

$$\beta = \frac{Q^2}{Q^2 + M_X^2 - t}$$

momentum fraction of parton w.r.t Pomeron

$$t = (p - p')^2$$

4-momentum transfer squared

Why diffraction ?

- Dynamics of **color singlet** object (Pomeron). Relation to confinement
- Sensitivity to **gluon** content, **low** x dynamics and **saturation**
- Relation to **shadowing**
- Limits of **factorization** and **universality** of diffractive PDFs

In nuclei

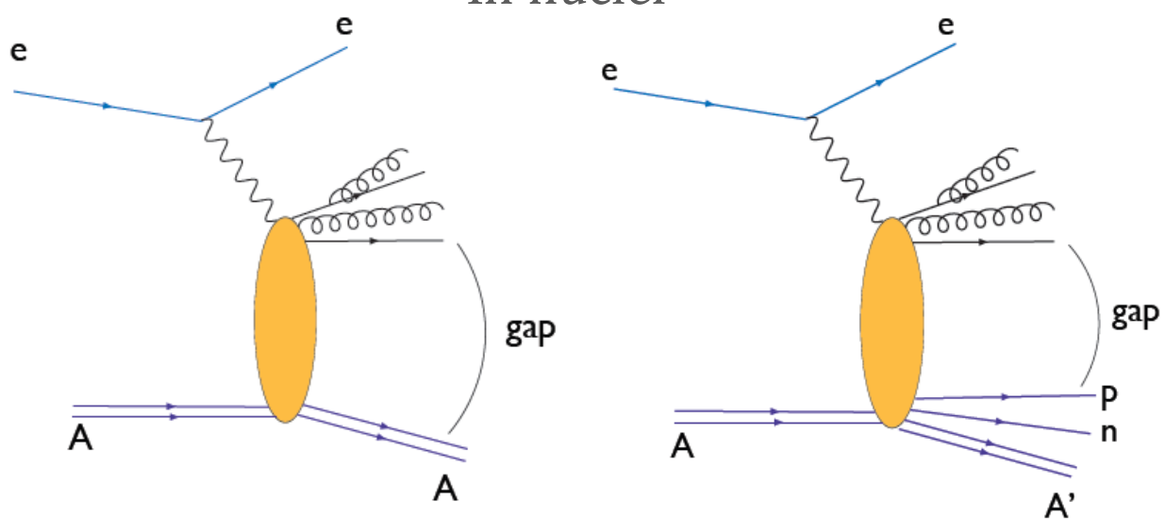

coherent incoherent

Scattering at ep collider HERA

Non-diffractive DIS event

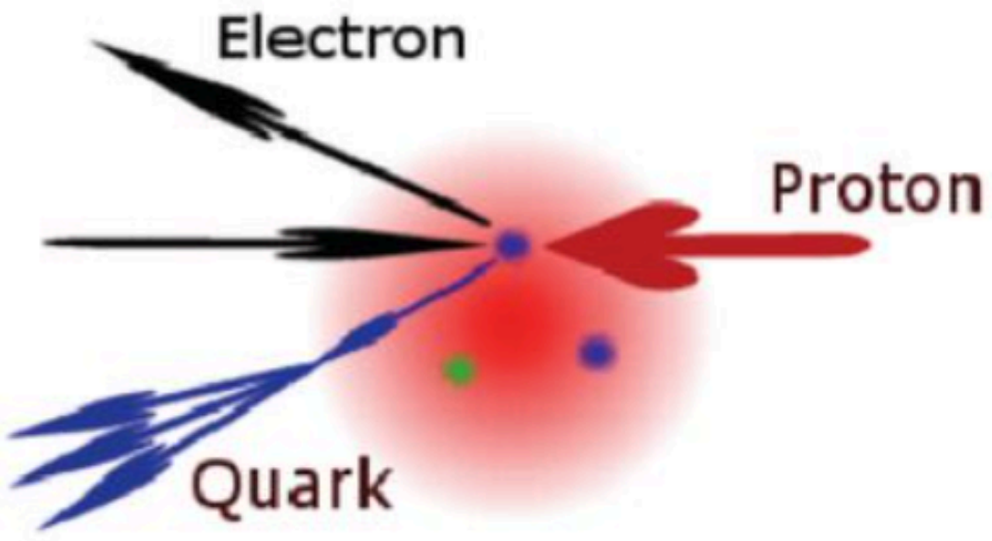

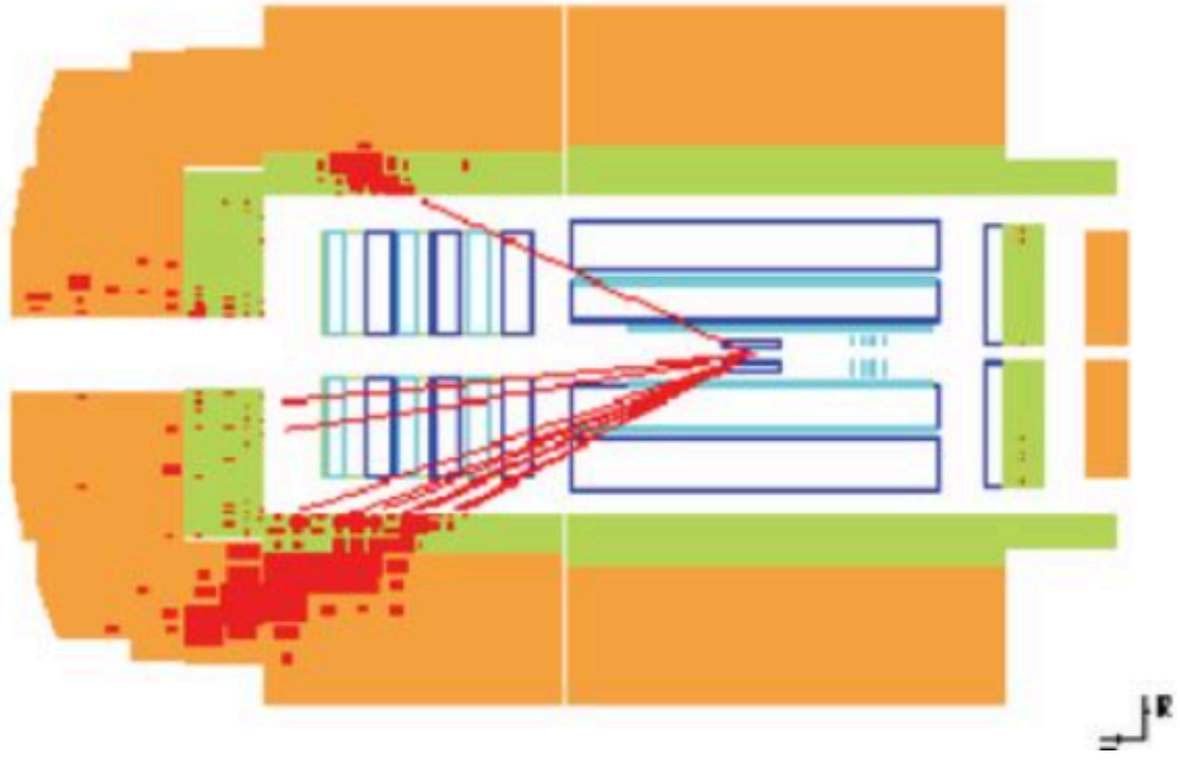

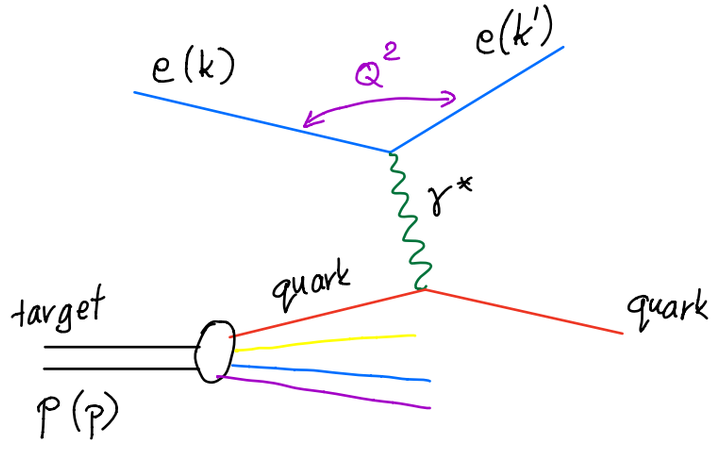

Diffraction at HERA

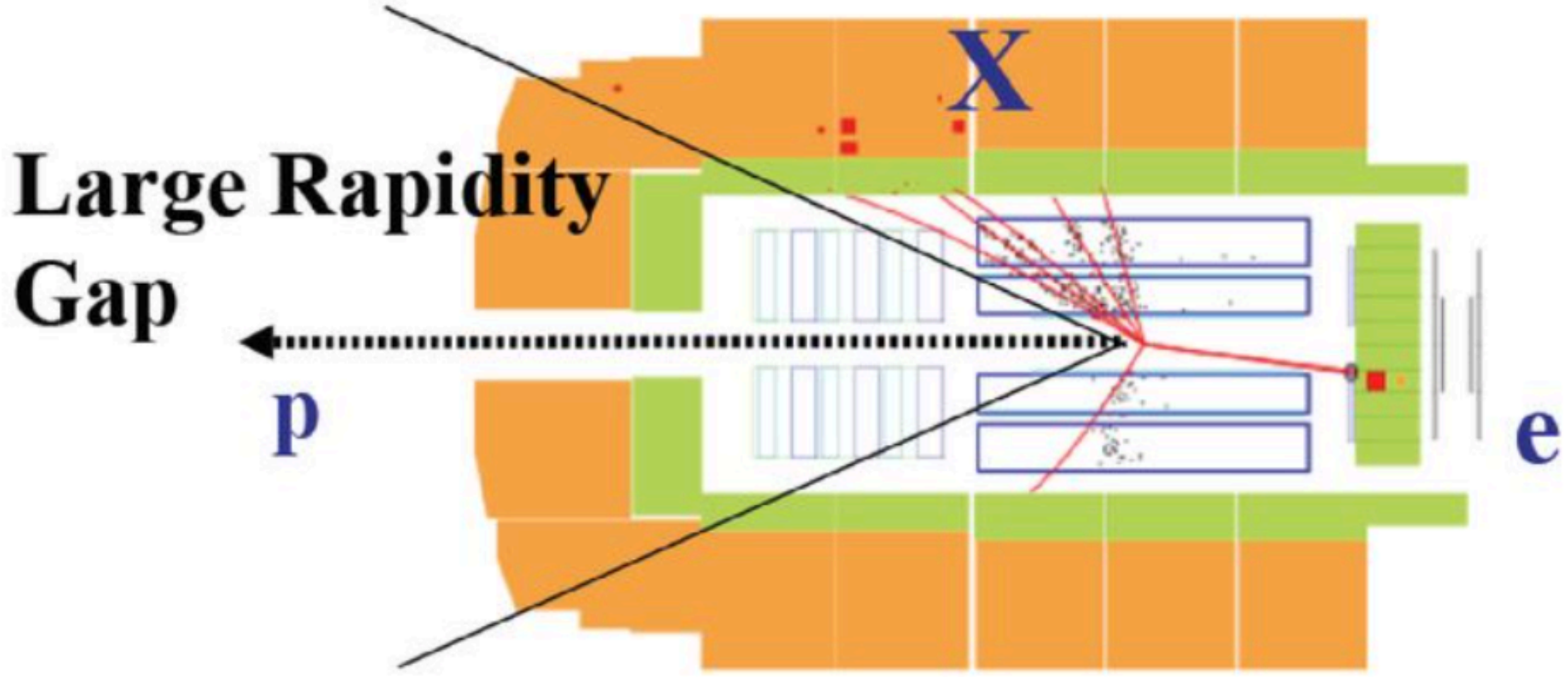

10% events at HERA were of diffractive type

Large portion of the detector void of any particle activity: **rapidity gap**

Proton stays intact despite undergoing violent collision with a 50 TeV electron (in its rest frame)

Phase space (x,Q^2) EIC–HERA in diffraction

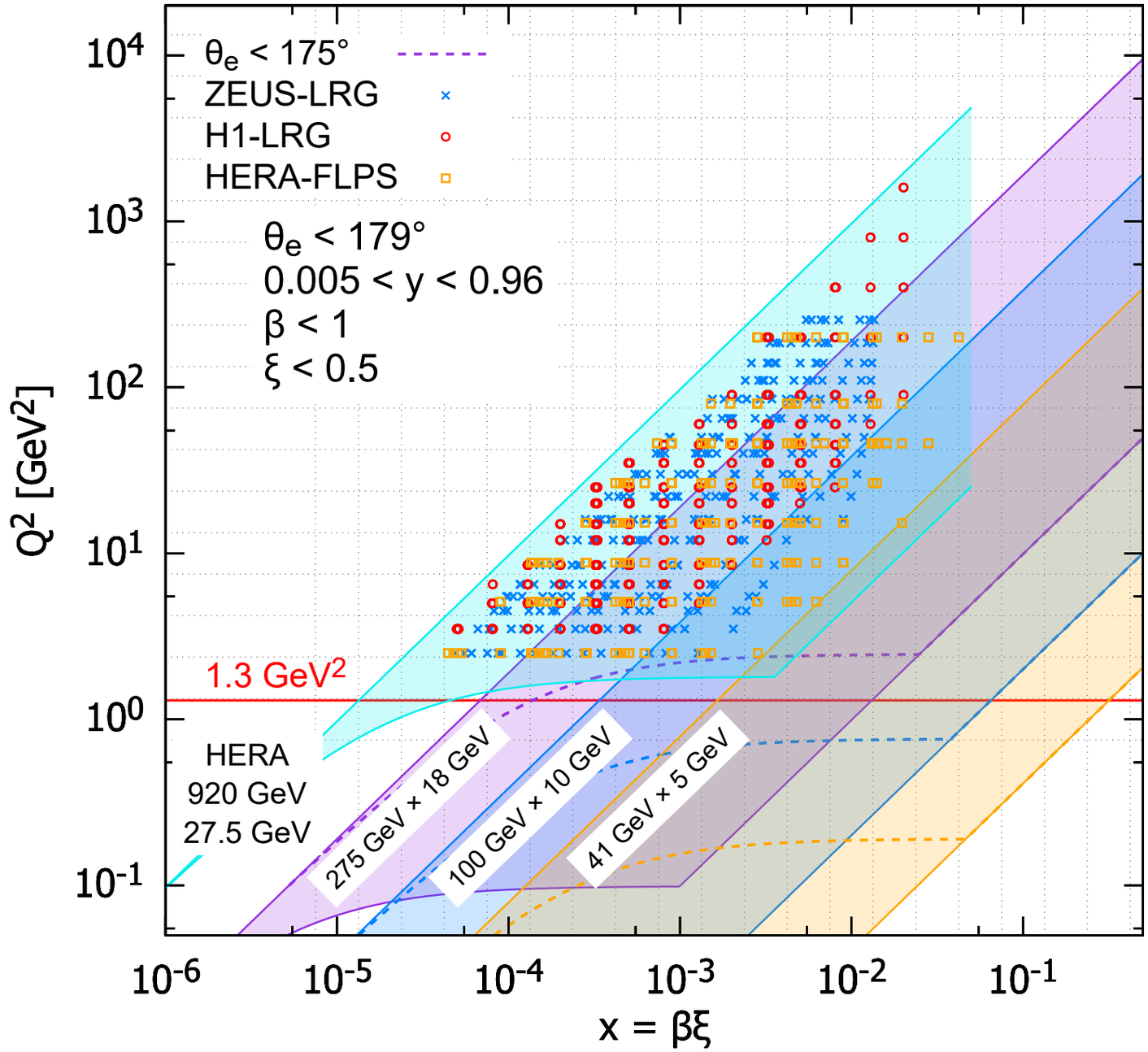

Rapidity range at EIC in diffraction

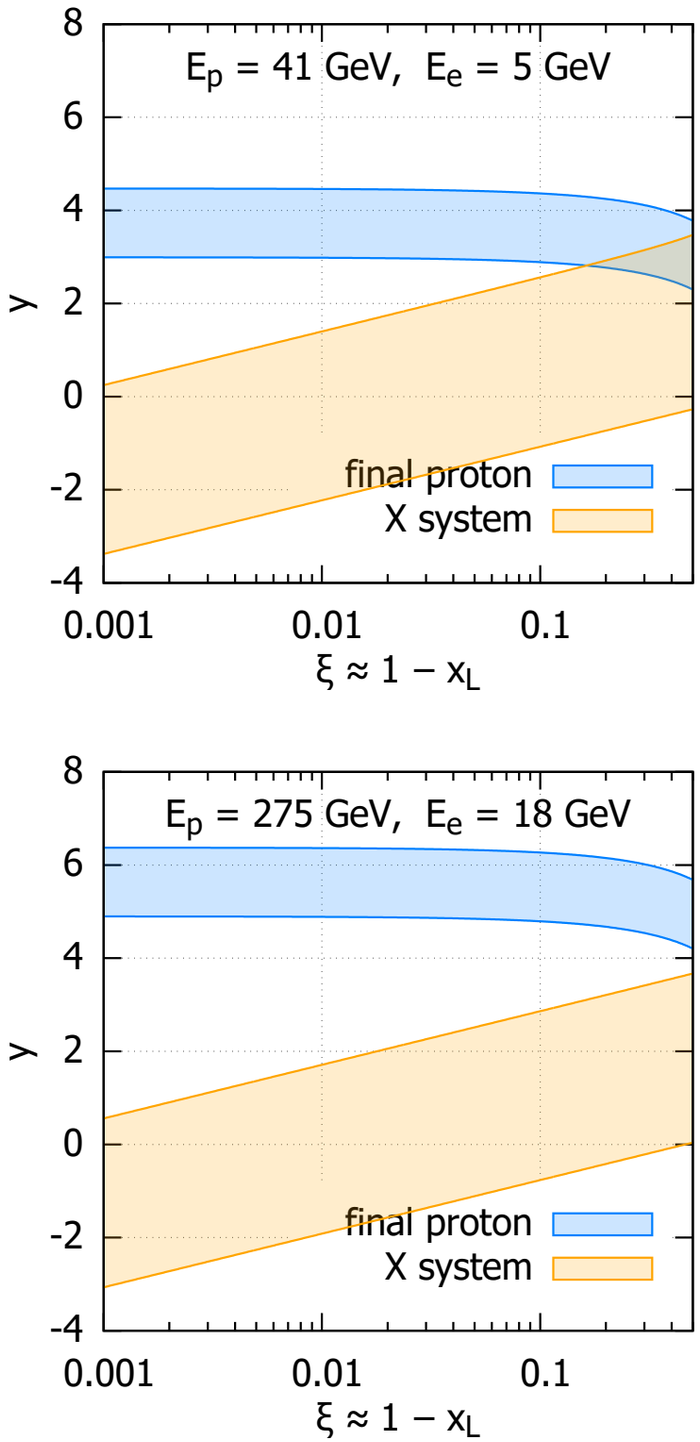

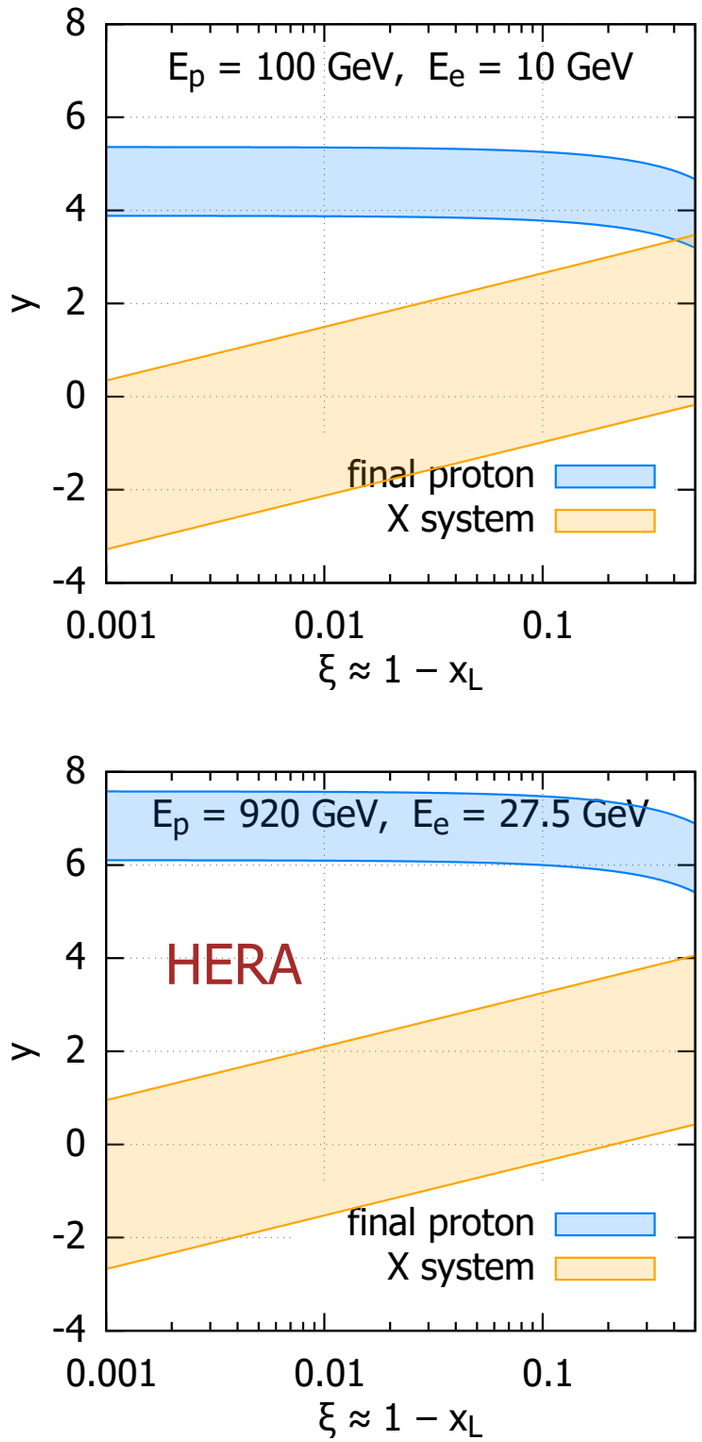

Rapidity range of proton and undecayed diffractive system X

$p_T^{proton} < 4\,\mathrm{GeV}$

$0.1 < \beta < 0.9$

$0.005 < y < 0.96$

HERA: LRG method reliable for gaps > 3 units of rapidity

EIC: fairly large gaps ($\Delta\eta \geq 4$) exist for smallest ξ and largest s

However, through most region LRG method may be challenging at EIC

Far forward detectors at EIC

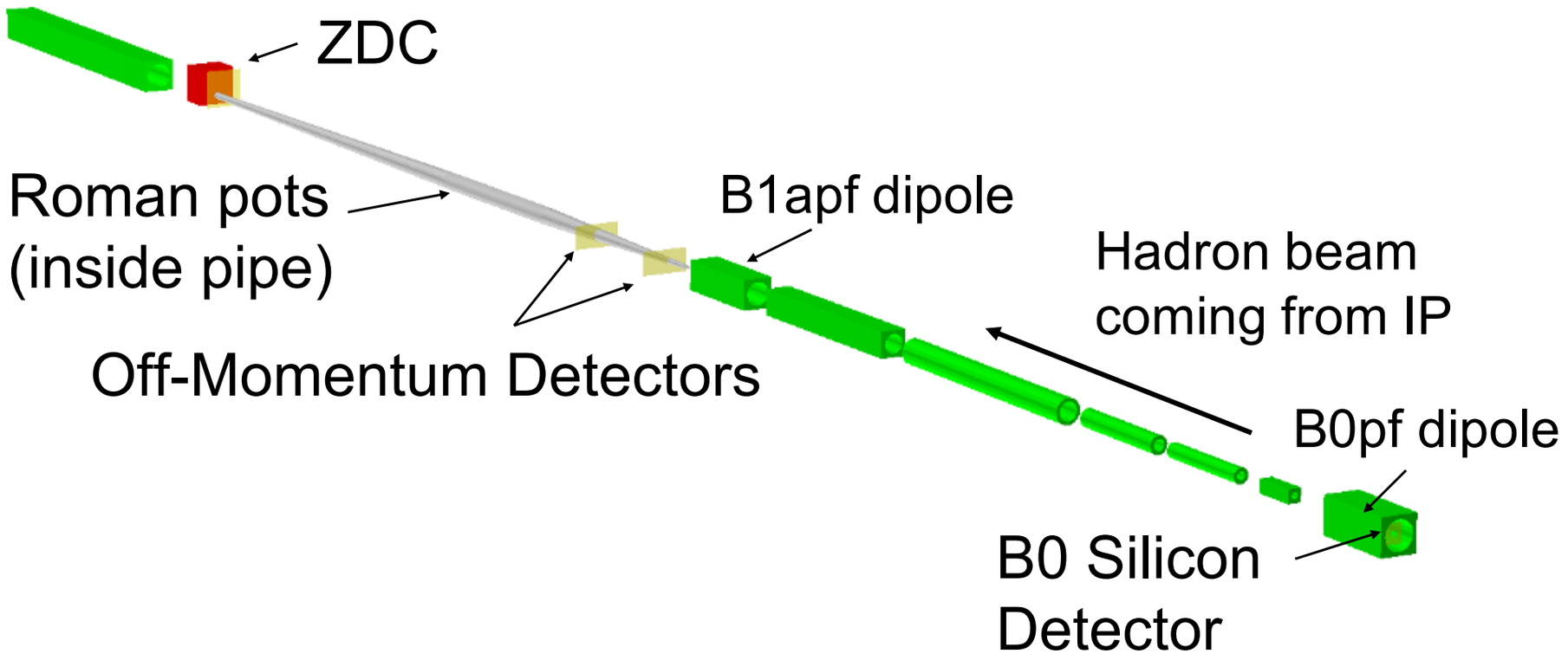

Detector	Angle	Position [m]
ZDC	$\theta<5.5$ mrad	37.5
Roman Pots	$0.5<\theta<5.0$ mrad	26.0, 28.0
Off-momentum detectors	$\theta<5.0$ mrad	22.5, 25.5
B0	$6.0<\theta<20.0$ mrad	$5.4<z<6.4$

Final proton tagging

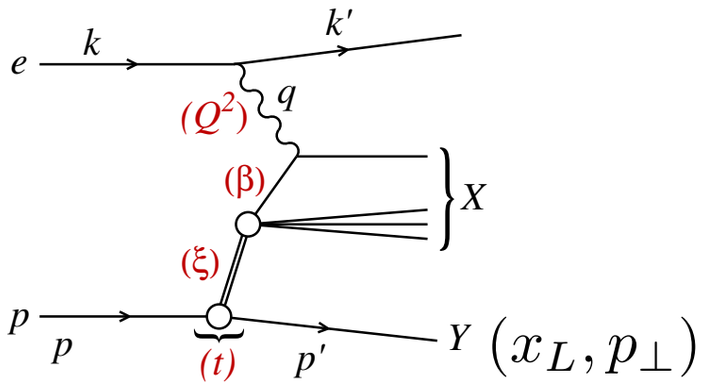

Small angle acceptance i.e. Roman pots

$(x_L, p_\perp, \theta)$ measured in LAB, collinear (e,p) frame

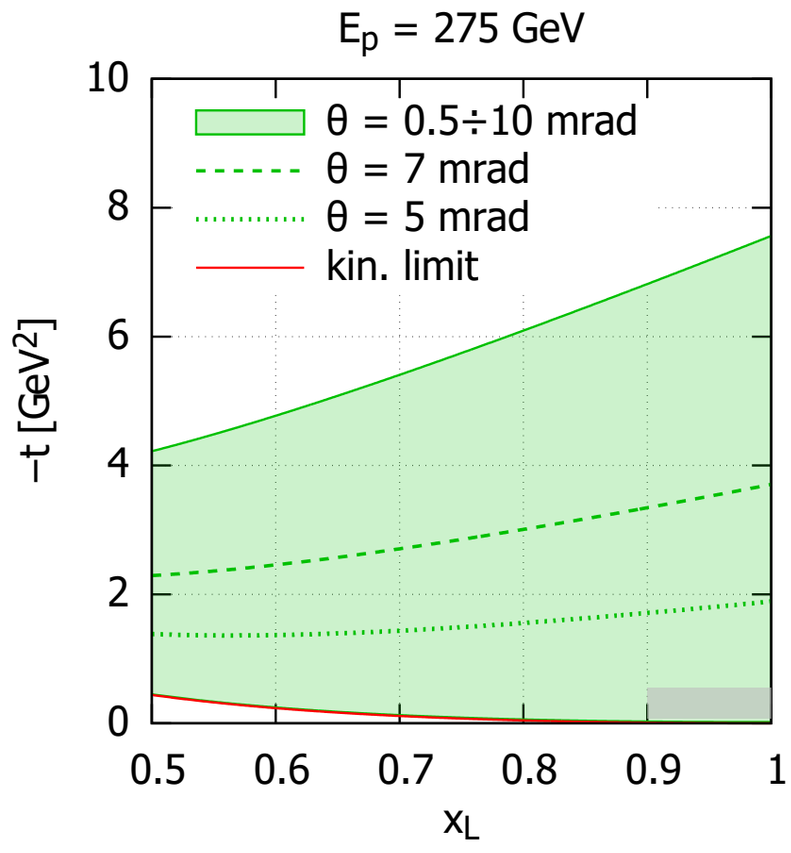

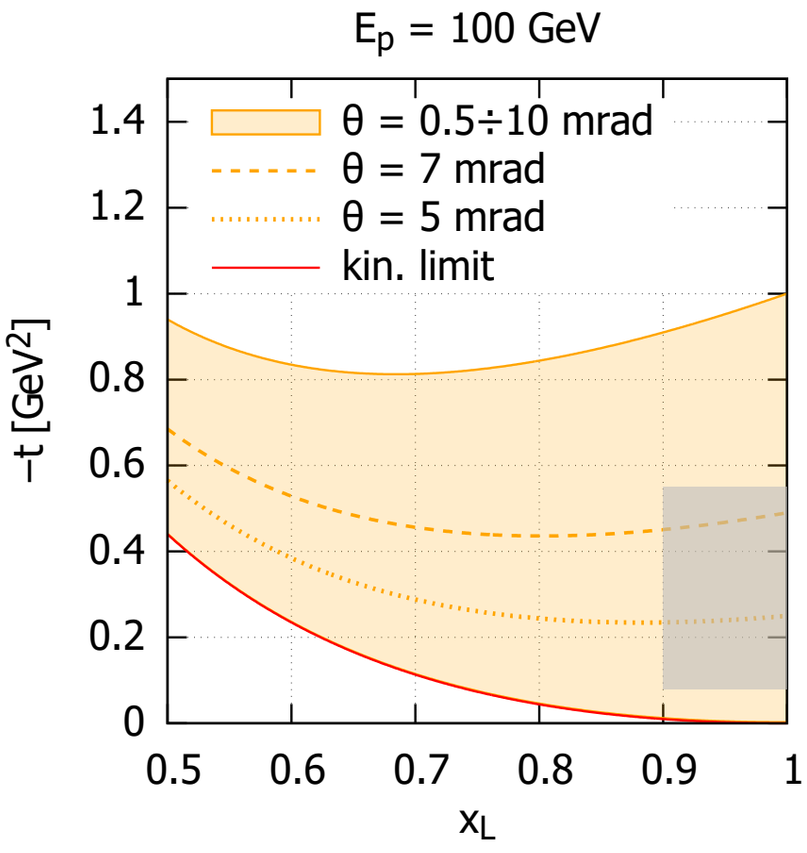

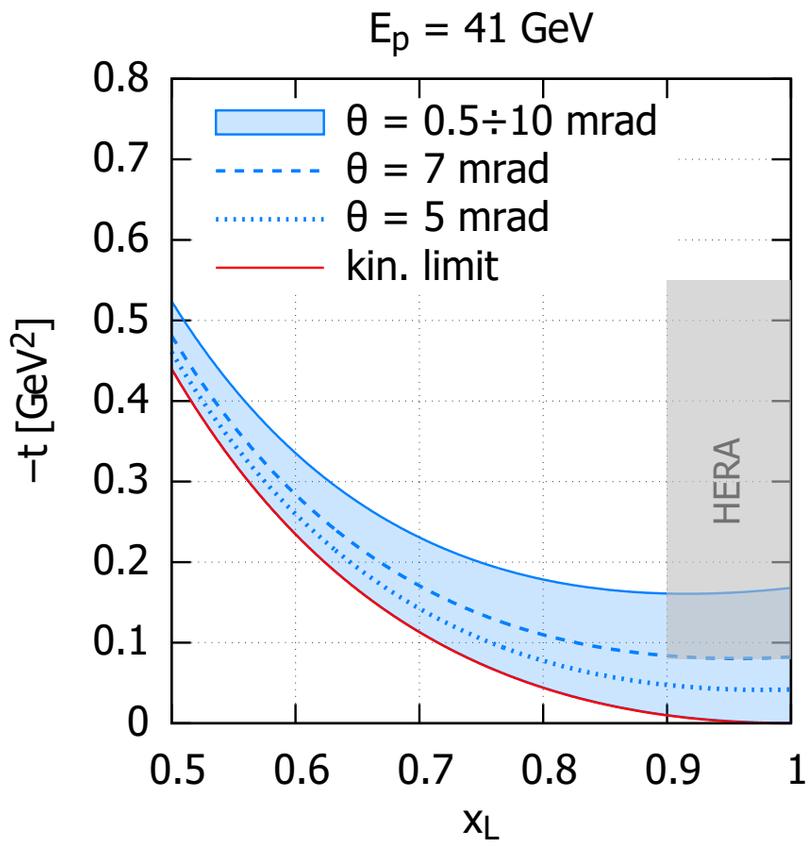

Much better than at HERA

Best way to select diffractive events through proton tagging

$$t = -\frac{p_\perp^2}{x_L} - \frac{(1-x_L)^2}{x_L} m_p^2$$

Diffractive cross section, structure functions

Diffractive cross section depends on 4 variables (ξ,β,Q^2,t):

$$\frac{d^4\sigma^D}{d\xi d\beta dQ^2 dt} = \frac{2\pi\alpha_{\rm em}^2}{\beta Q^4} Y_+ \sigma_{\rm r}^{\rm D(4)}(\xi,\beta,Q^2,t)$$

$$Y_+ = 1 + (1-y)^2$$

Reduced cross section depends on two structure functions:

$$\sigma_{\rm r}^{\rm D(4)}(\xi,\beta,Q^2,t) = F_2^{\rm D(4)}(\xi,\beta,Q^2,t) - \frac{y^2}{Y_+} F_L^{\rm D(4)}(\xi,\beta,Q^2,t)$$

Upon integration over t:

$$F_{2,L}^{\rm D(3)}(\xi,\beta,Q^2) = \int_{-\infty}^{0} dt\, F_{2,L}^{\rm D(4)}(\xi,\beta,Q^2,t)$$

Dimensions:

$[\sigma_{\rm r}^{\rm D(4)}] = {\rm GeV}^{-2}$

$\sigma_{\rm r}^{\rm D(3)}$ Dimensionless

When $y \ll 1$

$$\sigma_{\rm r}^{\rm D(4,3)} \simeq F_2^{\rm D(4,3)}$$

Pseudodata generation: collinear factorization for diffraction

Use the collinear factorization for the description of HERA and pseudodata simulation

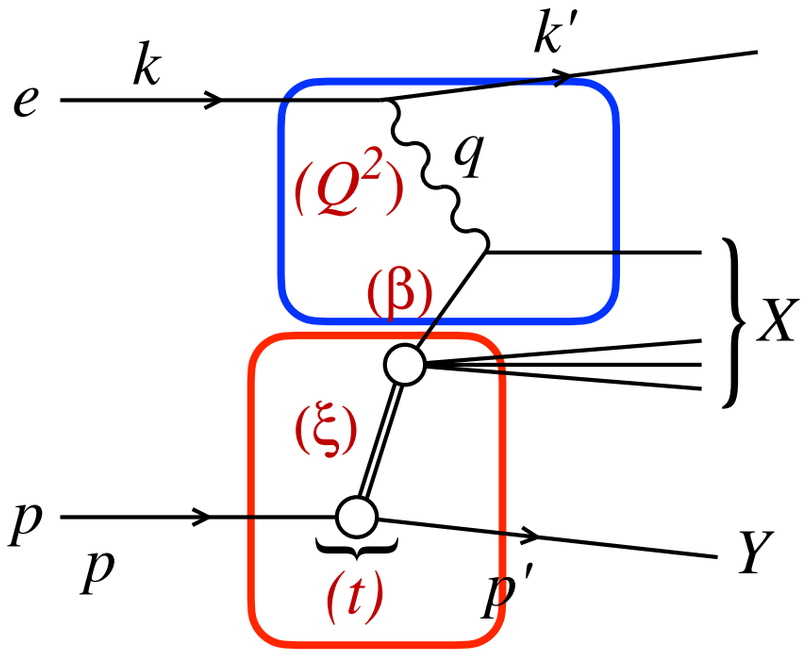

Collins

Collinear factorization in diffractive DIS

$$F_{2/L}^{D(4)}(\beta,\xi,Q^2,t) = \sum_i \int_\beta^1 \frac{dz}{z}\, C_{2/L,i}\left(\frac{\beta}{z},Q^2\right)\, f_i^{\mathrm{D}}(z,\xi,Q^2,t)$$

- Diffractive cross section can be factorized into the convolution of the perturbatively calculable partonic cross sections and diffractive parton distributions (DPDFs).
- The DPDFs represent (at least in LO) the probability distributions for partons i in the proton under the constraint that the proton is scattered into the system Y with a specified 4-momentum.

Model for diffractive structure functions

Regge factorization with Pomeron terms works for small ξ<0.01

At higher ξ additional exchanges `Reggeons' need to be included

$$f_i^{\mathrm{D}(4)}(z,\xi,Q^2,t) = f_{I\!P}^{p}(\xi,t)\, f_i^{I\!P}(z,Q^2) + f_{I\!R}^{p}(\xi,t)\, f_i^{I\!R}(z,Q^2)$$

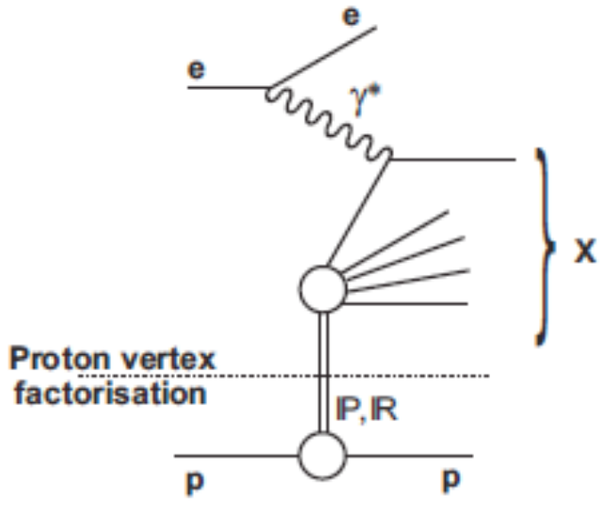

Regge type flux:

$$f_{I\!P,I\!R}^{p}(\xi,t) = A_{I\!P,I\!R}\frac{e^{B_{I\!P,I\!R}t}}{\xi^{2\alpha_{I\!P,I\!R}(t)-1}}$$

Trajectory:

$$\alpha_{I\!P,I\!R}(t) = \alpha_{I\!P,I\!R}(0) + \alpha'_{I\!P,I\!R}\, t.$$

For t-integrated case

$$f_i^{\mathrm{D}(3)}(z,\xi,Q^2) = \phi_{I\!P}^{p}(\xi)\, f_i^{I\!P}(z,Q^2) + \phi_{I\!R}^{p}(\xi)\, f_i^{I\!R}(z,Q^2)$$

Integrated flux:

$$\phi_{I\!P,I\!R}^{p}(\xi) = \int dt\; f_{I\!P,I\!R}^{p}(\xi,t)$$

Pomeron PDFs obtained via NLO DGLAP evolution starting at initial scale μ_0^2=1.8 GeV^2

$$z f_i(z,\mu_0^2) = A_i z^{B_i}(1-z)^{C_i} \qquad \text{k=q,g}$$

Pseudodata for $\sigma^{D(3)}$ in ep at EIC

Armesto, Newman, Slominski, Stasto

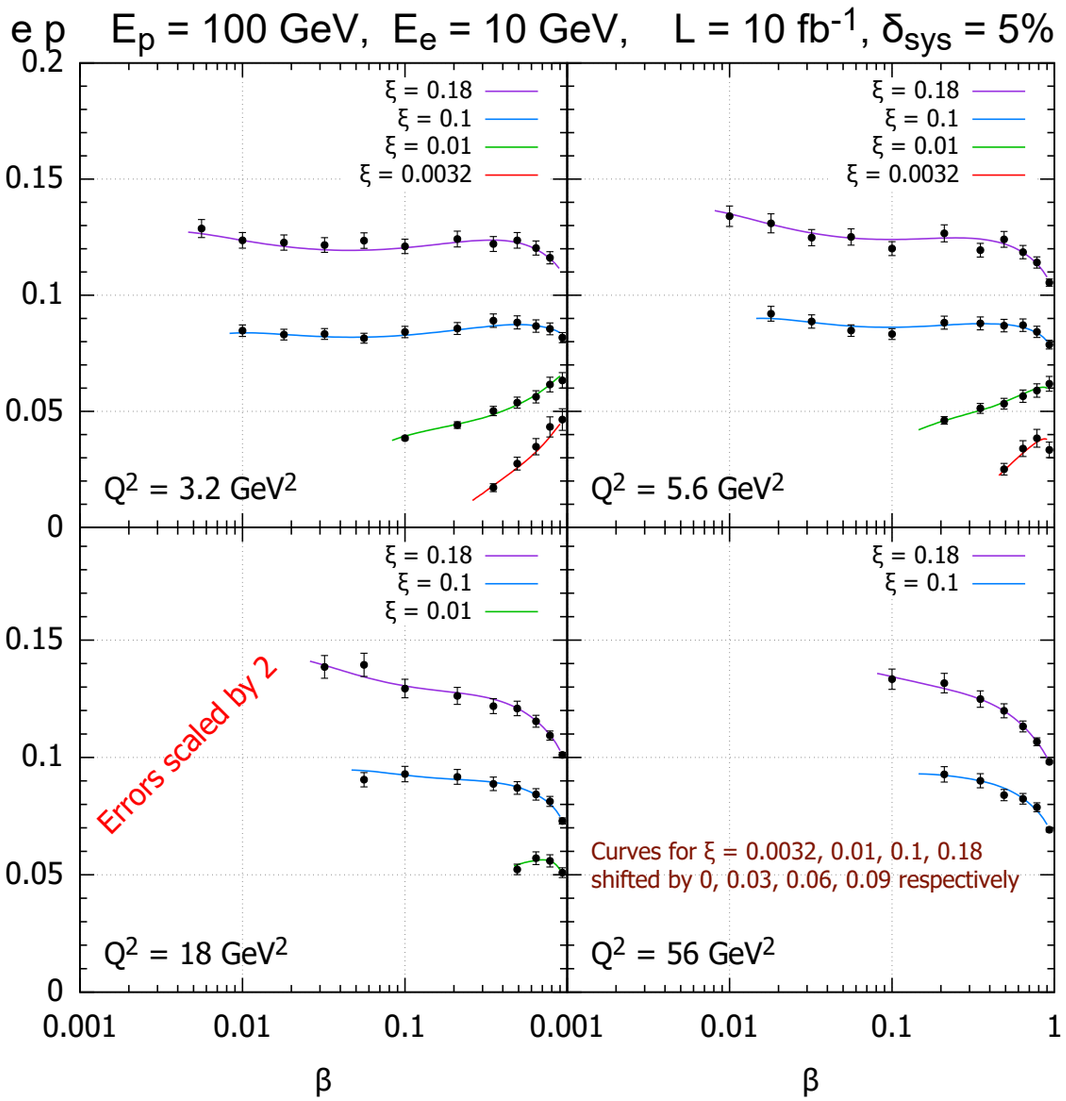

In total:

482 points for $1.3 < Q^2 < 1330\ \mathrm{GeV}^2$

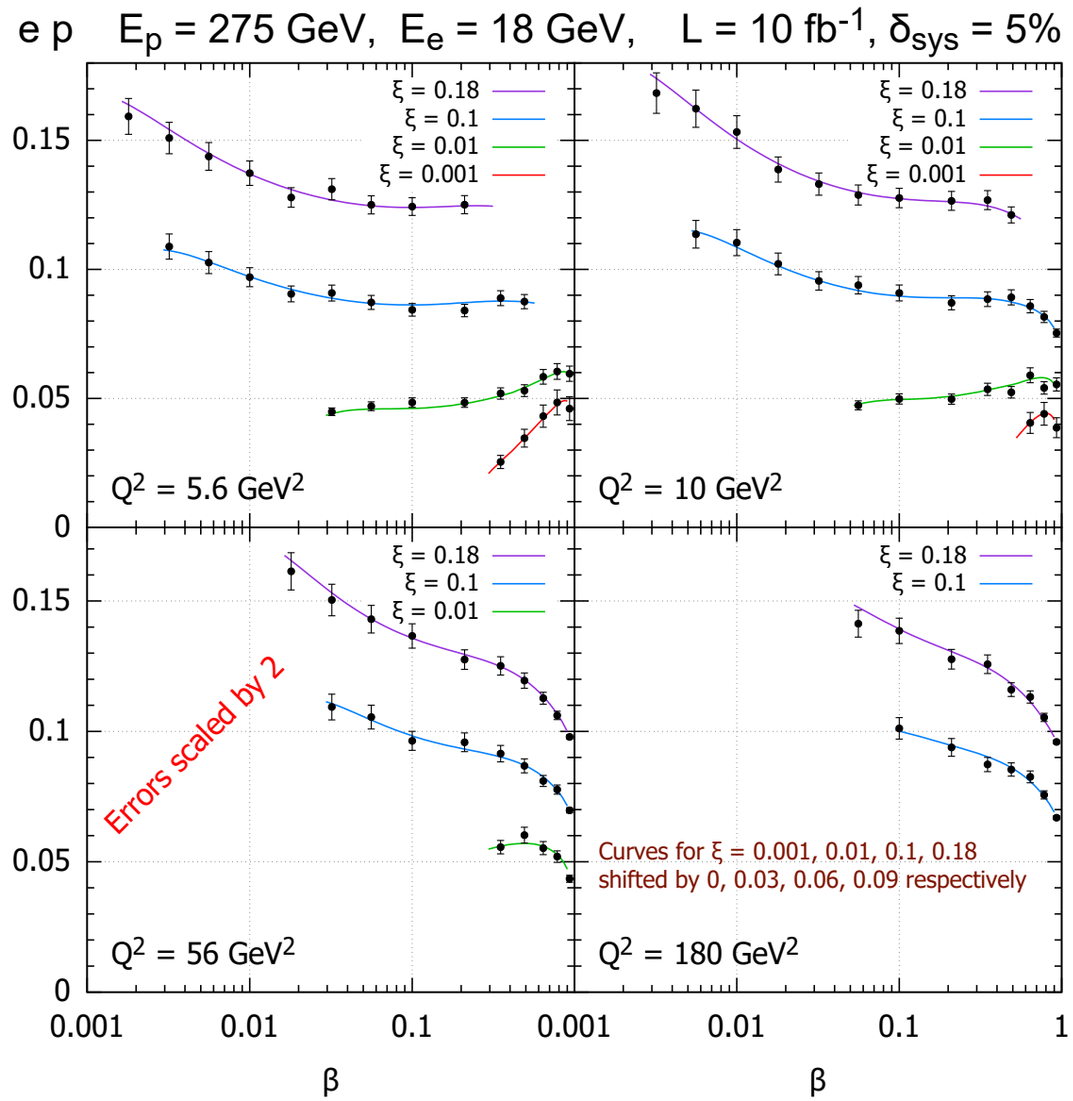

In total:

792 points for $1.3 < Q^2 < 4220\ \mathrm{GeV}^2$

Diffractive PDFs from EIC

Extraction of quark DPDF in bins of

Q^2 as a function of z

Reduction of uncertainty from HERA possible

Particularly constraints on quark at large z

Combining with diffractive dijet measurements, constraints on gluons possible

Similar precision for nuclei possible

Disentangle Pomeron & Reggeon (see later)

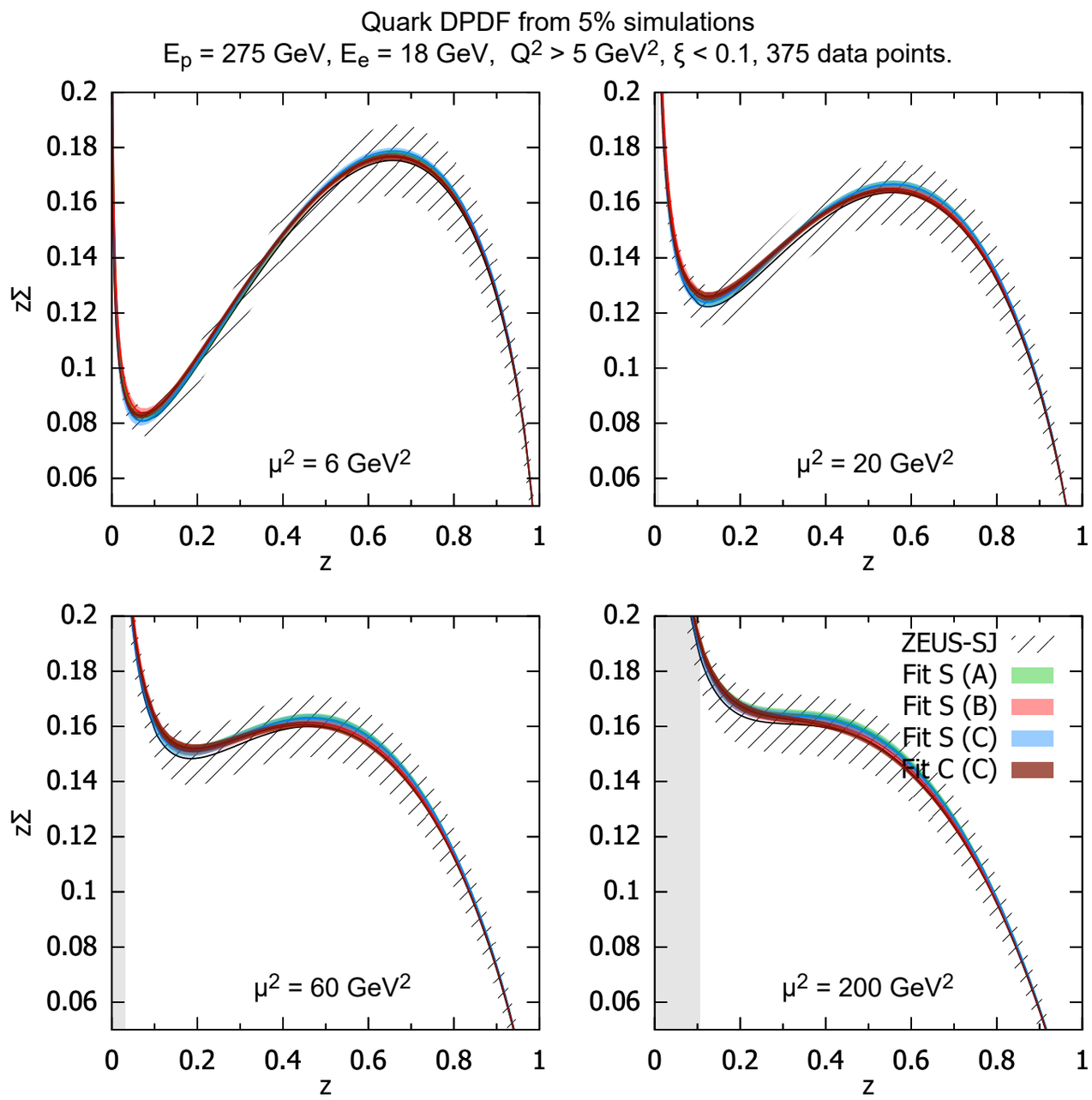

Armesto, Newman, Slominski, Stasto

Possibilities for $F_L^{D(3)}$ at EIC

Why F_L^D is interesting?

$$\sigma_{\mathrm{r}}^{\mathrm{D}(3)} = F_2^{\mathrm{D}(3)} - \frac{y^2}{Y_+} F_L^{\mathrm{D}(3)}$$

F_L^D vanishes in the parton model

Gets non-vanishing contributions in QCD

As in inclusive case, particularly sensitive to the diffractive **gluon density**

Expected large **higher twists**, provides test of the **non-linear, saturation** phenomena

Experimentally challenging…

Measurement requires several beam energies

F_L^D strongest when $y \to 1$. Low electron energies

H1 measurement: 4 energies, E_p=920, 820, 575, 460 GeV, electron beam E_e=27.6 GeV

Large errors, limited by statistics at HERA

Careful evaluation of systematics. Best precision 4%, with uncorrelated sources as low as 2%

$F_L^{D(3)}$ at HERA

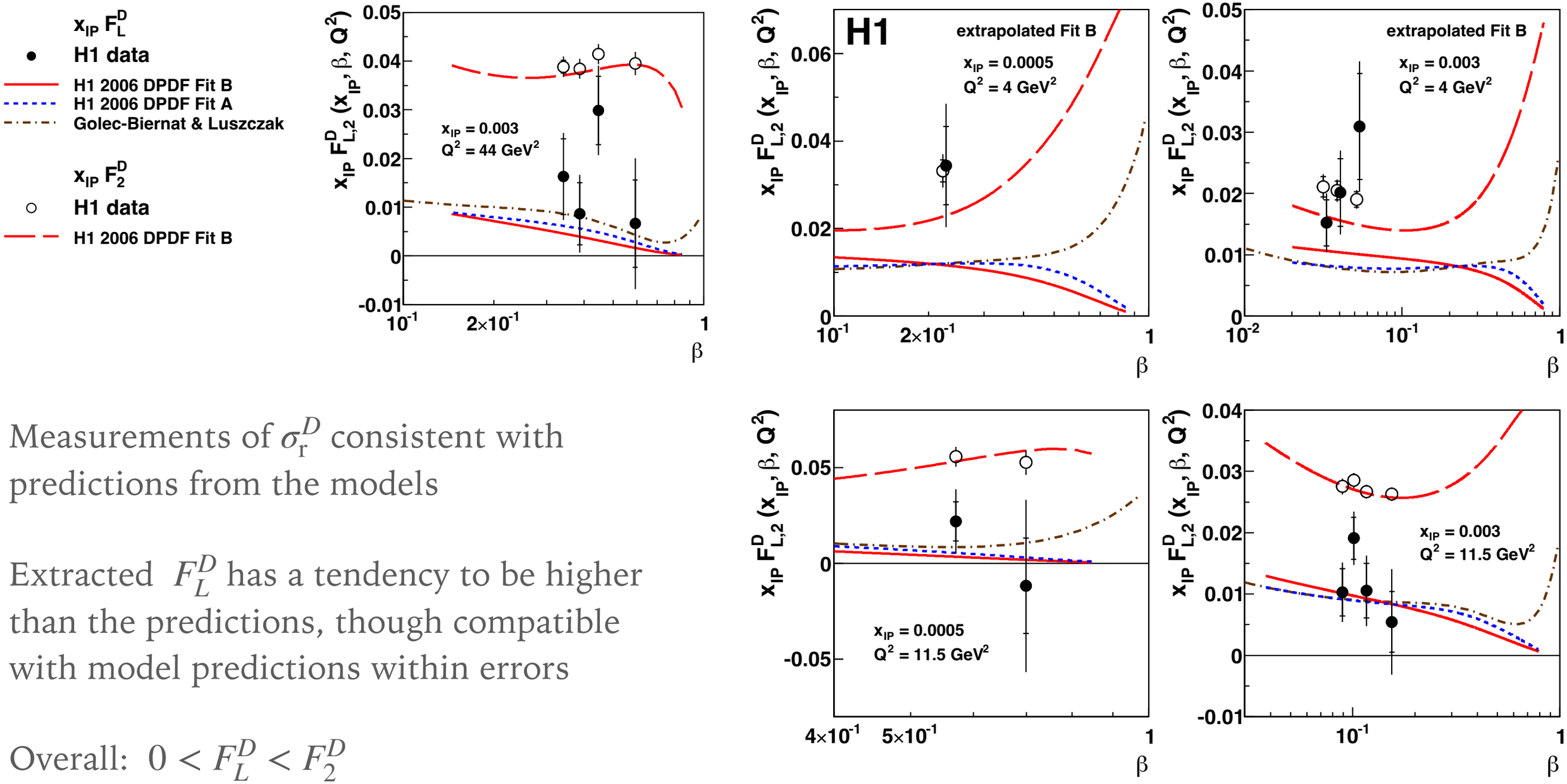

Measurements of σ_r^D consistent with predictions from the models

Extracted F_L^D has a tendency to be higher than the predictions, though compatible with model predictions within errors

Overall: $0 < F_L^D < F_2^D$

Pseudodata generation: energy choice

$$\sigma_{\mathrm{red}}^{\mathrm{D}(3)} = F_2^{\mathrm{D}(3)}(\beta,\xi,Q^2) - Y_{\mathrm{L}}\, F_{\mathrm{L}}^{\mathrm{D}(3)}(\beta,\xi,Q^2)$$

Integrated over t-momentum transfer

$$Y_{\mathrm{L}} = \frac{y^2}{Y_+} = \frac{y^2}{1+(1-y)^2}$$

Can disentangle $F_2^{D(3)}$ from $F_L^{D(3)}$ by varying energy and performing the linear fit.

$$y = \frac{Q^2}{xs} = \frac{Q^2}{\beta\xi s}$$

Need to vary the energy $\sqrt{s}$ to change y for fixed (β,ξ,Q²)

EIC energies for electron and proton:

$E_e = 5,10,18$ GeV

$E_p = 41,100,120,165,180,275$ GeV

E_e [GeV] \ E_p [GeV]	41	100	120	165	180	275
5	**29**	**45**	49	**57**	60	74
10	40	**63**	69	**81**	85	**105**
18	54	**85**	93	**109**	114	**141**

S-17 all 17 combinations

S-9 9 - bold red

S-5 5 - green (EIC preferred)

$F_L^{D(3)}$ extraction

$\sigma_r = F_2(\xi, \beta, Q^2) - Y_L F_L(\xi, \beta, Q^2)$ as a function of Y_L

Bins in (ξ, β, Q^2)

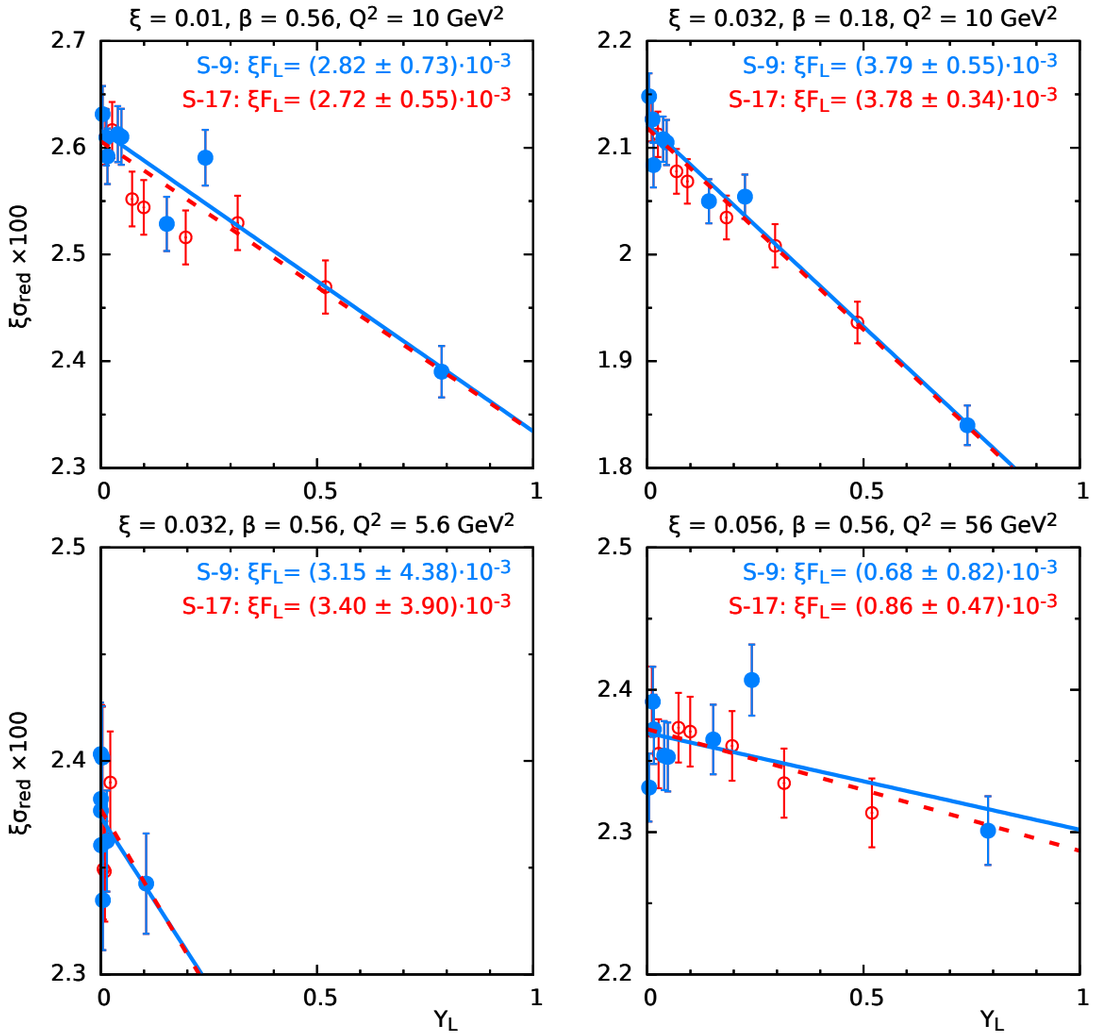

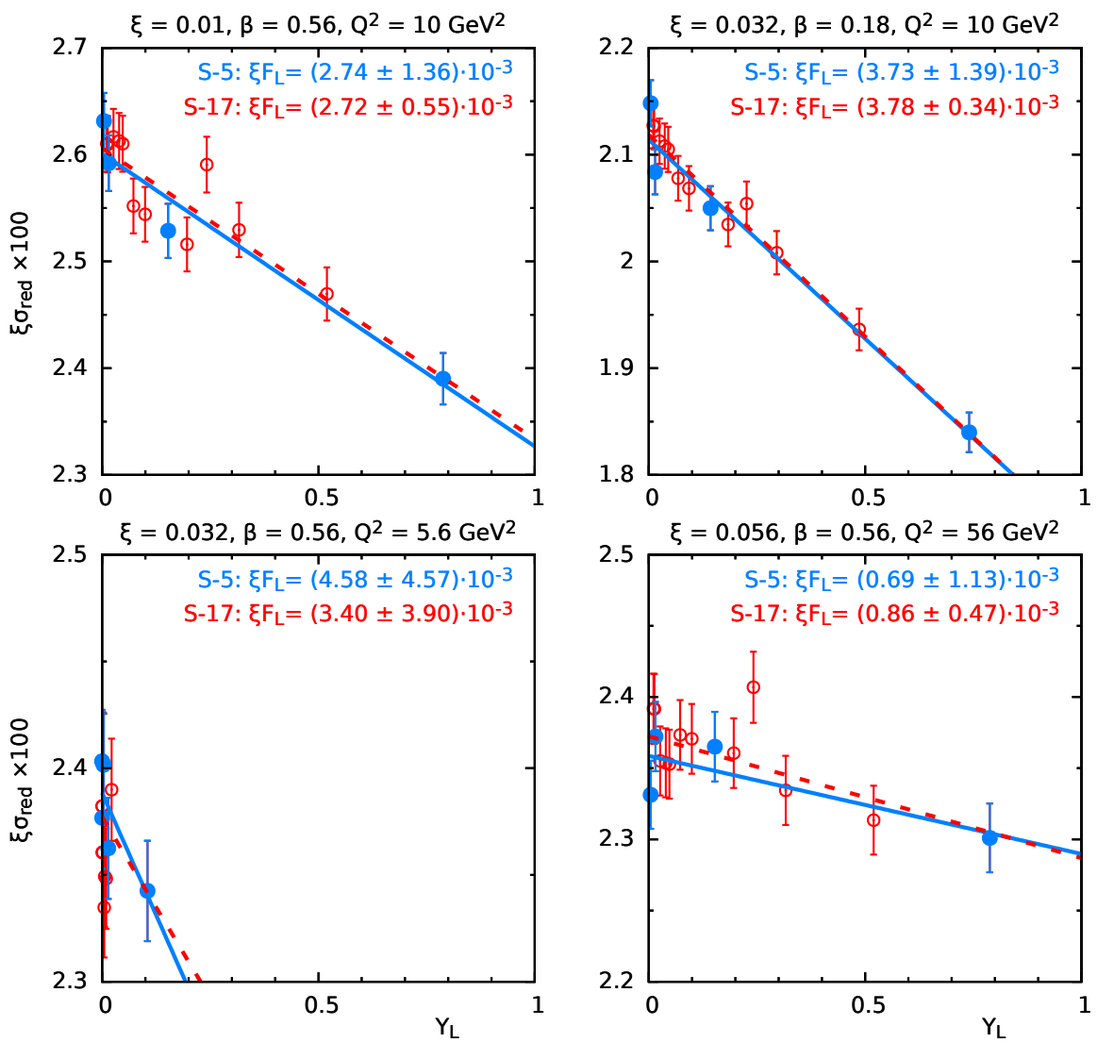

Uncorrelated systematics 1%

Differences between S-17 and S-9, S-5 small

Increase in error bar on the extraction when smaller number of energy points

Largest errors for bins with shortest range of Y_L

Simulated measurement of $F_L^{D(3)}$ vs β in bins of (ξ,Q^2)

Uncorr. systematic error 1%, 5 MC samples to illustrate fluctuations

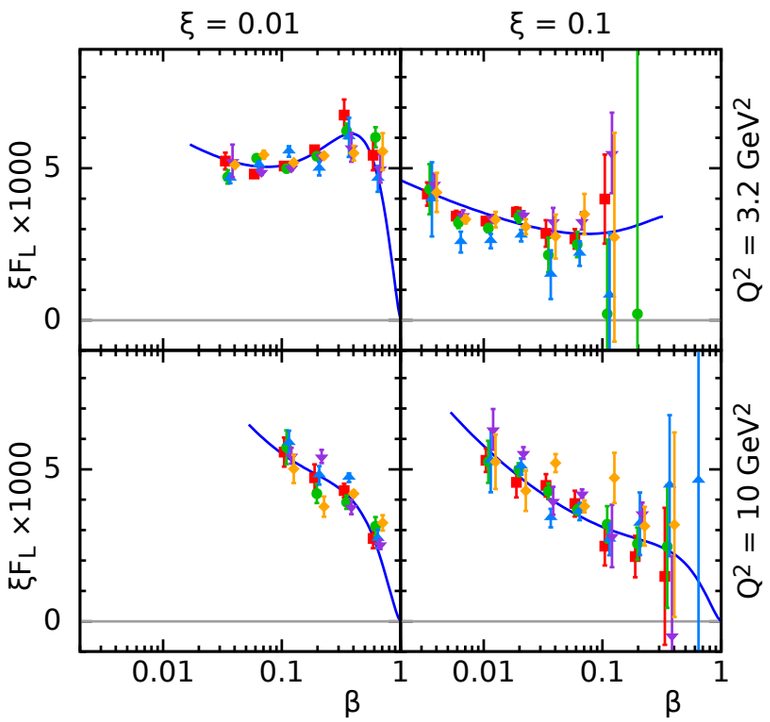

17 energies

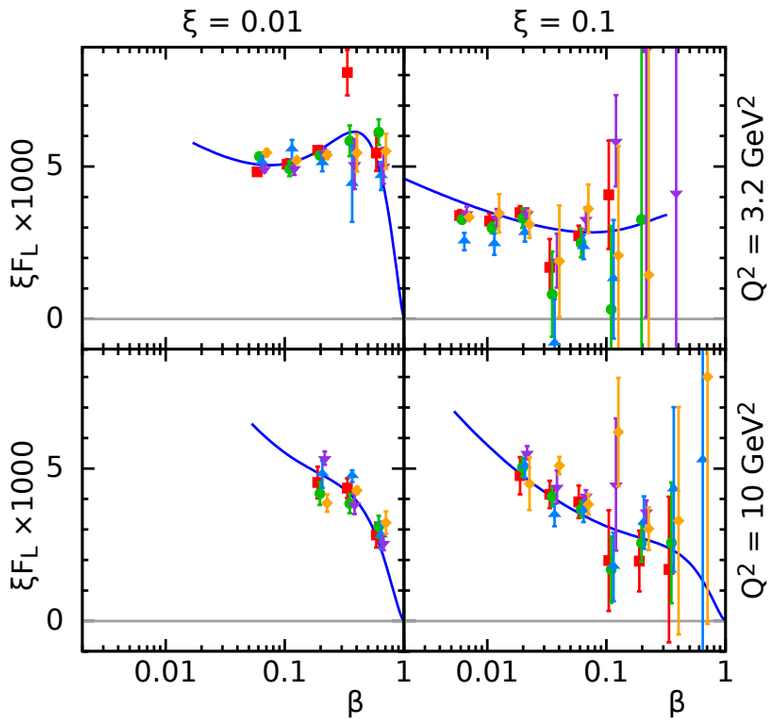

9 energies

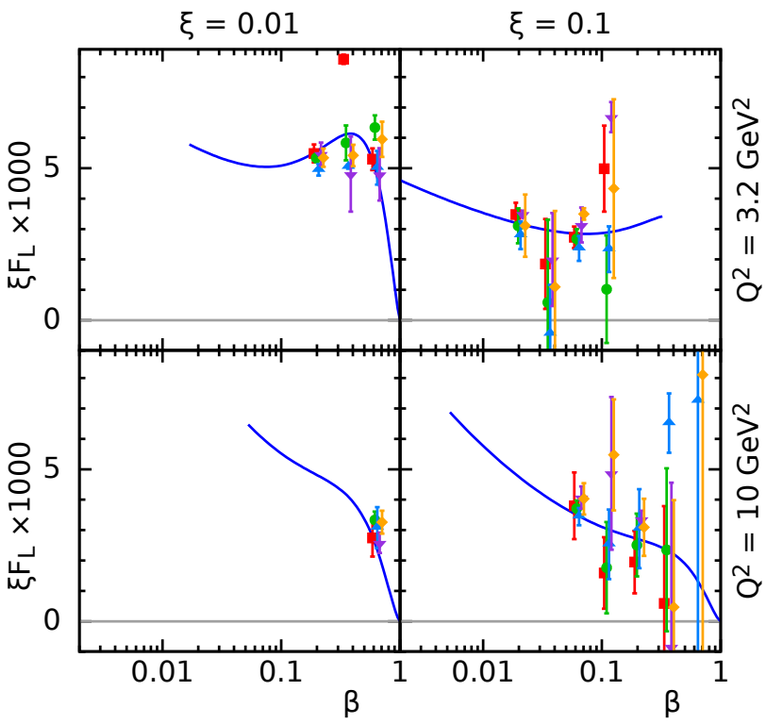

5 energies

Armesto, Newman, Slominski, Stasto

Small differences between S-17 and S-9, small reduction to range and increase in uncertainties.

More pronounced reduction in range and higher uncertainties in S-5.

An extraction of F^D_L possible with EIC-favored set of energy combinations

$F_L^{D(3)}$ fit accuracy

Estimate the accuracy of extraction for $F_L^{D(3)}$

Generate several MC samples of pseudodata and perform fits

Use direct arithmetic averaging

average

$$\bar{v} = \frac{S_1}{N}$$

variance

$$(\Delta v)^2 = \frac{S_2 - S_1^2/N}{N-1}$$

$$S_n = \sum_{i=1}^{N} v_i^n$$

Where v_i is the value of F_L^D

in Monte Carlo sample i

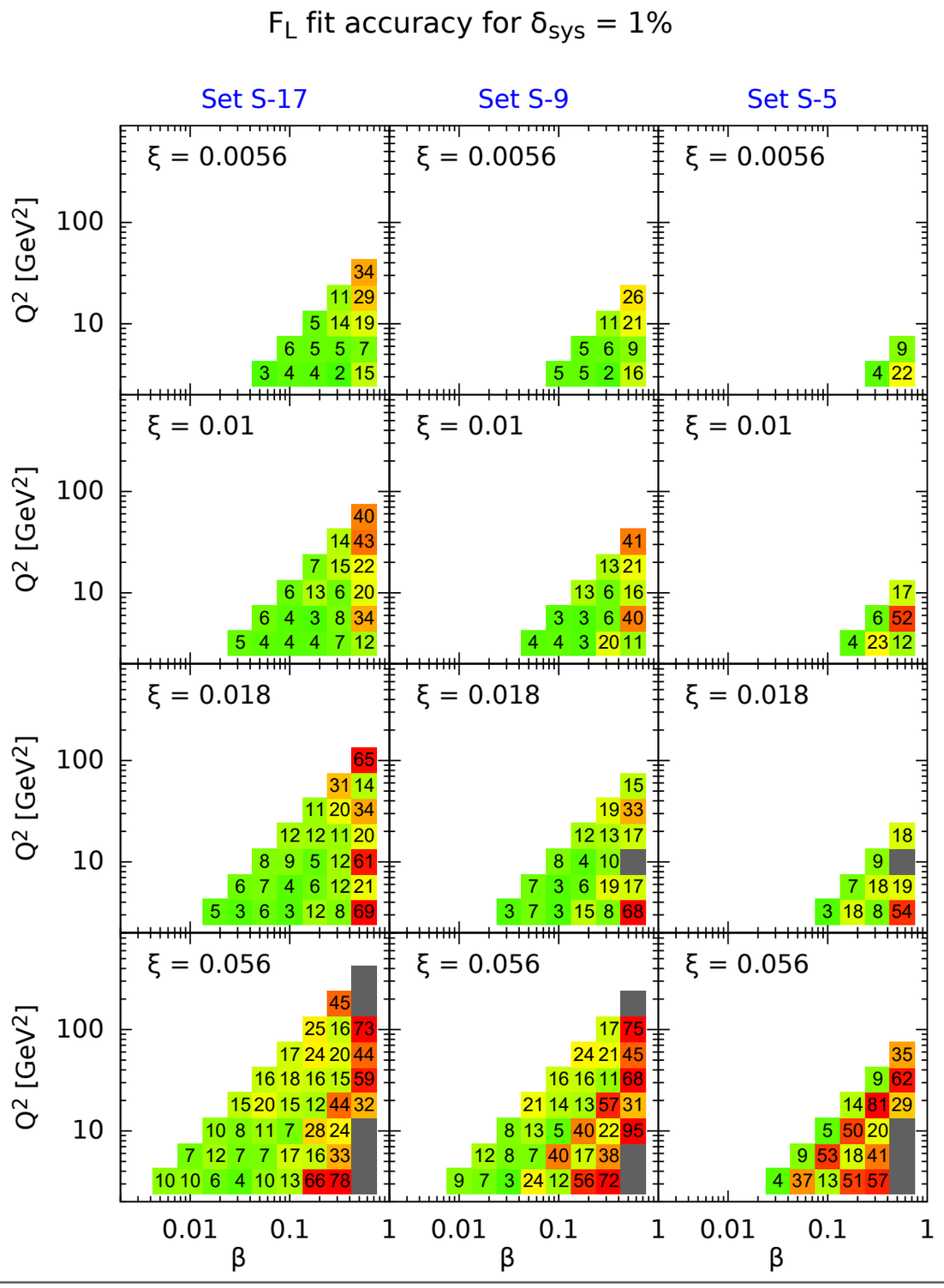

Simulations of $\sigma^{D(4)}$

What can we learn about the t-dependence of the diffractive structure function?

Diffractive cross section depends on 4 variables (ξ,β,Q^2,t):

$$\frac{d^4\sigma^D}{d\xi d\beta dQ^2 dt} = \frac{2\pi\alpha_{\rm em}^2}{\beta Q^4}\, Y_+\, \sigma_{\rm r}^{\rm D(4)}(\xi,\beta,Q^2,t) \qquad Y_+ = 1+(1-y)^2$$

$$d\sigma^{ep\to eXY}(\beta,\xi,Q^2,t) \;=\; \sum_i \int_\beta^1 dz\; d\hat{\sigma}^{ei}\left(\frac{\beta}{z},Q^2\right)\; f_i^{\rm D}(z,\xi,Q^2,t)$$

Ansatz for DPDFs:

$$f_i^{\rm D(4)}(z,\xi,Q^2,t) = f_{I\!P}^{p}(\xi,t)\, f_i^{I\!P}(z,Q^2) + f_{I\!R}^{p}(\xi,t)\, f_i^{I\!R}(z,Q^2)$$

Pomeron *Reggeon*

From the ZEUS-SJ fit

$$\xi\varphi_P(\xi,t) \propto \xi^{-0.22}\, e^{-7|t|}$$

$$\xi\varphi_R(\xi,t) \propto \xi^{0.6+1.8|t|}\, e^{-2|t|}$$

Very different slopes in t for Reggeon and Pomeron

At HERA Reggeon part could not be extracted precisely.

Is it possible to disentangle Pomeron/ Reggeon at EIC ?

$\sigma^{D(4)}$ vs t

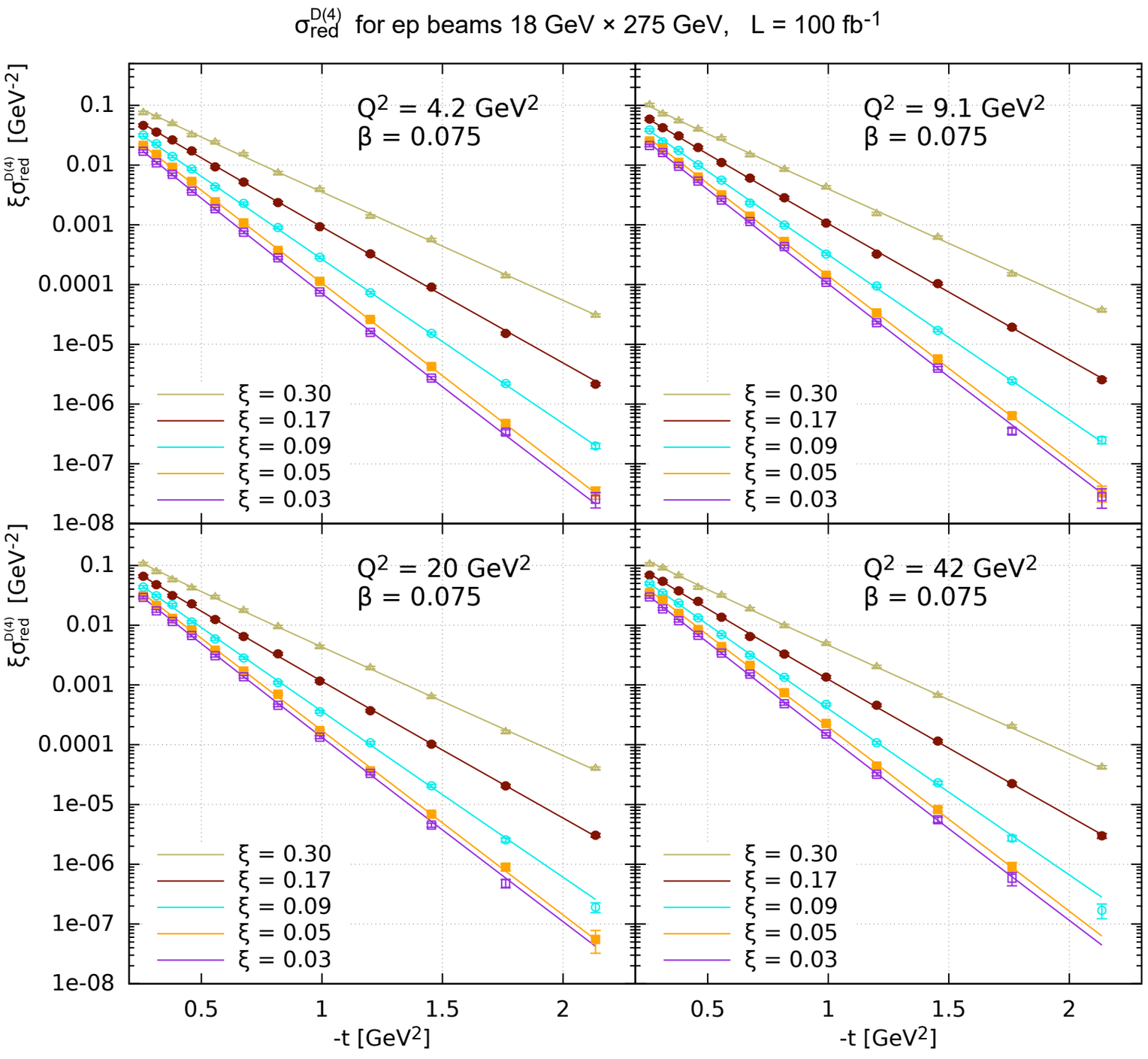

$E_e = 18\,\text{GeV}$

$E_p = 275\,\text{GeV}$

Lines-extrapolation

Points-simulation

Prospects for the very good measurement of the t-slope as a function of ξ

$\sigma^{D(4)}$ vs ξ

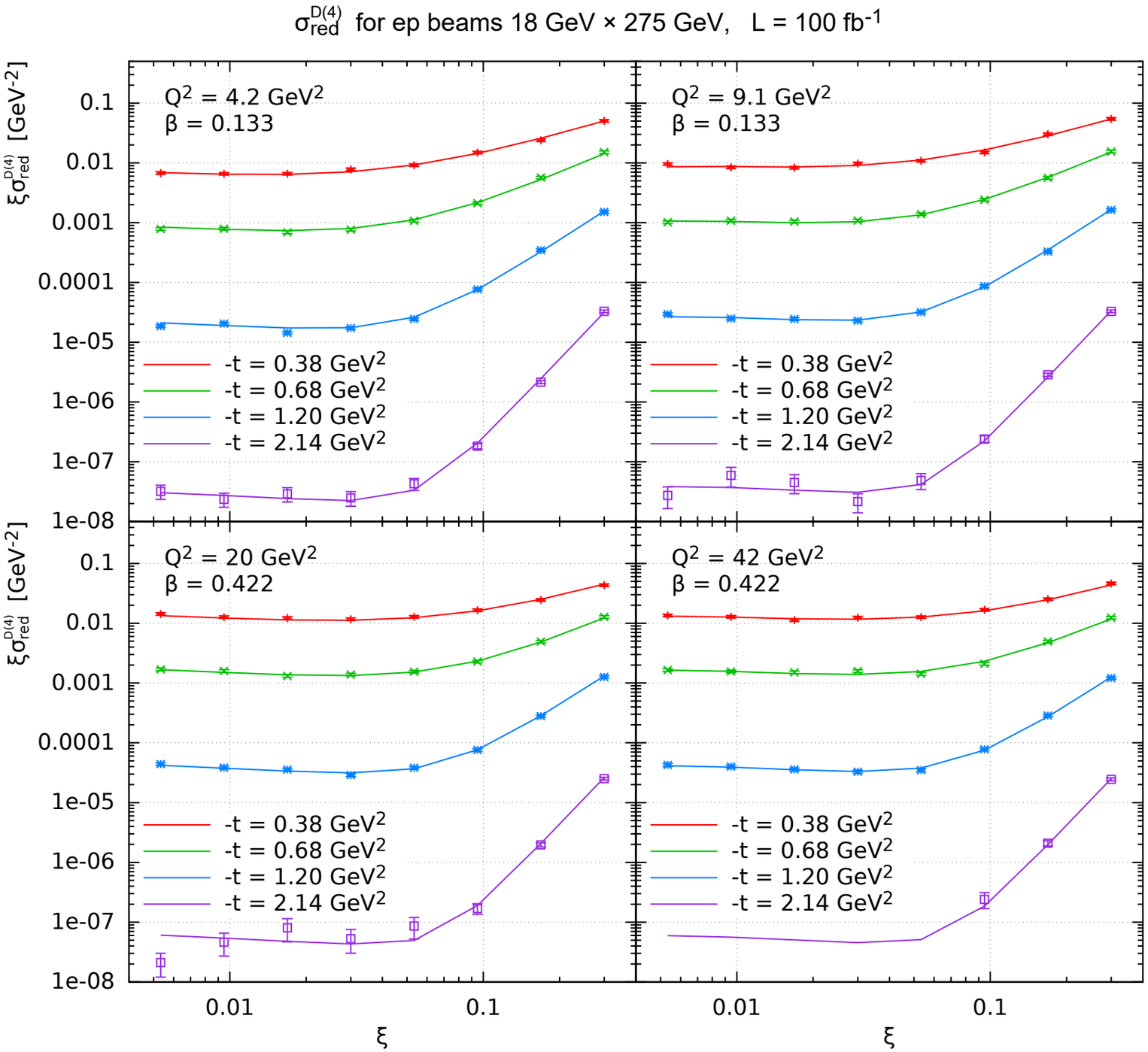

$E_e = 18\,\text{GeV}$

$E_p = 275\,\text{GeV}$

Lines-extrapolation

Points-simulation

Prospects for the very good measurement of the t-slope as a function of ξ

Double-slope structure: possibility to measure Reggeon contribution at EIC

Inclusive diffraction in eA DIS

- **Coherent** diffraction: sensitive to **global shape**; **incoherent** to **fluctuations**
- Extraction of **nuclear diffractive parton distributions** would be possible for the first time

Inclusive diffractive structure function in eA

Armesto, Newman,Slominski, Stasto
L & H models by Frankfurt, Guzey,Strikman

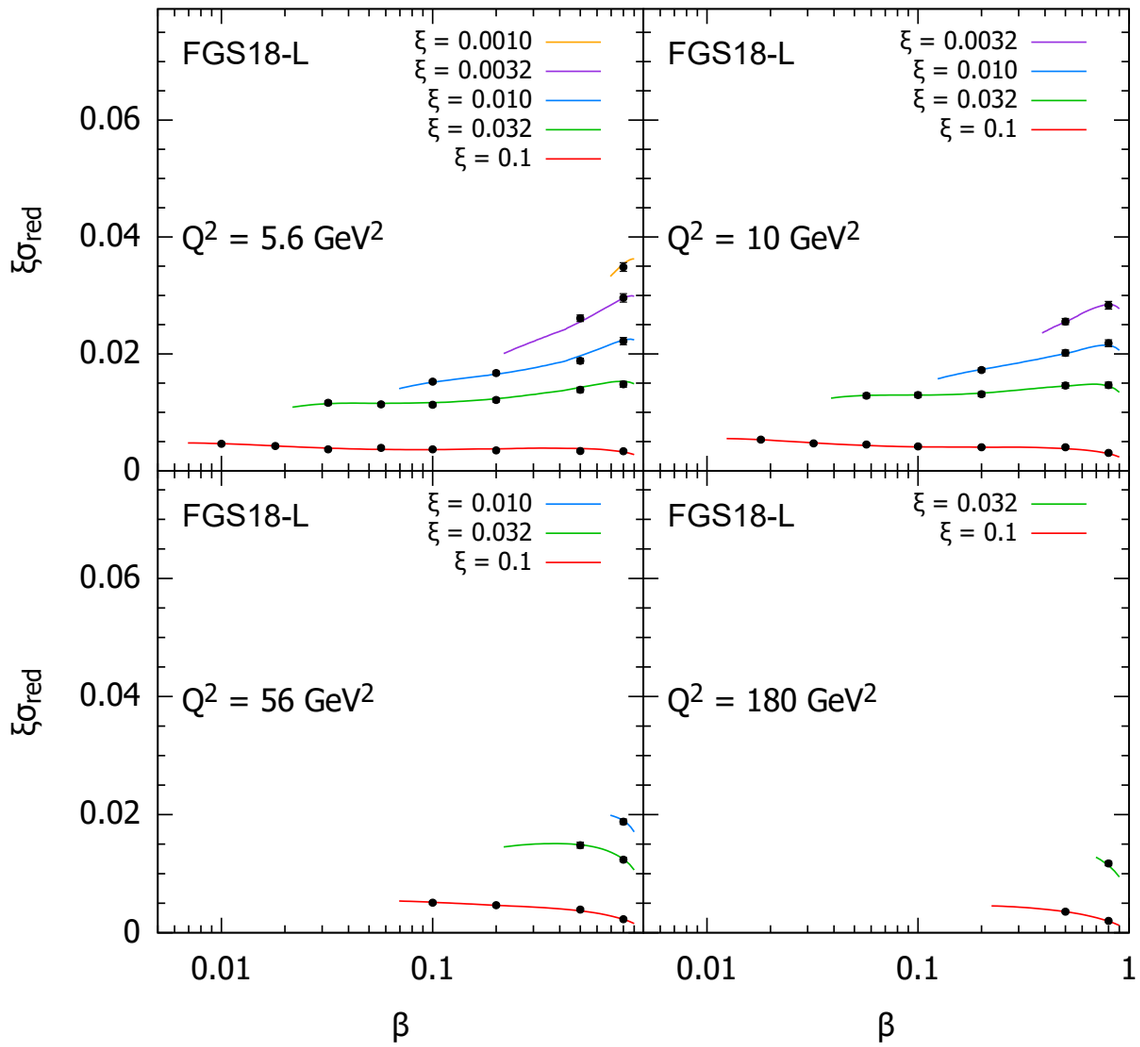

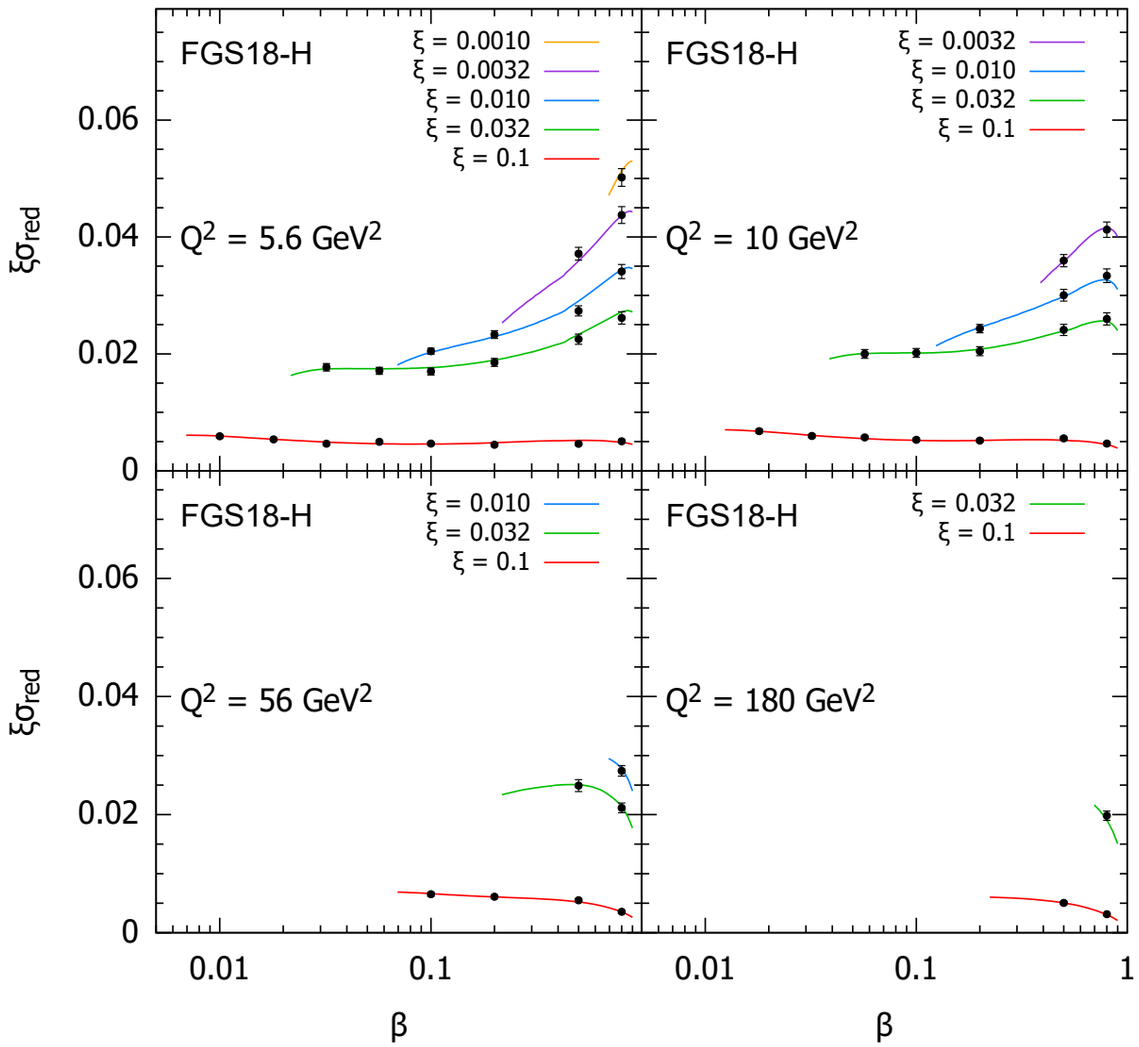

Inclusive diffraction in eA DIS

- Diffractive to inclusive ratio of cross sections **sensitive probe to different models** (ex. saturation vs leading twist shadowing)

Ratio in LT shadowing : suppression

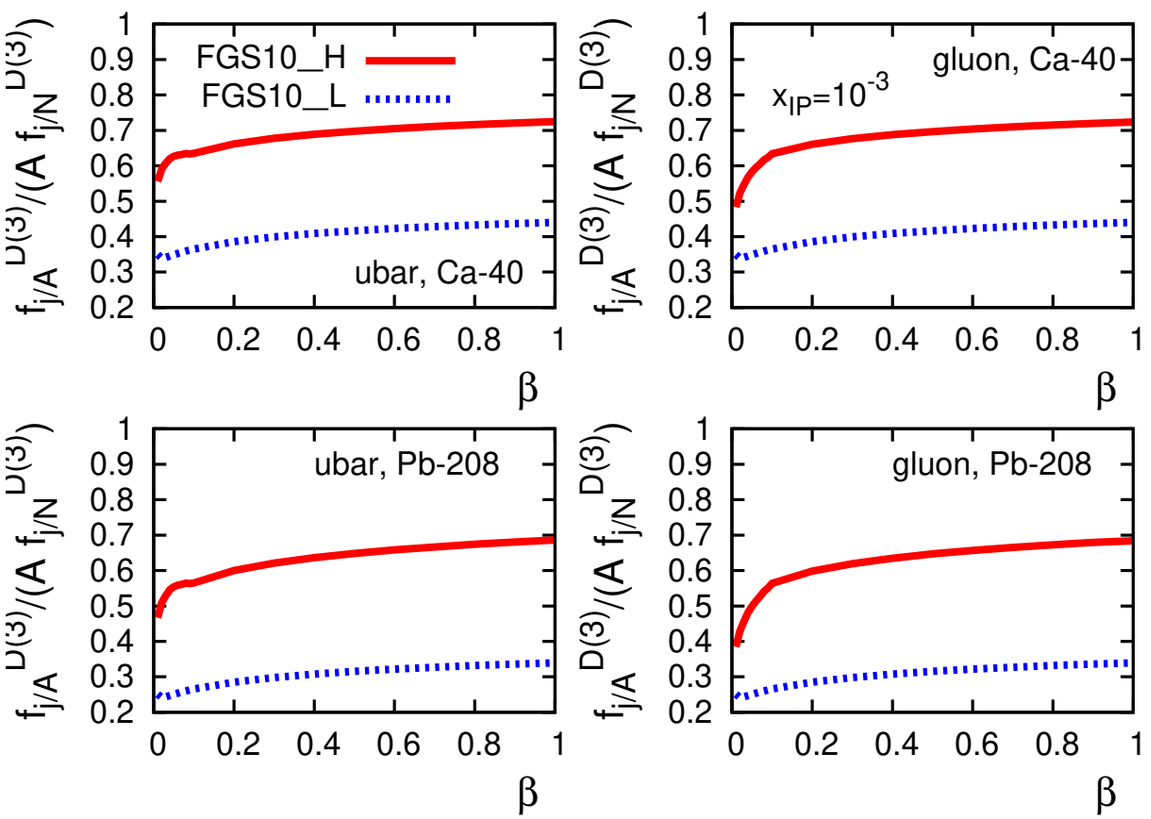

Ratio in saturation model: enhancement

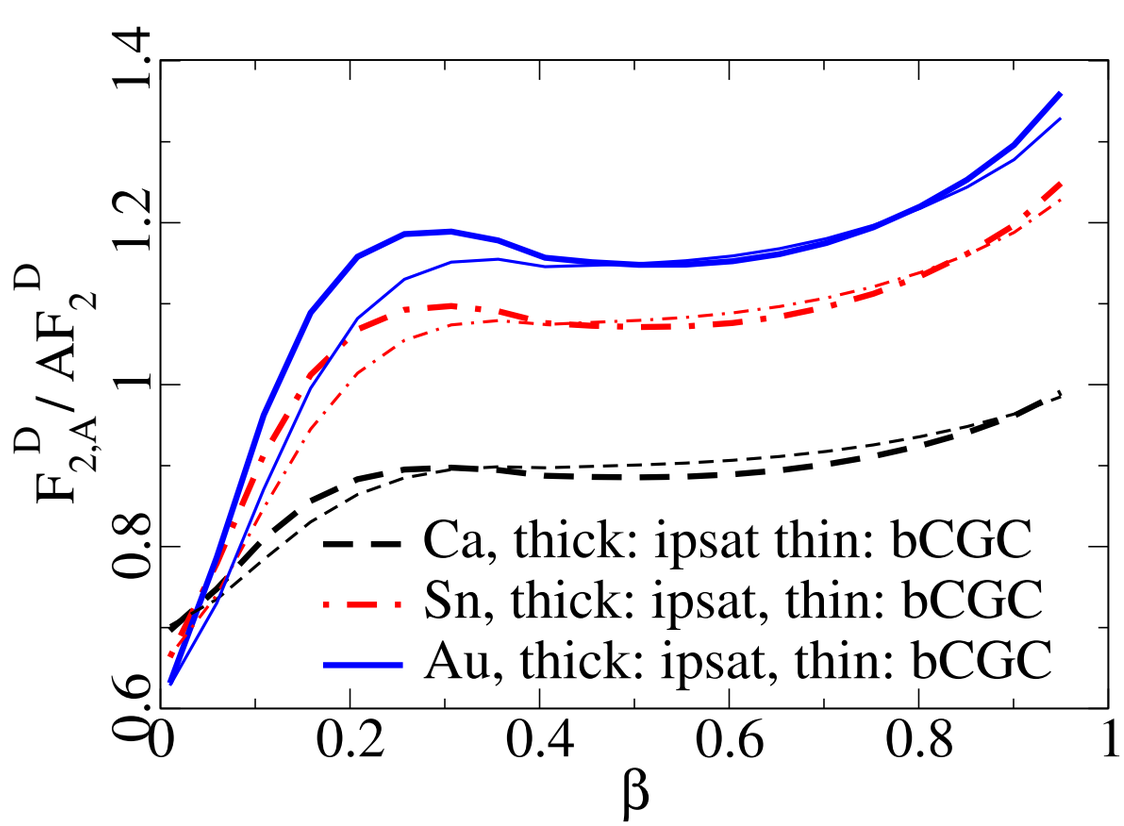

Yellow Report

Exclusive diffraction of VM

Exclusive diffraction of VM

$$e + A \to e + A + J/\psi$$

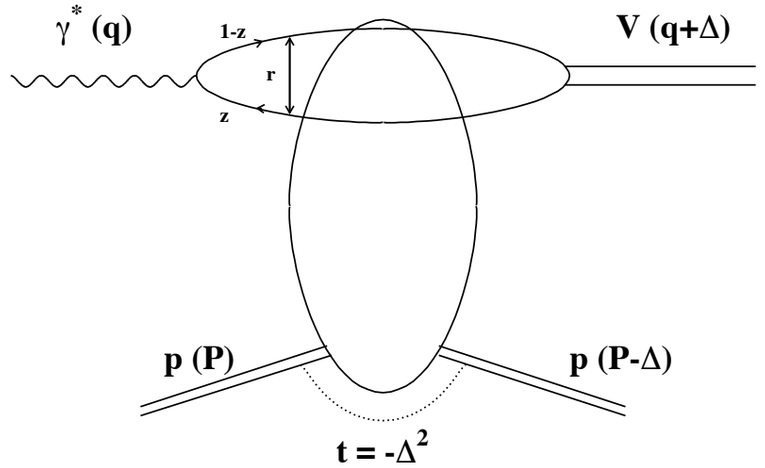

Good process to extract the shape of nucleus, sensitive to saturation at low x and large A

$$\frac{d\sigma^{\rm coh}}{dt} = \frac{1}{16\pi}\left|\langle \mathcal{A}^{\gamma^* A\to V A}\rangle_\Omega\right|^2$$

Ω target configurations

$$\mathcal{A}^{\gamma^* A\to V A} = \sum_{\lambda,\bar\lambda}\int d^2\mathbf{b}\, d^2\mathbf{r}\, dz\, e^{-i\mathbf{b}\cdot\boldsymbol{\Delta}}\Psi^{\lambda\bar\lambda}_{\gamma^*}(Q,z,\mathbf{r})\, N_\Omega(\mathbf{r},\mathbf{b},x)\, \Psi^{\lambda\bar\lambda}_{V}(z,\mathbf{r})$$

coherent Nucleus stays intact

$$\sigma_{\rm coh} \sim \left|\langle \mathcal{A}\rangle_\Omega\right|^2$$

Probing average density

incoherent Nuclear breakup

$$\sigma_{\rm incoh} \sim \langle|\mathcal{A}|^2\rangle_\Omega - \left|\langle \mathcal{A}\rangle_\Omega\right|^2$$

Probing fluctuations

Exclusive diffraction of VM: dips

$$e + p \to e + p + J/\psi$$

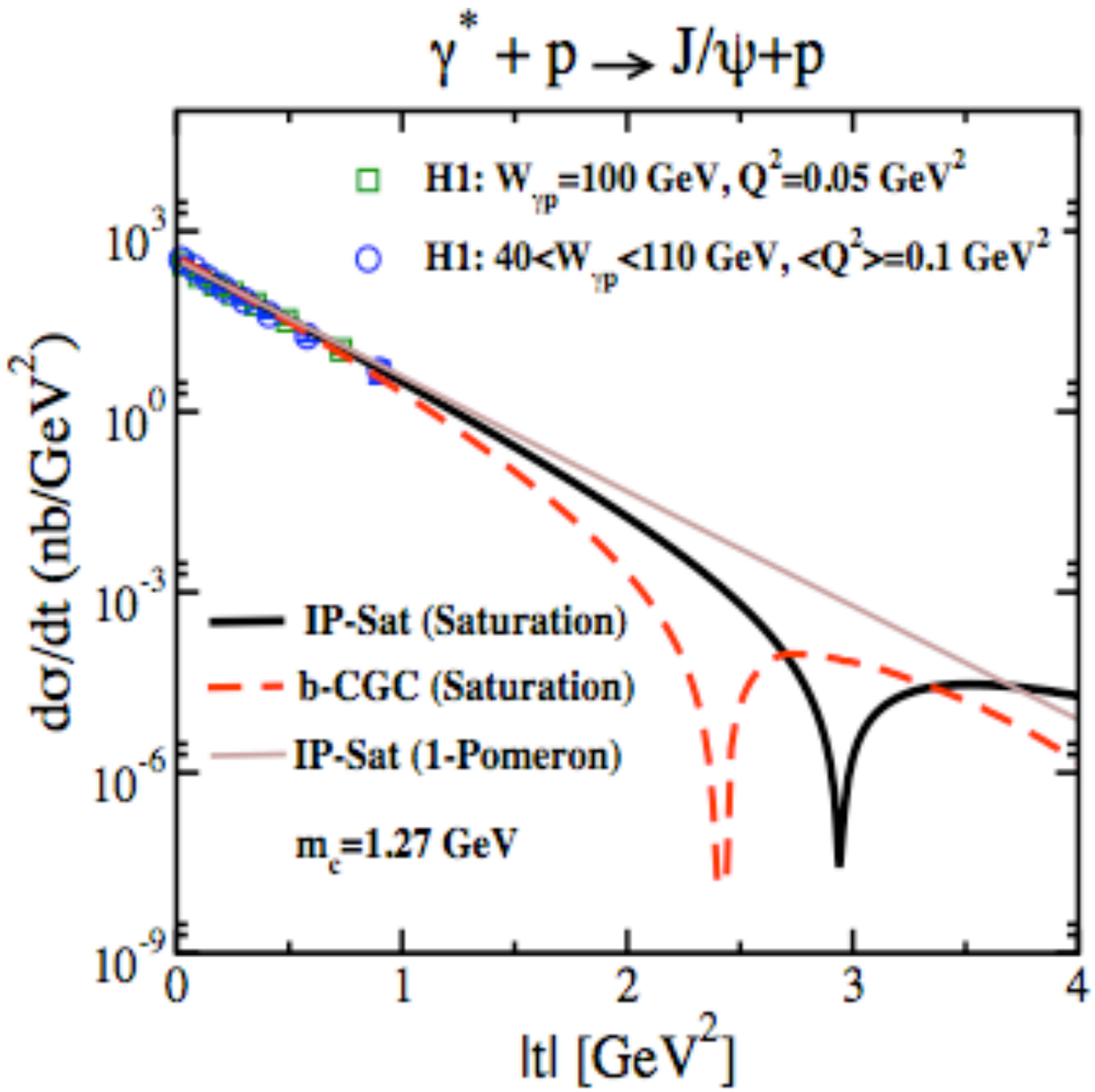

t-dependence is a Fourier transform of the impact parameter profile

Hard sphere: $N(x, r, b) \sim \theta(R - b)$, dips when $J_1(R\sqrt{t}) = 0$

Gaussian & linear: $N(x, r, b) \sim e^{-b^2/(2B)}$, Fourier transform is Gaussian, no dips

Saturation, for ex. exponentiation: $N(x, r, b) \sim 1 - \exp(-f(x, r)\, e^{-b^2/(2B)})$, dips present

Dips in general present for models with saturation

Position of dips depends on energy, scale, size of nucleus

Sensitive to modeling

Elastic diffraction of vector mesons

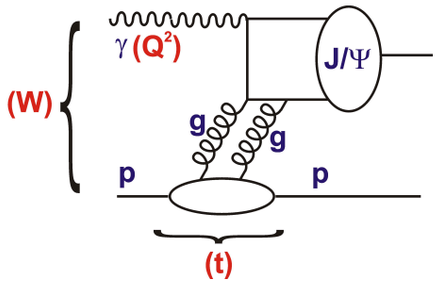

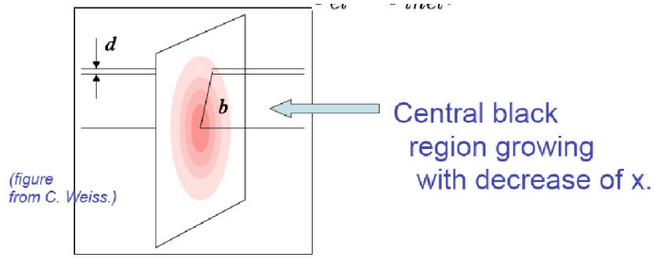

Examples for ep at very high energy (like LHeC)

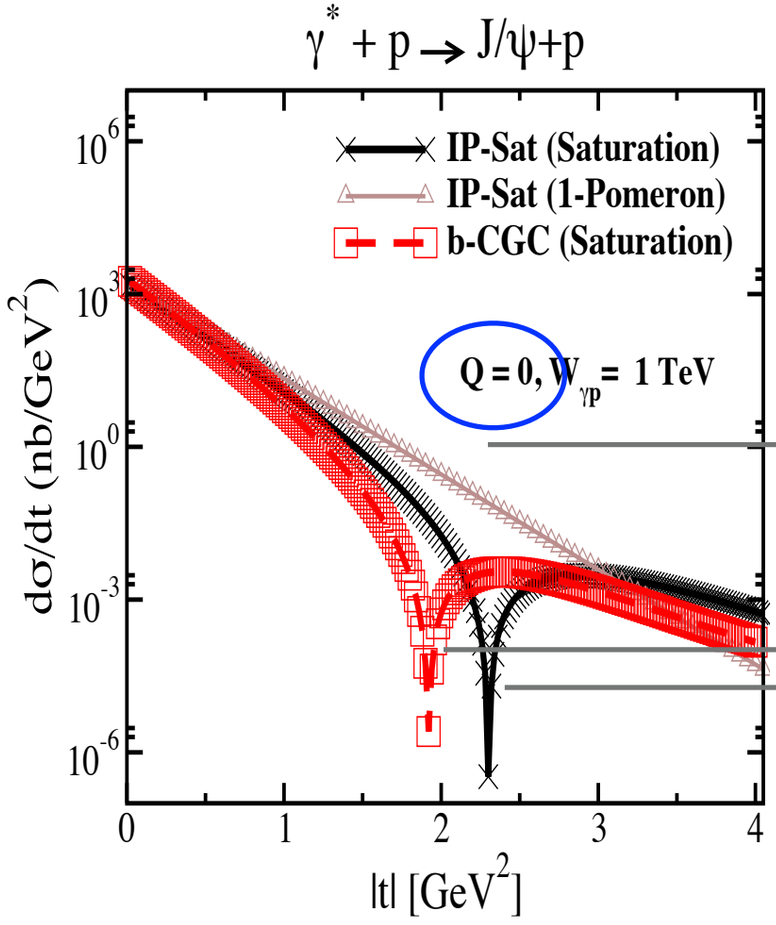

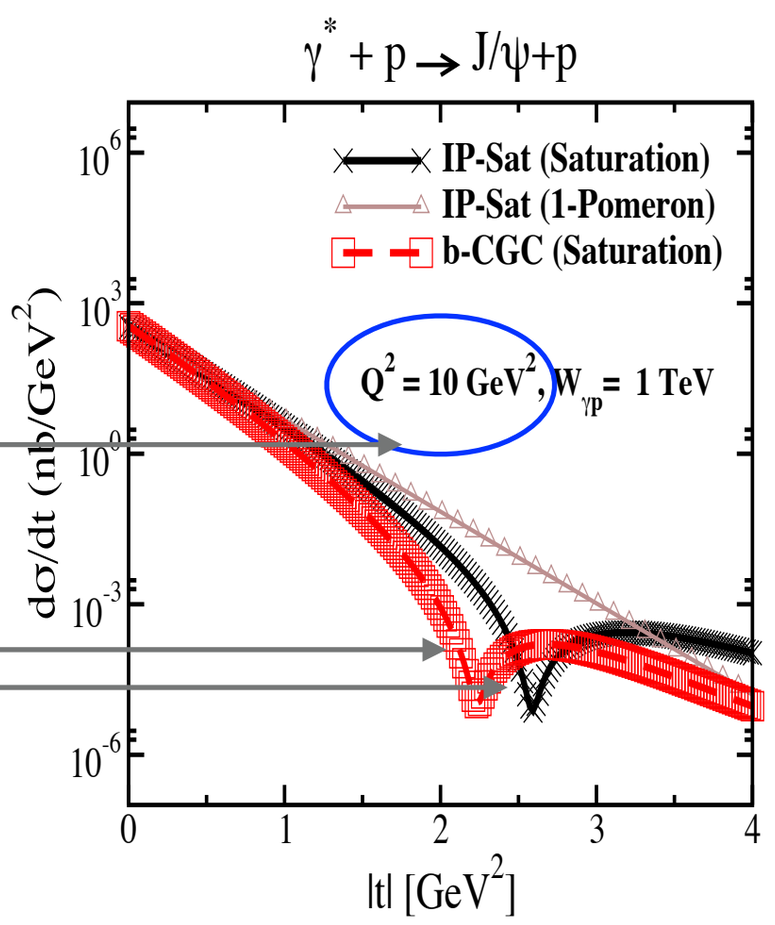

Advantage over UPC:

Q^2 dependence

Precision t, W and Q^2 dependence of vector mesons

Example : tests of saturation from the slope in t

One of the best processes to test for novel small *x* dynamics

Exclusive diffraction of VM: nuclei

Theory

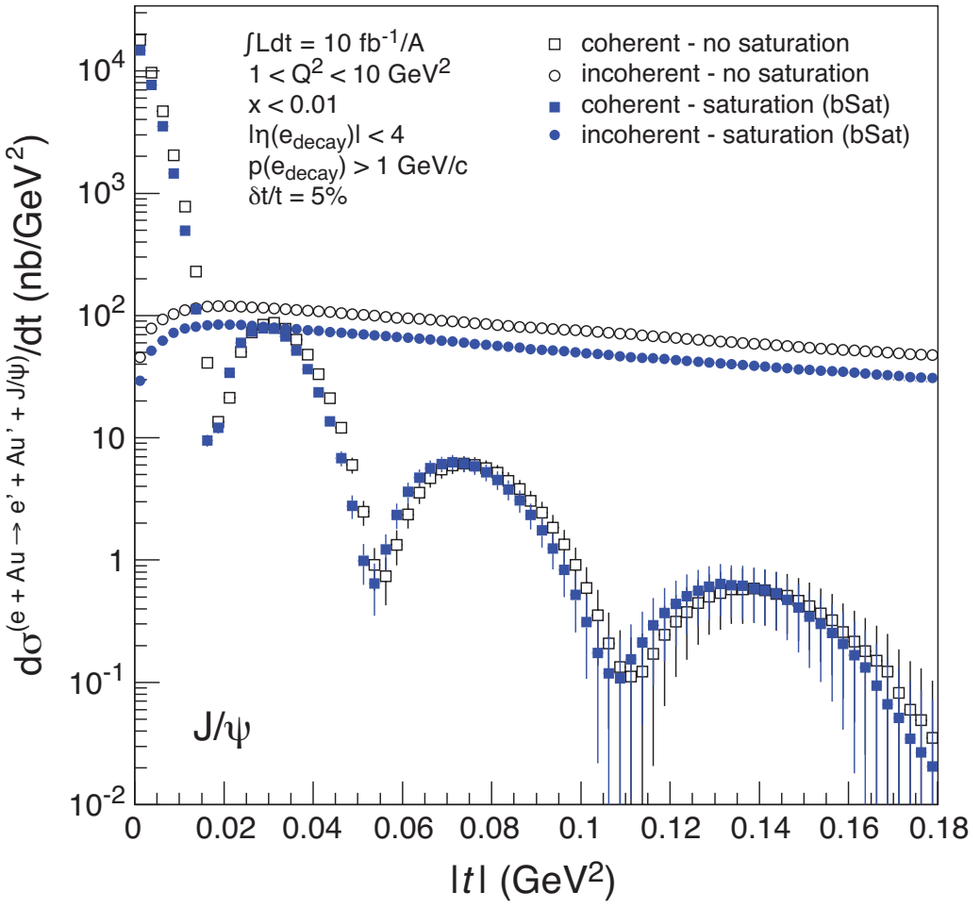

Experiment

plot from P.Steinberg et al

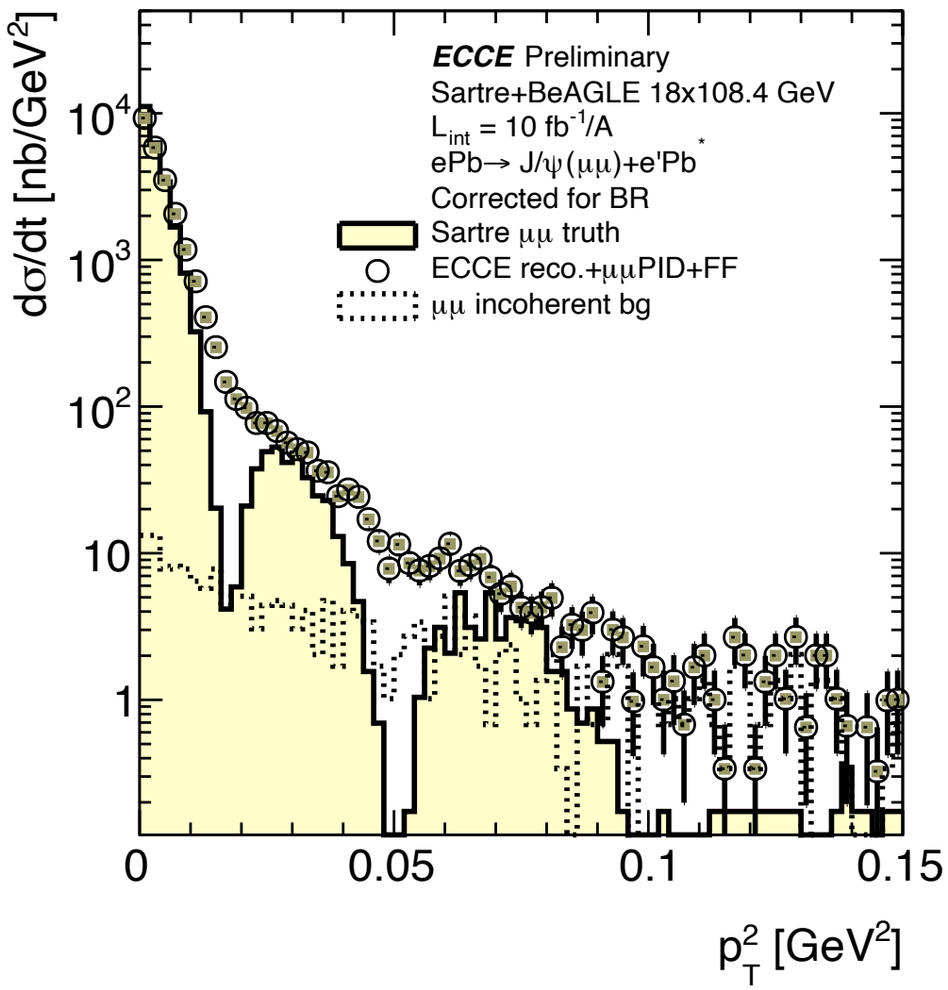

P.Steinberg quote from talk at EIC Theory WG:

'Measurement resolution (both e' and J/ψ) limit the ability to measure(or even) see diffractive dips. incoherent background can only be removed so much, esp. with acceptance of IP6. Begs the question: can these distributions be unfolded ?'

More theory work : robustness of dips, model dependence

More experimental work : detector design, unfolding method

J/ψ exclusive production in ^{4}He & ^{3}He

Coherent exclusive production of J/ψ with **light ions and deuteron**
Probing shadowing in a more controlled environment
Change of t-dependence depending on the number of scatterings

$$\frac{d\sigma_{\gamma^* A\to J/\psi A}}{dt}(t) = \frac{d\sigma_{\gamma^* N\to J/\psi N}}{dt}(t=0) \times \left| F_1(t) e^{[B_0(x)/2]t} + \sum_{k=2}^{A} F_k(t) \right|^2$$

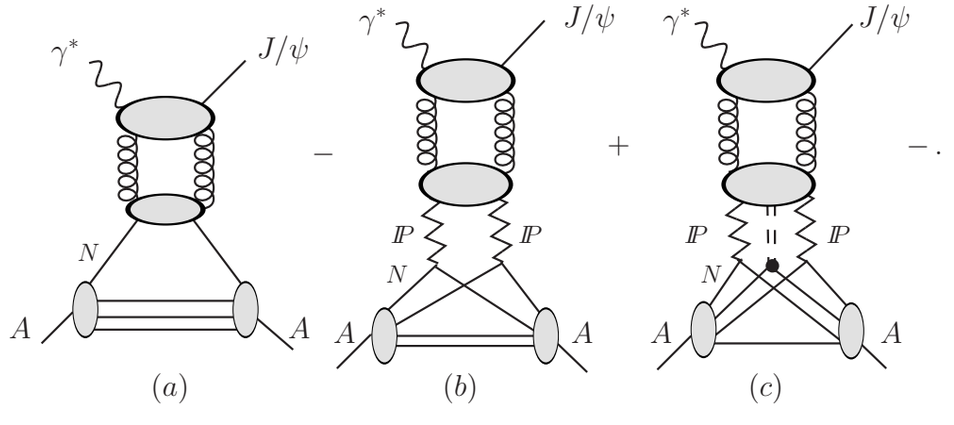

Guzey, Rinaldi, Scopetta,Strikman,Viviani

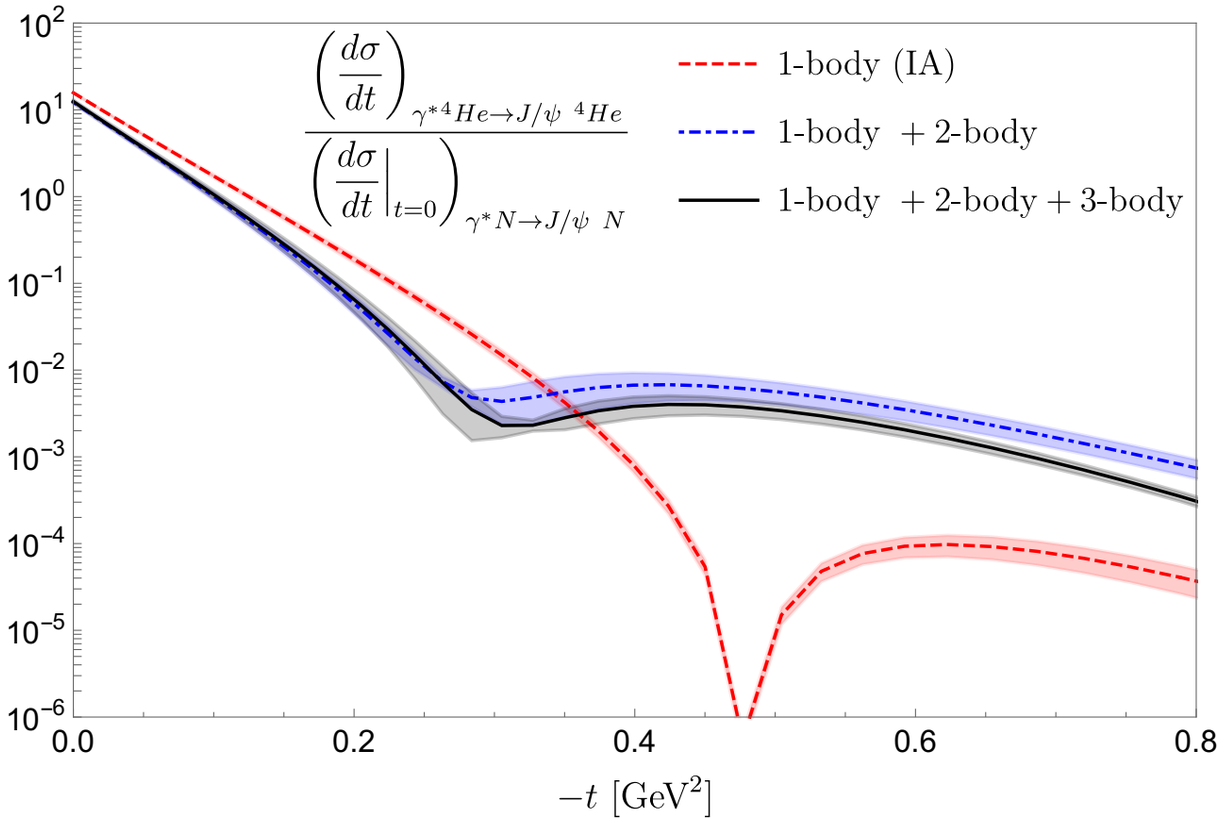

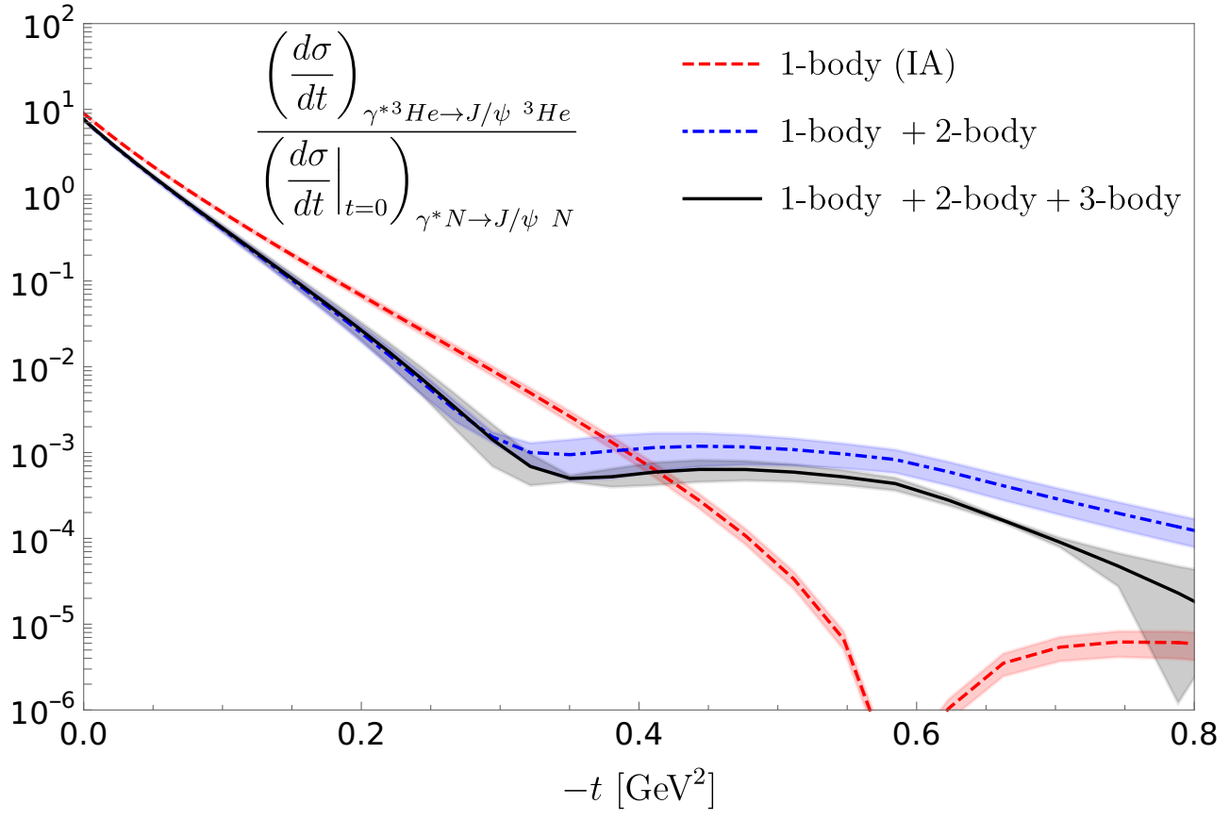

Physics with light ions at EIC

Examples of physics with light ions

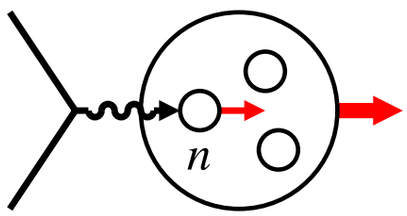

Neutron structure: standard PDFs/TMD/GPDs, improve flavor determination u/d ratio at large x, spin structure of neutron from polarized target

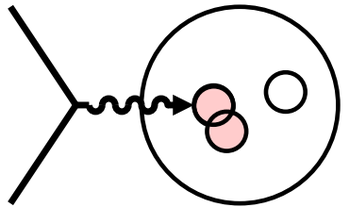

Nucleon interactions: nuclear modifications of quark and gluon densities, short-range correlations

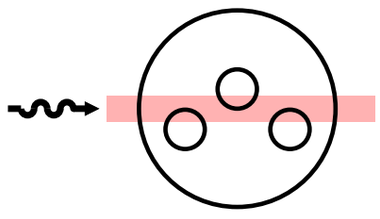

Coherent phenomena: coherent interaction of high-energy probe with multiple nucleons, shadowing, saturation

Light ions : simpler system, tagging allows for more controlled environment

Example: DIS on a deuteron with spectator tagging

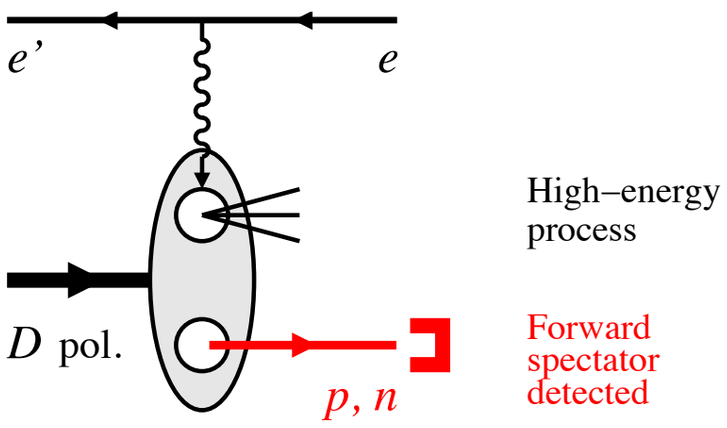

Spectator tagging allows to control the **nuclear configuration** in the deuteron initial state : active nucleon and relative momentum. Differential analysis of the nuclear effects

Unique method with several applications:

Free neutron structure function

Configuration dependence of the **EMC effect**

Proton structure function (analysis of nuclear effects)

Neutron polarization in polarized DIS (S, D waves)

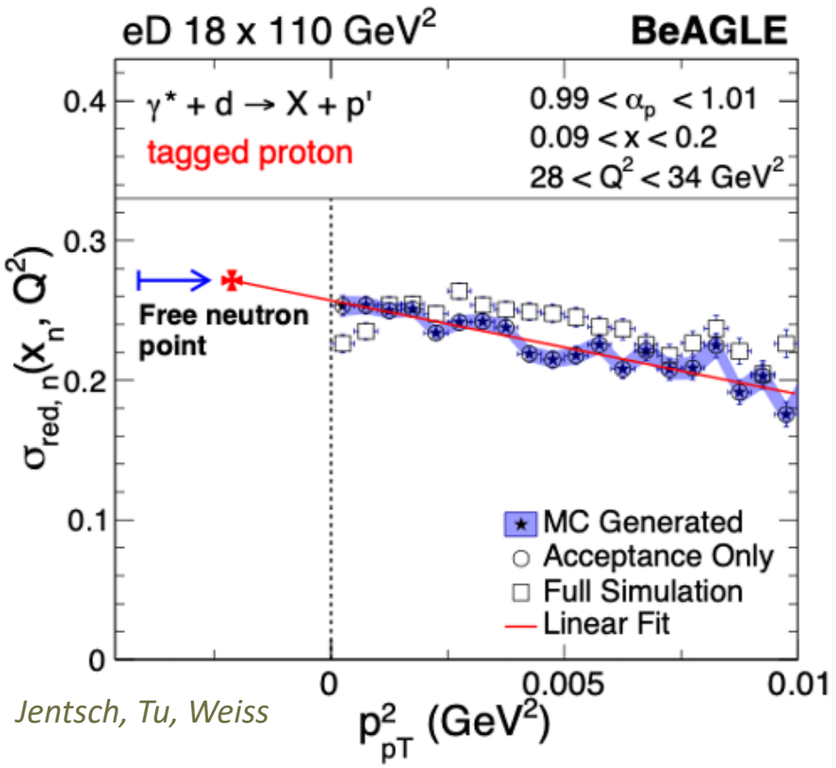

Jentsch, Tu, Weiss

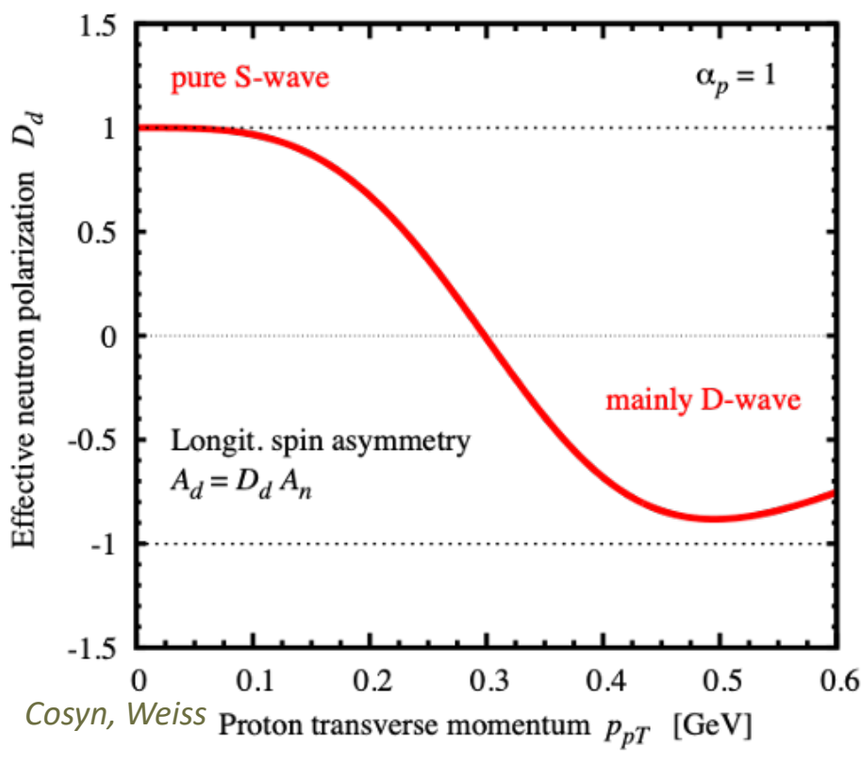

Cosyn, Weiss

Double tagging can be done with light nuclei: ^{3}He,^{3}H. Neutron, proton structure nuclear modifications

Diffractive J/ψ in electron-deuteron

Diffractive J/ψ scattering on a deuteron as a way to study short - range correlations (SRC)

Short-range correlated nucleon pairs with high internal nucleon momentum (quasi-deuteron inside the nucleus). Possible strong link of SRC to EMC effect.

Questions:

Role of gluons in SRC pairs?

Relation of SRC to shadowing and/or saturation ?

Spatial and momentum distribution of partons in high momentum configurations ?

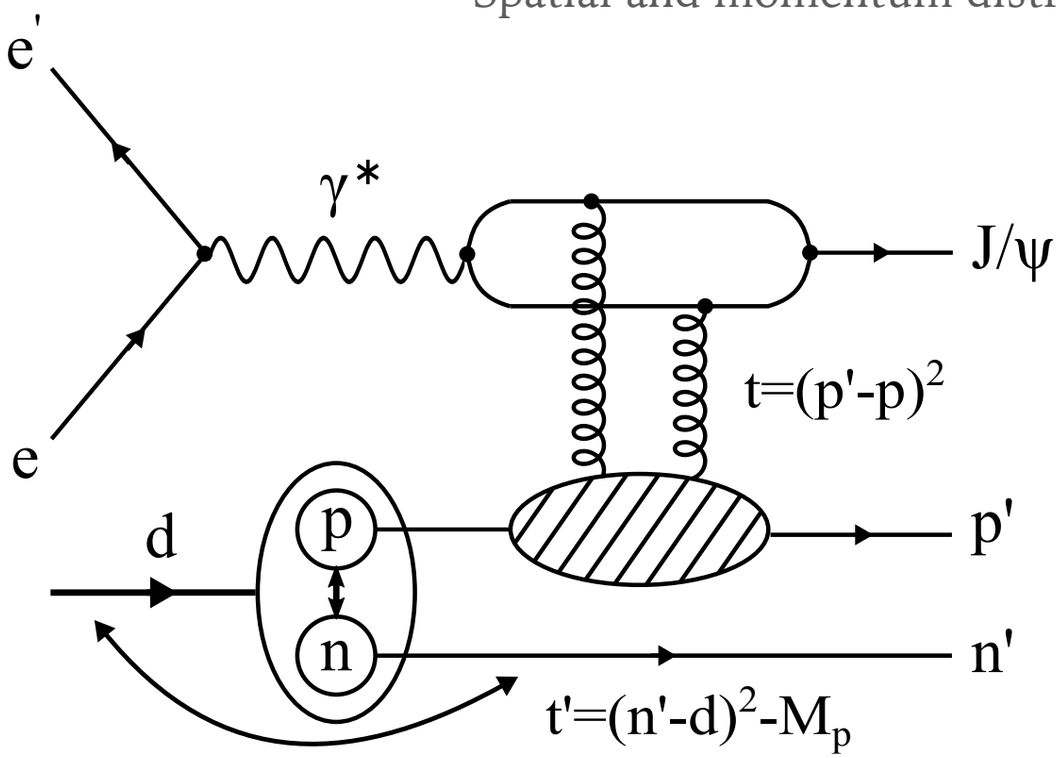

Momentum transfer t, the difference between outgoing proton momentum and incoming proton momentum, which is not known in ed, unlike in ep

$$t = (p' - p)^2$$

Reconstruction of t : through leading nucleon and spectator measurement (proton and nucleon are back-to-back in the rest frame of pn before the interaction)

$$t = (p' - (-n))^2$$

Simulation in impulse approximation

Diffractive J/ψ in electron-deuteron

3-momentum distribution of the spectator nucleon in the rest frame of deuteron

Reflects the internal nucleon momentum at the initial state of the deuteron wave function

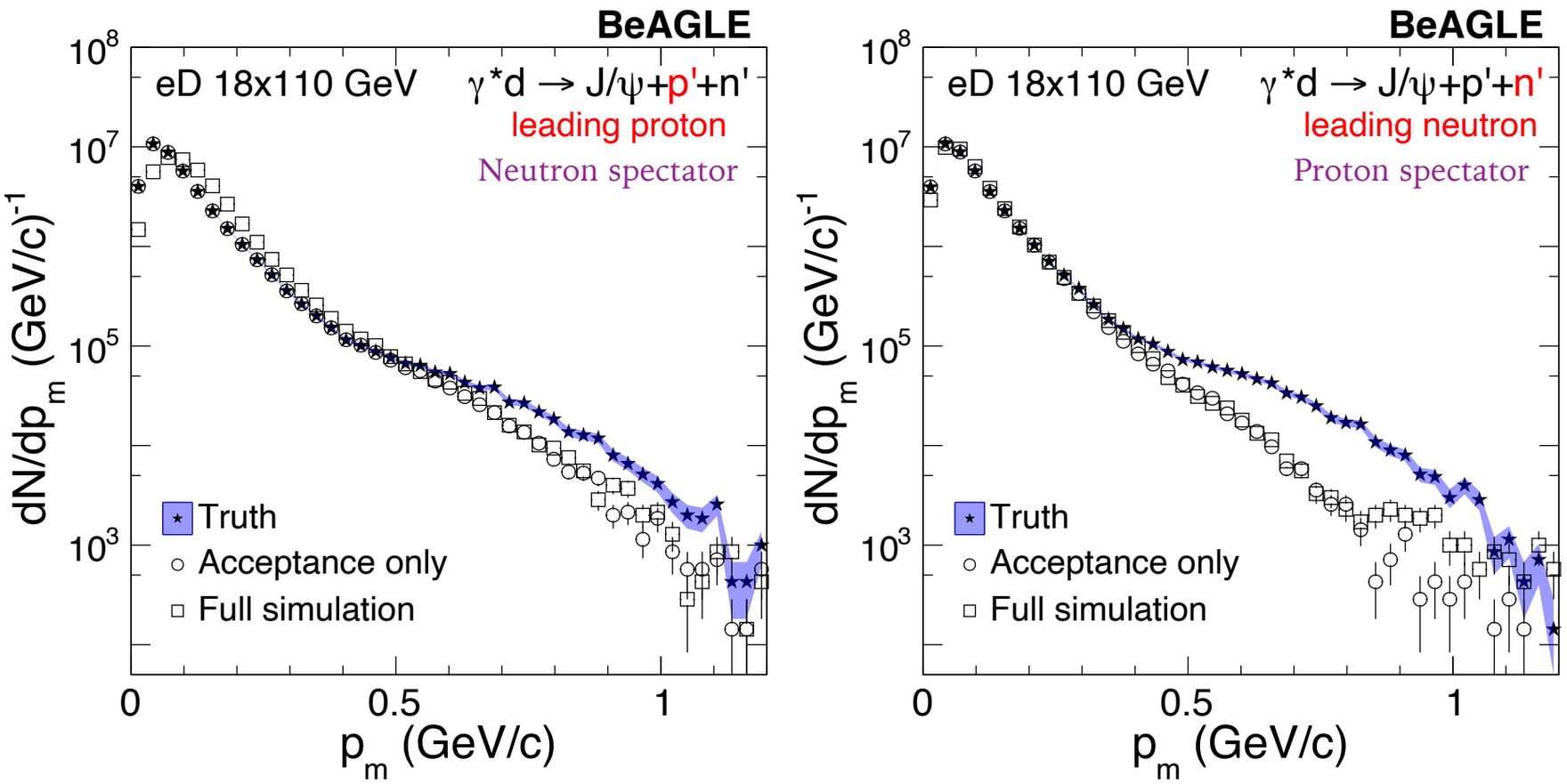

Neutron spectator: 4-6 mrad cone in the ZDC, 100% acceptance up to 0.6 GeV, momentum smearing up to 300 MeV

Proton spectator: Better resolution, less bin migration at low momenta

Distribution in t for diffractive J/ψ in electron-deuteron

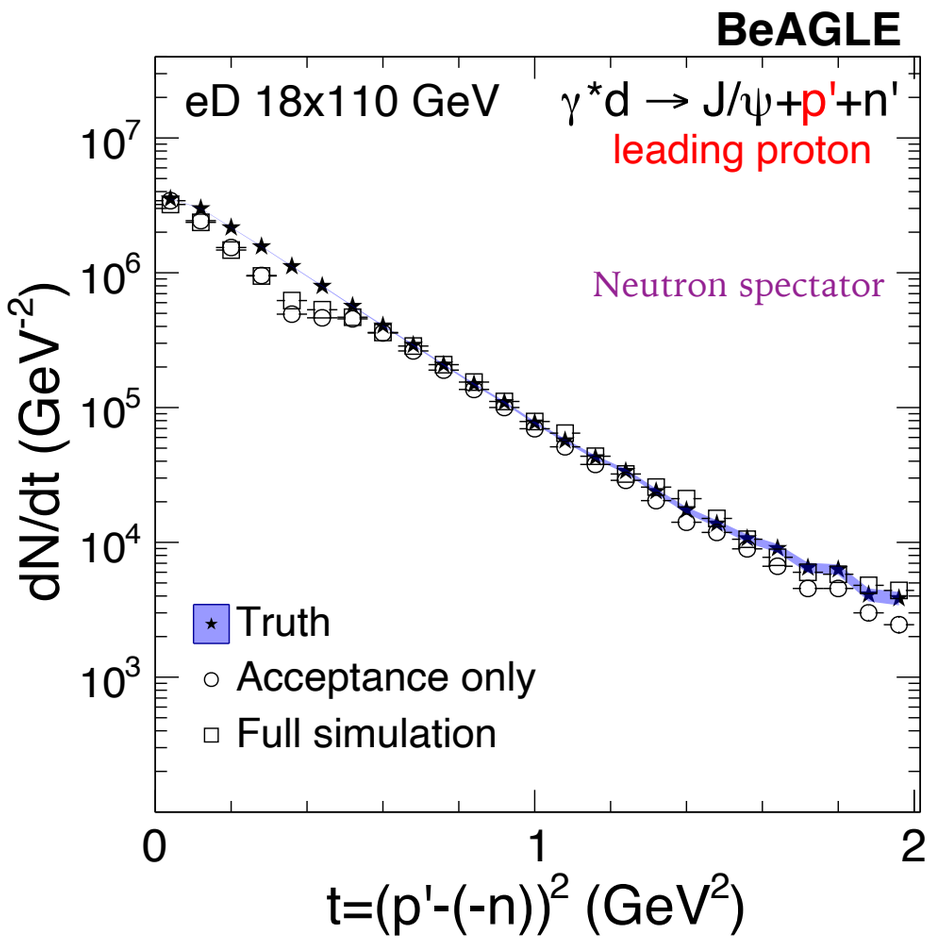

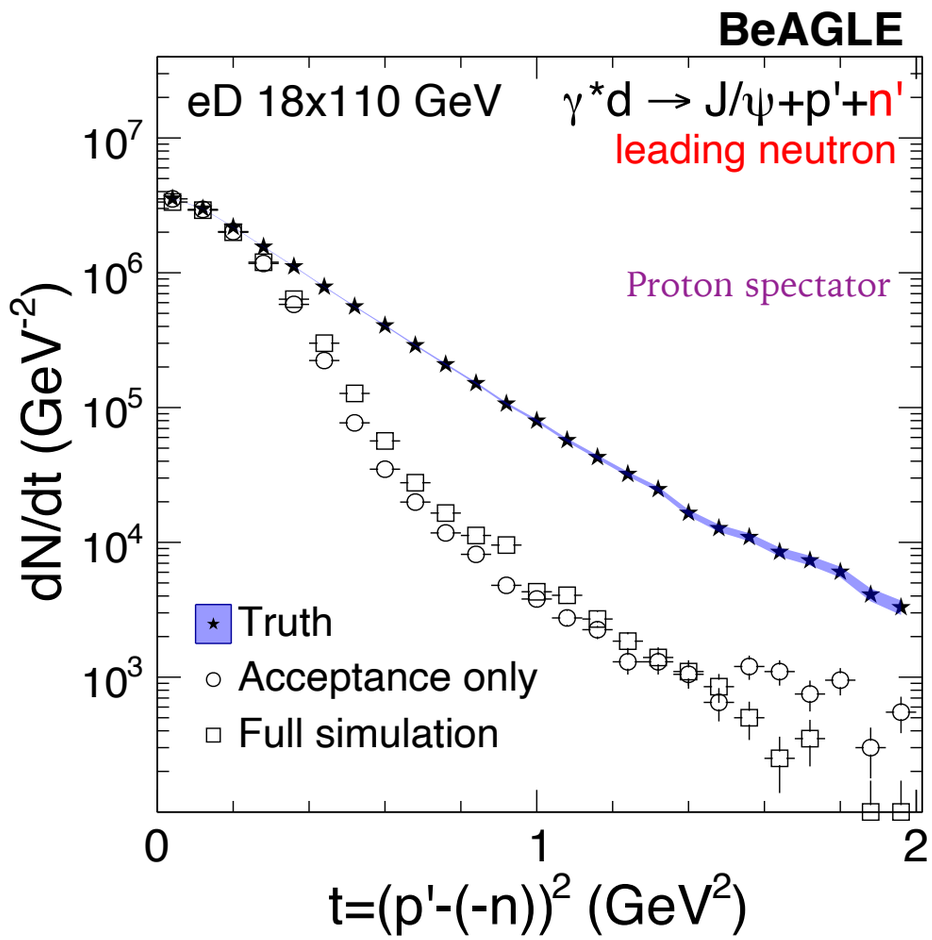

Integrated over a range of p_m

Method requires double tagging of both proton and neutron

In general t distribution affected by acceptance and resolution of nucleons

Good precision in neutron spectator case

Distribution in t for diffractive J/ψ in electron-deuteron

SRC dependent t-distribution

Distribution in t is a Fourier transform of the source distribution

Gluon distributions of the bound nucleon can be measured for different internal momentum ranges

Link between the role of gluons in the SRC and modifications of gluon structure functions

Assume 10% difference in the nucleon size for events p_m>0.6 GeV

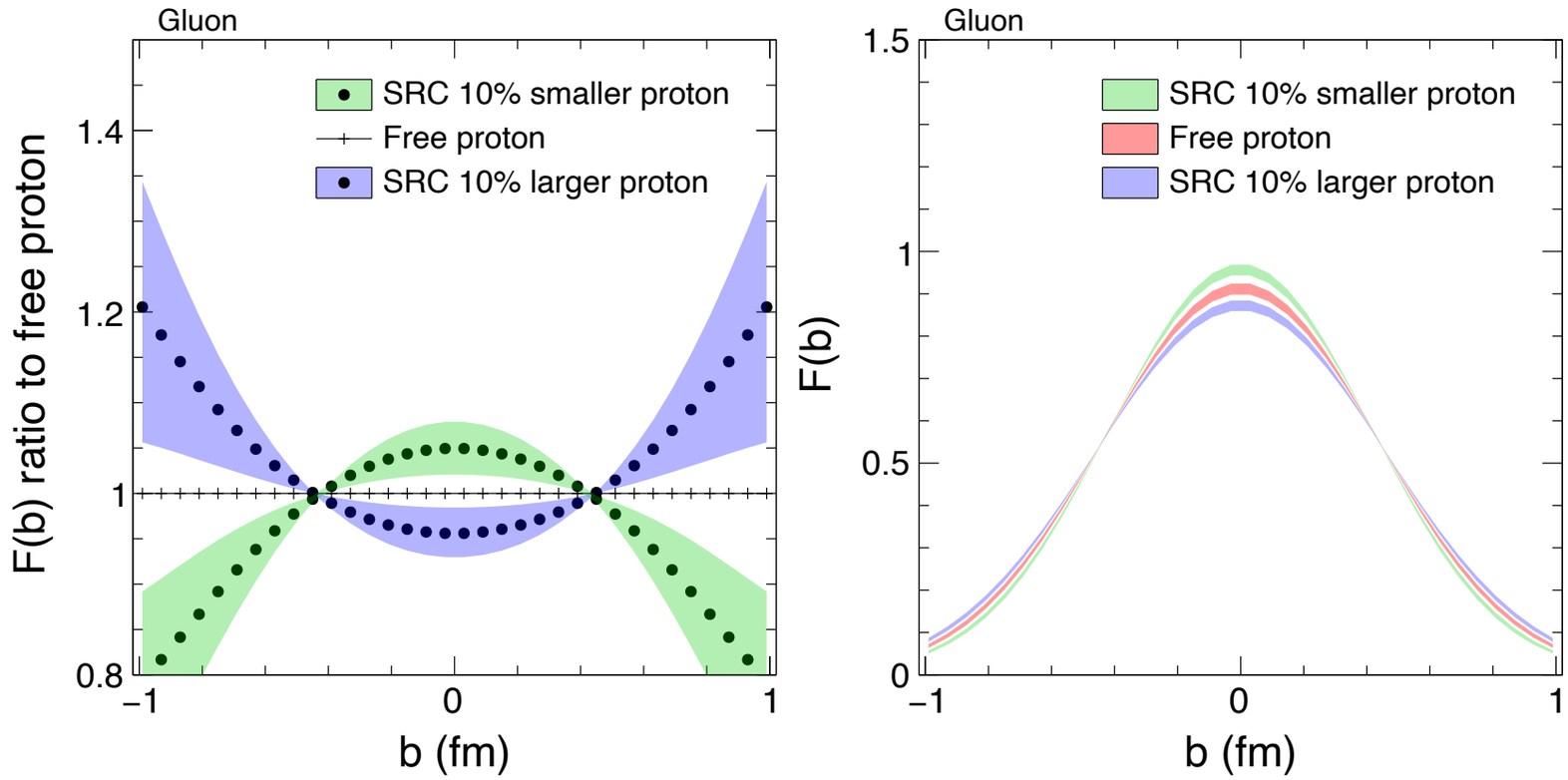

Gluon source distribution F(b) and ratio between SRC protons and free protons from the FT of the t distribution of elastic J/ψ

Passage of color charges through cold nuclear matter

- Modern theories of QCD in matter (such as $SCET_G$ and $NRQCD_G$) have enabled novel understanding of parton showers on matter. Capabilities to calculate higher order and resumed calculations in reactions with nuclei
- EIC will provide important input on **hadronization** mechanism in eA
- Different scenarios: **parton evolution in medium** or **hadron absorption**

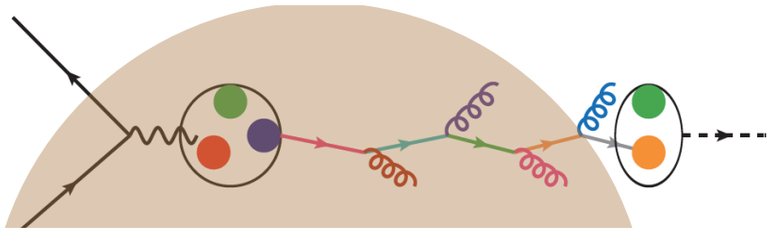

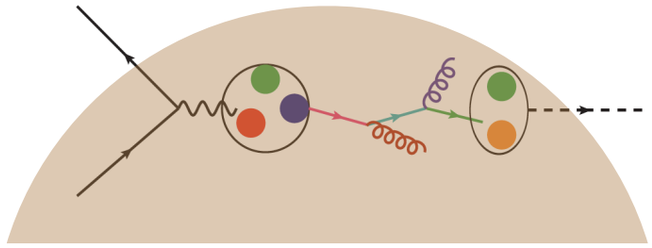

Parton energy loss and in-medium fragmentation function modification

$$\frac{d}{d\ln\mu^2}\tilde{D}^{h/i}(x,\mu) = \sum_j \int_x^1 \frac{dz}{z}\tilde{D}^{h/j}\left(\frac{x}{z},\mu\right)\left(P_{ji}(z,\alpha_s(\mu)) + P_{ji}^{\text{med}}(z,\mu)\right)$$

$$R_{eA}^h(p_T,\eta,z) = \frac{\left.\frac{N^h(p_T,\eta,z)}{N^{\text{inc}}(p_T,\eta)}\right|_{\text{e+Au}}}{\left.\frac{N^h(p_T,\eta,z)}{N^{\text{inc}}(p_T,\eta)}\right|_{\text{e+p}}}$$

Modification (e+A vs e+p) of light vs heavy mesons vs the fragmentation fraction z

Li, Liu, Vitev

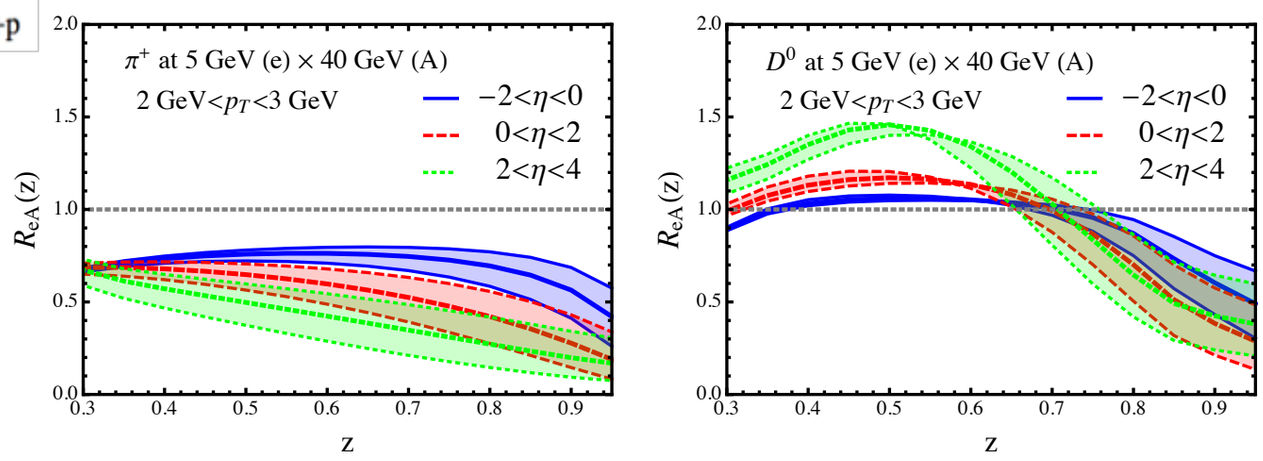

Constrain the space-time picture of hadronization.

Differentiate **energy loss** and **hadron absorption** models (based on ability to measure heavy flavors)

Lower energy beams better for this process

Jets as probes of cold nuclear matter

Jets emerged as a premier diagnostic tool for **hot** nuclear matter at RHIC and LHC

Also excellent probes for **cold** nuclear matter. Using jets, elucidate the properties of in-medium parton showers.

$$d\sigma \sim \underbrace{f_a(z,\mu)}_{\text{initial}} \otimes \overbrace{H_{ab}(x,z;p_T,\eta)}^{\text{partonic cross section}} \otimes \underbrace{J_b(z,\mu,R)}_{\text{final}}$$

PDF

jet function

Yellow Report

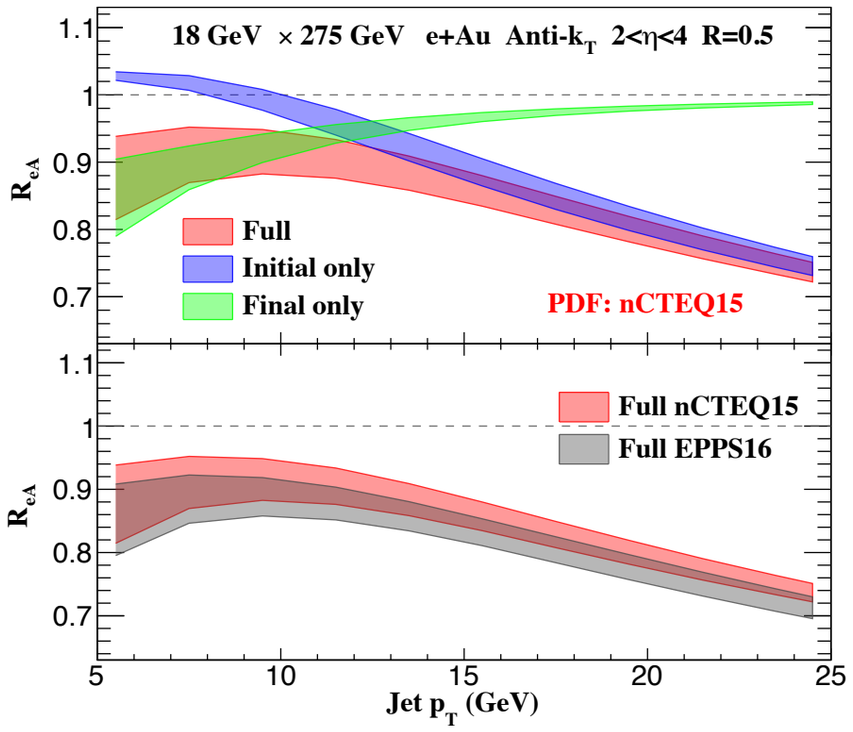

- IS (large and small p_T) vs FS (small p_T) contributions to nuclear ratio
- Small nPDF effects
- Ratios with different jet cone allow to separate parton shower effects

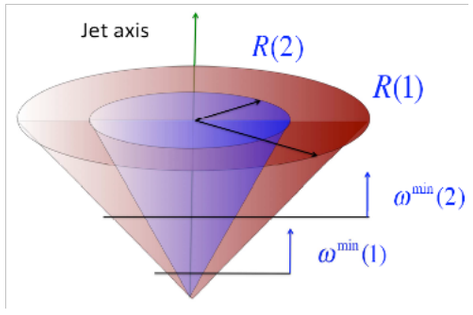

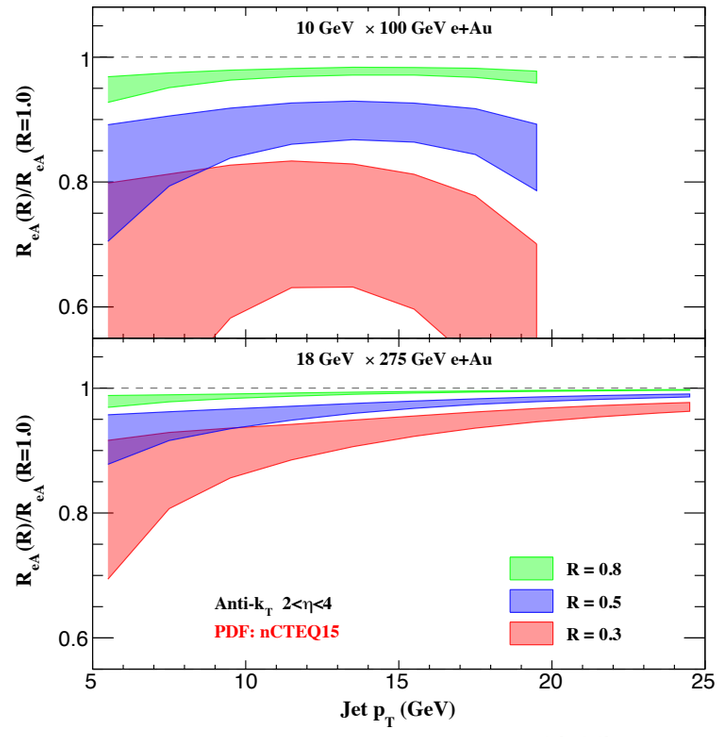

Li, Vitev

- Pioneer jet **substructure** studies with heavy quark initiated jets performed in a EIC regime very different from the one probed in heavy ion collisions *Li, Liu, Vitev*
- Pave the way to a qualitatively new level of understanding of the role of **heavy quark mass**

Summary

- **EIC : precision tool for high energy nuclear physics**
- Nuclear structure functions, precision extraction of nuclear PDFs, testing the limits of collinear factorization in nuclei. Initial conditions for hot QCD.
- Explore the onset of saturation in eA, DGLAP vs non-linear evolution, x,A, and Q dependence. Precise measurement of F_L needed (variable energies)
- Extraction of diffractive nuclear PDFs possible for the first time, potential for F_L^D. Prospects for measuring Reggeon. Diffractive to inclusive ratios needed to distinguish between the different scenarios (saturation vs leading twist shadowing).
- Exclusive diffraction of vector mesons, excellent process to map spatial distribution and test saturation. Experimental challenges.
- Test the mechanism of hadronization with hadrons and jets (heavy flavors, low energy beams). Initial vs final state effects.
- Rich program with light ions: spectator tagging, configuration dependence, neutron structure, SRC, coherent nuclear processes, polarization